ME

18 SEPTEMBER 1980 NO. 6, JUNE 1980 1 OF 3

JPRS L/9304

18 September 1980

USSR Report

METEOROLOGY AND HYDROLOGY

No. 6, June 1980

FBIS FOREIGN BROADCAST INFORMATION SERVICE

NOTE

JPRS publications contain information primarily from foreign newspapers, periodicals and books, but also from news agency transmissions and broadcasts. Materials from foreign-language sources are translated; those from English-language sources are transcribed or reprinted, with the original phrasing and other characteristics retained.

Headlines, editorial reports, and material enclosed in brackets [] are supplied by JPRS. Processing indicators such as [Text] or [Excerpt] in the first line of each item, or following the last line of a brief, indicate how the original information was processed. Where no processing indicator is given, the information was summarized or extracted.

Unfamiliar names rendered phonetically or transliterated are enclosed in parentheses. Words or names preceded by a question mark and enclosed in parentheses were not clear in the original but have been supplied as appropriate in context. Other unattributed parenthetical notes within the body of an item originate with the source. Times within items are as given by source.

The contents of this publication in no way represent the policies, views or attitudes of the U.S. Government.

For further information on report content call (703) 351-2938 (economic); 3468 (political, sociological, military); 2726 (life sciences); 2725 (physical sciences).

APPROVED FOR RELEASE: 2007/02/08: CIA-RDP82-00850R000300030024-9

JPRS L/9304

18 September 1980

USSR REPORT

METEOROLOGY AND HYDROLOGY

No. 6, June 1980

Translation of the Russian-language monthly journal METEOROLOGIYA I GIDROLOGIYA published in Moscow by Gidrometeoizdat.

CONTENTS

 [III - USSR - 33 S&T FOUO]

UDC 551.524.34(215-17)

MODERN CHANGES IN CLIMATE OF THE NORTHERN HEMISPHERE

Moscow METEOROLOGIYA I GIDROLOGIYA in Russian No 6, Jun 80 pp 5-17

[Article by Candidate of Physical and Mathematical Sciences K. Ya. Vinnikov, Professor G. V. Gruza, Candidates of Geographical Sciences V. F. Zakharov and A. A. Kirillov, N. P. Kovyneva and Candidate of Physical and Mathematical Sciences E. Ya. Ran'kova, State Hydrological Institute, All-Union Scientific Research Institute of Hydrometeorological Information-World Data Center, Arctic and Antarctic Scientific Research Institute and USSR Hydrometeorological Scientific Research Center, submitted for publication 15 January 1980]

[Text]

Abstract: The article presents empirical data on the change of mean annual air surface temperature in the northern hemisphere during the period 1881-1978. The authors analyze the linear trends for different parts of the series. The conclusion that during the period 1966-1975 the mean annual air surface temperature of the extra-equatorial part of the northern hemisphere (17.5-87.5°N) has increased gradually is confirmed. Materials are presented which characterize the integral ice content of the north polar basin. It is demonstrated that a peculiarity of the development of the arctic ice cover during recent years is its contraction.

Change in Surface Air Temperature

In many recent studies the mean annual surface temperature of the air, averaged over the area of individual hemispheres or wide latitudinal zones, is used in characterizing changes in the global temperature regime.

The longest uniform series of mean characteristics of air surface temperature for the northern hemisphere were obtained in the studies of Willett [30, 31], Mitchell [22, 23], Callendar [18], L. P. Spirina [13], Ye. S. Rubinshteyn [11], I. I. Borzenkova, et al. [1], Landsberg, et al. [21].

In all these studies it was established that from the end of the last century to the 1940's a process of warming of the northern hemisphere developed which in the 1940's was replaced by a cooling. Both these processes were expressed most clearly in the high latitudes.

For a considerably shorter time interval, taking in the 1950's, 1960's and 1970's, similar data were obtained in the studies of Angell and Korshover [14, 15], Yamamoto, et al. [32], Brinkman [17], Kukla, et al. [20], Walsh [28, 29] and Barnett [16].

Willett [31] was the first to draw attention to the fact that the cooling trend, beginning in the 1940's, for the first time noted on the basis of data for the high latitudes, had gradually shifted into the lower latitudes. In the middle latitudes of the northern hemisphere it has been observed only since the 1950's, and in the tropical and equatorial latitudes -- considerably later. With the beginning of the 1970's Willett has noted an incipient weak tendency to warming. This preliminary conclusion found confirmation in a study by I. I. Borzenkova, et al., in which the conclusion was drawn that in the mid-1960's the cooling process in the northern hemisphere had ended and had been replaced by a warming process whose mean intensity during the period 1964-1975 was estimated at about 0.3°/10 years for the mean annual air temperature at the surface in the extra-equatorial part of the hemisphere (87.5-17.5°N).

Although the quantitative information contained in the mentioned studies differs not only with respect to the scales of spatial and temporal averaging, but also with respect to accuracy, there are virtually no significant contradictions in the data of the principal studies. The contradictions in the interpretation of data are greater. In particular, in the studies of Kukla, et al. [20] and Borzenkova, et al. [1] contradictory opinions are expressed concerning the recently observed tendencies in change in the thermal regime of the northern hemisphere.

In this connection we note that it makes sense to retain the traditional use of the terms "global warming" or "cooling" relative to the processes of change in the mean annual or seasonal air temperature at the surface over the greater part of a hemisphere. The desirability of such an application of these terms is dictated by the fact that data on changes in the air temperature at the surface over a sufficiently long period of time could be obtained from materials obtained by relatively reliable instrumental measurements. This does not exclude the necessity for monitoring changes of the thermal regime of the free atmosphere.

During 1977-1978 specialists at the All-Union Scientific Research Institute of Hydrometeorological Information-World Data Center created [5] a supplementary archives (on magnetic tapes) of anomalies of surface mean monthly air temperature for the northern hemisphere for the period 1891-1978. The basis for the archives is the same sources of information

[8, 12] as were used in a study by I. I. Borzenkova, et al. [1]. However, the reading of data from the maps of monthly temperature anomalies was accomplished anew using a somewhat differing latitude-longitude grid with a spacing of 5° in latitude x 10° in longitude. With the use of these data for the period 1891-1978 we obtained time series of monthly air temperature anomalies for the principal latitude zones of the northern hemisphere (87.5-72.5°N, 72.5-57.5°N, 57.5-37.5°N, 37.5-17.5°N, 87.5-17.5°N).

A comparison of the primary mean annual temperature anomalies obtained using data in the new archives and averaged for the mentioned latitude zones with the similar values obtained in carrying out study [1] does not reveal the presence of significant random errors for any of the latitude zones. The differences between the data in [1] and the data in the archives of the All-Union Scientific Research Institute of Hydrometeorological Information-World Data Center for the 1960's and 1970's, for the zone 87.5-17.5°N in general reveal a systematic negative error for the second half of the 1960's, being of the order of -0.05°C. These differences from 1960 through 1975 were equal to 0.00, 0.00, 0.02, -0.03, -0.03, -0.05, -0.03, -0.06, -0.07, 0.03, 0.00, -0.01, 0.01, -0.01, 0.00 respectively. The new data for the period 1961-1969 are more precise. In the remaining cases the nonclosures in the comparison of data are not great and the materials can be considered equally precise.

The resulting time series of mean monthly air temperature anomalies are not uniform because the anomalies for the period 1891-1940 and 1961-1969 were computed relative to the means for the period from 1881 through 1935 (40); the anomalies for the period from 1941 through 1960 -- relative to the means for the period from 1881 through 1960, and the anomalies for the period from 1970 through 1978 -- relative to the means for the period from 1931 through 1960 [8, 12].

Now we will discuss in greater detail the principles for restoring uniformity of the considered time series.

In [1] Borzenkova, et al. developed a system of corrections making it possible to eliminate the nonuniformity of series of air temperature anomalies when using only the primary values of the anomalies without making use of information on the "norms." The corresponding corrections for the mean monthly anomalies, averaged by latitude circles, were published in [4] also for anomalies of the mean annual surface temperature of the principal latitude zones of the northern hemisphere are given in Table 1. This system of corrections is denoted by the letter A.

In order to apply the mentioned correction method to the data in the archives of the All-Union Scientific Research Institute of Hydrometeorological Information-World Data Center it is necessary to take into account the circumstance that the data in this archives begin in 1891, not in 1881, as the data in [1].

This circumstance is no obstacle to obtaining a similar system of corrections for the data in the archives of the All-Union Scientific Research Institute of Hydrometeorological Information-World Data Center if as an additional condition use is made of the assumption that the sum of the primary air temperature anomalies during the period from 1881 through 1935 or 1940 is equal to zero. This condition is almost obvious since the primary temperature anomalies for this period of time were computed relative to the "norms" for the period 1881-1935(40); some uncertainty in the end of the period makes this condition approximate.

In order to ensure a comparability of these results to the materials in [1], in correcting the data we will reduce them to the "norms" for the period 1881-1975.

This system of corrections will be denoted by the letter B.

A third independent system of corrections, C, can be obtained using information on the "norms" for air temperature present in the archives of the All-Union Scientific Research Institute of Hydrometeorological Information-World Data Center.

Earlier, in [4], it was postulated that corrections of the C type, evaluated using the air temperature "norms" and relating to different intervals of years, have a lesser accuracy. Computation of these corrections involved reduction of air temperature data to sea level, with plotting, drafting of maps and visual interpolation of data at the points of intersection of a regular grid. In computing the differences in the "norms" for the two periods, that is, the corrections of interest to us, we obtain small differences of high values, whose random errors are summed. These differences, even if they are caused by errors entering into the corrections, are introduced into the series of observations, impairing their uniformity. However, having a lesser accuracy (in comparison with the systems of corrections A and B) for regions well covered with observational data, the system of corrections C can be less reliable for poorly covered regions, especially for the areas of the world ocean.

Accordingly, henceforth in the representation and analysis of data we will use the system of corrections B for the points of grid intersection situated over the continents and the system of corrections C for the remaining points of grid intersection.

Such a combined system of corrections will be denoted by the letter D.

All the mentioned systems of corrections for correction of the time series for mean annual air temperature at the surface in the northern hemisphere are presented in Table 1.

The closeness of the corrections relating to systems A and B must not cause surprise because these systems are virtually identical. The differences between the systems of corrections A and B, on the one hand, and C, on the other, are especially significant for the latitude zones 72.5-57.5° and 57.5-37.5°N. These differences can be considered as measures of the inhomogeneity of the series after their correction. For the mean annual surface temperature in the extra-equatorial part of the North Atlantic (87.5-17.5° N) the uncertainty in the evaluation of the jumplike disruption of homogeneity of the series is 0.03-0.04°C between 1940 and 1941, less than 0.05°C between 1960 and 1961 and a value of about 0.1°C between 1969 and 1970.

The problem of the forms of representation of the empirical characteristics of the secular variation of climatic parameters was examined at a special conference of the representatives of three institutes: USSR Hydrometeorological Institute, All-Union Scientific Research Institute of Hydrometeorological Information-World Data Center and State Hydrological Institute in February 1979. The conference adopted the following recommendations:

1. In the representation of the secular variation of climatic parameters it is considered necessary that the following be given in tabular or graphic form:

a) actual values of the parameters for individual years;
b) results of five-year moving averaging;
c) evaluations of linear trends obtained by the least squares method for 10-, 20- and 30-year periods for intervals of years ending with the last year of a time series which is a multiple of 5 and also during the last decade and the entire observation period.

2. The following should be used as evaluations of trend:

a) the angle coefficient of the linear trend;
b) the relative contribution of the linear trend to the total dispersion for the considered period.

Table 1

Systems of Corrections (°C) for Restoring the Homogeneity of Time Series of Anomalies of the Mean Annual Air Temperature at the Surface in Various Latitude Zones of the Northern Hemisphere

Северная широта, град A	1881—1940, 1961—1969				1941—1960				1970—1978			
	A	B	C	D	A	B	C	D	A	B	C	D
87,5—72,5	0,04	−0,15	−0,14	−0,15	0,05	0,03	0,07	0,09	0,63	0,55	0,56	0,41
72,5—57,5	−0,09	−0,14	−0,08	−0,12	0,01	0,02	0,02	0,02	0,38	0,38	0,21	0,31
57,5—37,5	−0,09	−0,10	−0,02	−0,07	−0,02	−0,02	−0,01	−0,02	0,16	0,16	0,02	0,07
37,5—17,5	−0,07	−0,08	−0,01	−0,04	0,00	−0,01	−0,01	−0,01	0,12	0,12	0,14	0,11
87,5—17,5	−0,07	−0,10	−0,03	−0,07	0,00	0,00	0,00	0,00	0,21	0,2	0,14	0,15

KEY:
A) North latitude, degrees

Table 2

Deviations of Mean Annual Air Temperature at Surface in Extra-Equatorial Part of the Northern Hemisphere (Zone 87.5-17.5°N) from Mean During Period 1881-1975

Годы (A)	0	1	2	3	4	5	6	7	8	9
1880		−0,14	−0,28	−0,21	−0,50	−0,50	−0,42	−0,42	−0,30	−0,08
1890	−0,15	−0,27	−0,28	−0,31	−0,29	−0,18	−0,16	−0,05	−0,18	−0,03
1900	0,03	0,03	−0,30	−0,28	−0,28	−0,32	−0,08	−0,32	−0,16	−0,19
1910	−0,27	−0,06	−0,26	−0,21	0,00	0,04	−0,12	−0,32	−0,23	−0,10
1920	−0,01	0,17	0,05	0,12	0,09	0,16	0,24	0,16	0,23	−0,09
1930	0,27	0,29	0,26	−0,11	0,30	0,15	0,17	0,39	0,53	0,33
1940	0,32	0,17	0,26	0,35	0,33	0,07	0,18	0,29	0,20	0,16
1950	0,05	0,22	0,21	0,41	0,12	0,09	−0,12	0,11	0,22	0,24
1960	0,22	0,15	0,16	0,13	−0,19	−0,11	−0,07	0,15	−0,05	−0,19
1970	0,15	−0,01	−0,29	0,17	0,11	0,14	−0,12	0,17	0,08	

KEY:
A) Years

In accordance with these recommendations, in Fig. 1 for the five considered latitude zones of the northern hemisphere we have represented the secular variation of anomalies of the mean annual air temperature at the surface. In addition, data on the mean annual air temperature at the surface for the greater part of the northern hemisphere (zone 87.5-17.5°N) are given in Table 2. In Fig. 1 and Table 2 the materials from the archives of the All-Union Scientific Research Institute of Hydrometeorological Information-World Data Center, relating to the period 1891-1978, are supplemented by data for the periods 1881-1890 from [1].

Evaluations of the linear trend parameters for the mean annual surface temperature for the principal latitude zones of the northern hemisphere are presented in Table 3. We use m to denote the number of years in time intervals for which the angle coefficient β of the linear trend in °C/10 years is evaluated, $\bar{t}$°C is the mean value in this interval and α % is the relative contribution of the linear trend in the dispersion of the series in the particular interval. The evaluation algorithm was described in detail in [10].

On the left side of Table 3 we have given the recommended evaluations and on the right side -- one of the possible methods for piecewise-linear approximation of secular variation of air temperature at the surface in the northern hemisphere.

An analysis of the evaluations for the extra-equatorial part of the northern hemisphere (87.5-17.5°N) shows that on the average for the period from 1891 through 1978 about 20% of the dispersion of the series was attributable to the positive trend.

After a more detailed examination of this series it can be concluded that:

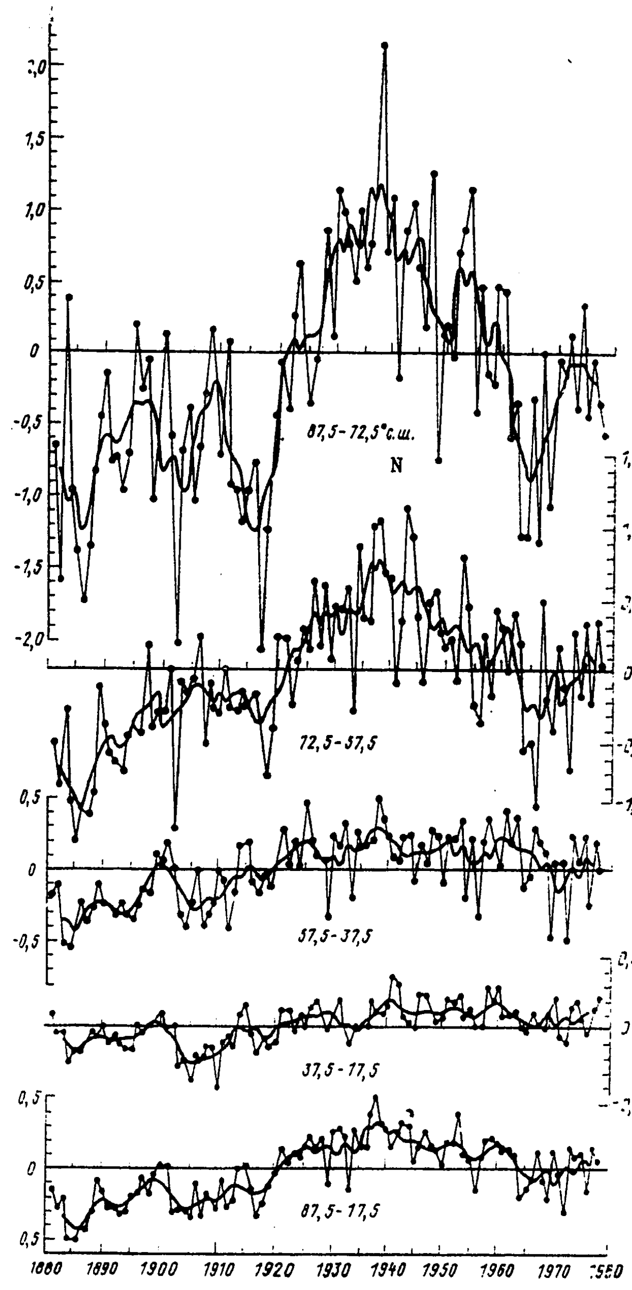

Fig. 1. Secular variation of annual and five-year mean air temperature anomalies (relative to the "norm" for 1881-1975) for different latitude zones in the northern hemisphere. Correction system D.

Table 3

Evaluations of Linear Trend Parameters for Mean Annual Air Temperature at Surface in the Main Latitude Zones of the Northern Hemisphere for Different Parts of the Time Series

Северная широта, град (A)	Параметры (B)	1891—1978	1946—1975	1956—1975	1966—1975	1969—1978	1891—1940	1940—1964	1964—1978
	m	88	30	20	10	10	50	25	15
87,5—17,5	β	0,039	0,086	−0,057	0,15	0,21	0,125	−0,087	0,15
	$\bar{r}$	0,04	0,10	0,05	0,01	0,02	0,02	0,18	−0,01
	α	22	22	4	7	14	62	27	19
87,5—72,5	β	0,070	−0,307	−0,103	0,94	−0,24	0,390	−0,564	0,49
	$\bar{r}$	−0,08	−0,08	−0,29	−0,32	−0,18	−0,14	0,22	−0,38
	α	5	16	1	29	7	45	34	21
72,5—57,5	β	0,053	−0,170	−0,075	0,51	0,46	0,248	−0,241	0,47
	$\bar{r}$	0,05	0,05	−0,06	−0,12	−0,04	−0,01	0,27	−0,14
	α	9	13	1	11	16	58	21	24
57,5—37,5	β	0,037	−0,056	−0,073	−0,08	0,35	0,114	0,009	0,02
	$\bar{r}$	0,04	0,12	0,09	0,05	−0,02	−0,01	0,16	0,02
	α	15	4	3	1	15	44	0	0
37,5—17,5	β	0,031	−0,048	−0,038	0,04	0,05	0,050	−0,031	0,08
	$\bar{r}$	0,04	0,12	0,09	0,07	0,09	−0,02	0,15	0,07
	α	28	16	4	2	2	26	5	11

KEY:

A) North latitude, degrees
B) Parameters

-- by the 1940's the intensive warming of the northern hemisphere which had begun at the end of the preceding century had ended;
-- this warming was replaced by a cooling process which began in the 1940's and which ended in the 1960's;
-- since the mid-1960's the changes in air temperature at the surface in the northern hemisphere have been characterized by a positive trend of 0.1-0.2°C/10 years.

By combining the warming of the northern hemisphere during the last 10-15 years with the preceding cooling, it is easy to arrive at the conclusion that in the present period there is a continuation of the cooling which began in the 1940's. In actuality, the evaluations of the linear trend are negative for the periods 1946-1975 and 1956-1975.

In this connection it must be noted that the authors evaluate the trends only as a diagnostic procedure. In their opinion, the basis for any global climatic predictions must not be a formal extrapolation of empirical data, but an analysis of the physical mechanisms of climatic change.

By examining similar evaluations for the narrower latitude zones 87.5-72.5, 72.5-57.5, 57.5-37.5, 37.5-17.5°N we discover that:
-- the trend parameter β has the same sign for almost all the mentioned latitude zones;
-- in absolute value the β evaluations reveal a clearly expressed tendency to an increase from the low to the high latitudes.

Three evaluations of the parameter do not fit into these patterns. Two of them for the intervals 1966-1975 and 1940-1964 for the zone 57.5-37.5°N are not statistically significant because the linear trend for these periods does not describe any appreciable part of the variability of the mean annual air temperature at the surface. The third evaluation, relating to the period 1969-1978 for the zone 87.5-72.5°N for this same reason has a low statistical significance. However, if we compare this period with the partially overlapping period 1966-1975 we discover an increase in the mean air temperature values during these time intervals. It can be surmised that a 10-year period is too short for a reliable determination of the linear trend sign for air temperature in the high latitudes.

In order to compare data published by different authors we will examine evaluations of the trend parameter β for the mean annual air temperature at the surface in the northern hemisphere for one and the same period 1964-1975 (see Table 4).

The first evaluation, based on the materials published in a study by I. I. Borzenkova, et al. [1], was obtained by M. I. Budyko and K. Ya. Vinnikov [2] and was 0.31°C/10 years. The use of the refined primary data makes it possible to conclude that the real value of this parameter falls between 0.28 and 0.15°C/year and is evidently close to 0.19°C/10 years.

The use of data published in a study by Angell and Korshover [15] makes it possible for mean annual conditions to obtain the evaluation β = 0.28°C/10 years, close to the first of the cited evaluations. The data of Yamamoto, et al., presented in a study by Kukla, et al. [20], give the evaluation β = 0.12°C/10 years. Finally, the materials published by Barnett give the least evaluation β = 0.07°C/10 years.

Evaluations of Linear Trend Parameter for Mean Annual Air Temperature at the Surface in the Northern Hemisphere for the Period 1964-1975 According to Data of Different Publications

Data source	North latitude, °	°C/10 years
Borzenkova, et al. [1]	17.5-87.5	0.31
Angell and Korshover [15]	0-90	0.28
Kukla, et al. [20]	0-90	0.12
Barnett [16]	15-65	0.07
This study		
System of corrections:		
B	17.5-87.5	0.28
C	same	0.15
D	same	0.19

All the evaluations cited above coincide in sign and their quantitative differences can be attributed rather easily to the difference in the latitude zones to which they belong. For example, the data of Barnett [16] do not include the region of the high latitudes to the north of 65°N, where the changes in air temperature at the surface are several times greater than in the low latitudes, as a result of which the β evaluation obtained using his data are the lowest. The data of Angell and Korshover [15], relating to surface temperature, are much inferior to the accuracy of the data of Yamamoto, et al., cited in the study by Kukla, et al. [20]; the latter evidently give the best evaluation for the entire northern hemisphere. But the evaluation β = 0.12°C/10 years, according to the data of Yamamoto, et al. for the entire hemisphere (0-90°N), agrees satisfactorily with the evaluation β = 0.19°C/10 years obtained for the extra-equatorial part of the hemisphere (87.5-17.5°N) according to the data cited in Table 2.

We also note the good correspondence between the materials in Fig. 1, pertaining to the high latitudes of the northern hemisphere, and the data obtained in a study by Walsh [28].

Thus, modern data characterizing modern changes in air temperature at the surface in the northern hemisphere virtually do not contradict one another, and if its changes during the last 10-15 years are considered, it is discovered that during this period there was some warming of the northern hemisphere as a whole, although unambiguous evaluations of the trends for

1966-1978, associated with the cooling beginning in 1975 in the zone of the high latitudes, force one to exhibit care and refrain from categorical conclusions in the interpretation of the presented materials.

Evidently, due to the fact that the period of aerological observations is relatively short and during this entire period there was a rapid improvement of instruments and methods for obtaining information the data in the scientific literature on change in the global characteristics of the thermal regime of the free atmosphere exhibit inadequate agreement. And the differences no longer pertain to interpretation of materials, but the data themselves.

The recent changes in the mean temperature in the lower half of the troposphere, determined from the thickness of the layer between the 500- and 1000-mb surfaces, are presented in the studies of Kukla, et al. [20] (materials obtained by Dronia), Painting [25] and Harley [19].

An analysis of the data presented by Dronia in [20] show that the mean temperature of the lower half of the troposphere in the zone 35-90°N is decreasing rapidly, beginning from the end of the 1950's, but in the zone to the north of 65°N this decrease has slowed down or completely stopped from the mid-1960's. Dronia does not discover any tendency to a temperature increase.

The data of Painting [25] somewhat contradict the materials of Dronia. The materials presented in [25] show that approximately from the mid-1960's the tendency to a cooling changes to the opposite in the high latitudes of the northern hemisphere (75, 80, 85°N). In the lower latitudes (50-60°N) the cooling, beginning from the end of the 1950's, was continuing to the mid-1970's.

Similar materials, relating to the extra-equatorial part of the northern hemisphere for the period from 1949 through 1976, are presented in a study by Harley [19]. These data show that on the average for the zone 25-85°N the very intensive decrease in temperature in the lower half of the troposphere, transpiring in the first half of the 1960's, in the mid-1960's was replaced by a warming. This warming is clearly traced in the data for the latitude zone 25-40°N. On the other hand, in the high latitudes (70-85°N) Harley's data do not indicate any definite tendency to a change in the temperature of the lower half of the troposphere for the period 1965-1976.

The contradictions in the data of Dronia, Painting and Harley cannot be resolved without a detailed analysis of the measurement data used by the authors and the methods used in their processing.

As a more complete characteristic of the thermal regime of the atmosphere in a hemisphere Starr and Oort [27] introduced a new parameter -- mean atmospheric temperature weighted by mass. In studies [27, 24] this temperature was computed for the periods 1958-1963 and 1968-1973. The first of these periods was characterized by a rapid decrease in the temperature of the entire northern hemisphere atmosphere -- by 0.6°C in 5 years. During the second period the changes in temperature had a wavelike character in the absence of an apparent linear trend.

Later Angell and Korshover [15] studied the change in mean temperature of the troposphere (the part of the atmosphere in the layer from the earth's surface to the 100-mb surface) during the period 1958-1977 and drew the conclusion that in the extratropical part of the northern hemisphere the cooling noted in the first half of the period is continuing to the present time, although on a somewhat lesser scale.

Everything said above is evidence that at the present time the available evaluations of change in air temperature at the surface in the northern hemisphere are more reliable in comparison with the evaluations of change in the thermal regime of the free atmosphere.

Evolution of the Ice Cover in the Arctic Ocean in the Modern Period

Arctic sea ice is one of the most important links in the global climatic system.

Recently steps have been taken in the direction of generalizing available material on the distribution of ice in the Arctic Ocean for the purpose of determining total ice content and analyzing its variability [6, 7]. As a result it was established that from the beginning of the 1940's and to the mid-1960's there was an increase in this ice content, amounting to 0.6 million square kilometers. Thereafter its decrease began and parallel with this process there was an increase in atmospheric temperature which some authors have been inclined to regard as the beginning of a long epoch of warming, whereas others regard it as disruption of a normal cooling regime.

The data on the basis of which conclusions were drawn concerning the nature of the changes in the area of the arctic ice cover during the last 30 years apply entirely to the three summer months: July, August and September. Due to the fact that observations of the distribution of ice in a number of regions in the Arctic Ocean began many years after culmination of the warming, and it is important to evaluate the change in the area of the ice cover precisely from that moment, the research region was limited. This region, with an area of 10.9 million square kilometers (about 74% of the area of the entire ocean), included the Arctic basin proper and the following seas: Greenland, Norwegian, Barents, Kara, Laptev, East Siberian and Chukchi. These circumstances, naturally, could not but cause questions concerning the validity of applying the conclusions drawn in general to individual years and the entire Arctic Ocean.

Now we will make an attempt at generalizing and analyzing the available data on the development of the ice cover during the course of the entire annual cycle and thus answer the first part of the question.

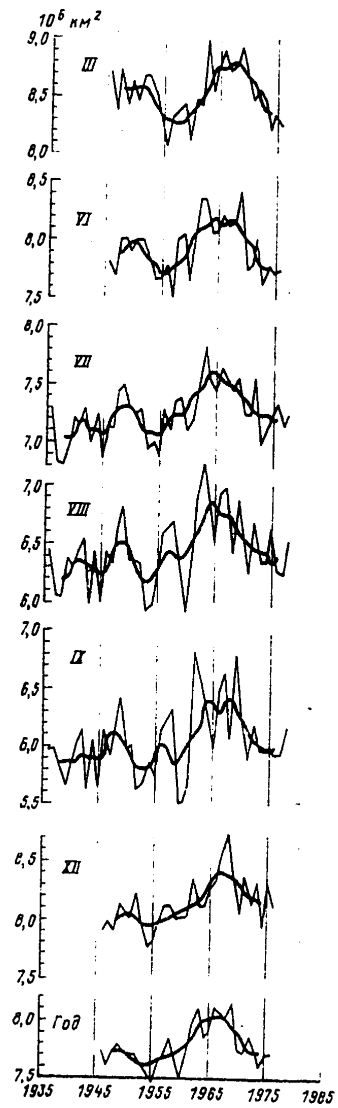

Fig. 2. Changes in area of ice cover of Arctic Ocean in individual months and as average for year. Thick curves -- result of five-year moving averaging.

The basis for the investigation was primarily data from ice aerial reconnaissance surveys made regularly in the marginal zone of the ocean, beginning in 1946. Unfortunately, the evaluation of the accuracy of these data involved great difficulties and for this reason it was not done. Nevertheless, they undoubtedly must be regarded as sufficiently reliable for judging the trends in variations of ice area in the modern period. This is particularly correct for the warm half of the year when the geographical position of the boundary of the sea ice is surveyed with great detail several times a month. Data on the distribution of ice in the Greenland Sea were taken from a study by A. A. Kirillov and M. S. Khromtsova [9]. The authors used all available data characterizing the state of ice in this sea contained in the Danish Ice Yearbooks (period 1946-1962), in the journal MARINE OBSERVER (period 1959-1968), and finally, on British maps of ice conditions in the North Atlantic, the basis for which was observations from artificial earth satellites (period 1966-1977). In giving a general evaluation of the data used in this study it must be said that their reliability within the year increases from winter to summer, but within the investigated period -- from its beginning to the end.

Figure 2 shows the long-term variation of area of the ice cover in the Arctic Ocean during the course of March, June, July, August, September, December and as an average for the year. Each of the cited monthly curves is characteristic for its season, but taken together they give a full idea concerning the intra-annual characteristics of long-term changes.

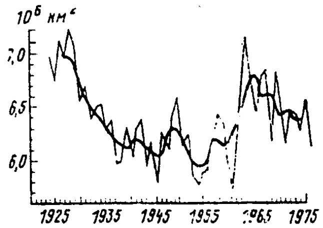

Fig. 3. Change in area of ice cover in Arctic Ocean in second half of August. For annotations see Fig. 2.

We note that the nature of the long-term changes in area of the ice cover within the year for the most part remains constant. After a period of lessened ice content in the mid-1950's the ice area began to increase and in 1967 attained maximum values during the entire investigated period. In the late 1960's the area of the ice cover began to decrease. This process also continued in the 1970's. As a result, the extent of the ice cover in the Arctic Ocean approached close to that which was observed prior to its expansion.

The conclusions drawn by V. Yu. Vise [3] concerning the scales of change in the area of occurrence of arctic ice during the warming epoch were based, as is well known, on data on the ice content of arctic seas, including an earlier period 1924-1939. In discussing these data, the author mentioned their low quality and the extremely approximate nature of the evaluations obtained using them. Nevertheless, it would be incorrect today, under conditions of increasingly recognized need for studying prolonged trends in the development of natural conditions in the past, to ignore these data completely, without making use of them in the analysis. Despite shortcomings, it must be admitted that they give a true idea concerning the principal tendencies in development of the ice cover in the 1920's and 1930's. This is confirmed by numerous types of evidence concerning the behavior of other environmental elements during this period. It is therefore desirable to supplement the data of V. Yu. Vize and obtain a picture of continuous evolution of the ice cover in the course of the last 50 years. This picture is presented in Fig. 3.

It can be seen that the area of the ice cover in the course of a half-century has experienced considerable changes. The curve of five-year moving averages from the end of the 1920's drops steeply downward; in the 1940's and in the first half of the 1950's it does not exhibit any significant tendencies and then moves upward. As indicated by V. Yu. Vize, the reduction in the area of the ice cover in the first stage was about 1 million square kilometers. An expansion of the ice cover in the 1950's and 1960's resulted in an increase in the area by 0.8 million square kilometers, that is, almost reduced to zero the preceding improvement in ice conditions. In the years which followed the area of the ice again began to decrease and by the middle of the 1970's had decreased by 0.4 million square kilometers in comparison with the maximum in the 1960's.

It is interesting to know whether the curve reproduced in Fig. 3 reflects the nature of the change in the mean annual area of the ice cover in the Arctic Ocean or whether it is correct only for August. A positive answer to this question would make it possible to judge the nature of the long-term changes in the mean annual area of the ice cover on the basis of regular observations in one of the summer months.

For this purpose we evaluated the correlation between the mean annual and August ice areas in the investigated region. The result was entirely satisfactory: the correlation coefficient was 0.82. The presence of correlation with such a coefficient can serve as an adequate basis for drawing the conclusion that the curve shown in Fig. 3 correctly reflects the main characteristics of the long-term variability of the mean annual area of the ice cover. Taking this into account, an attempt was made to determine the mean annual extent of the ice cover in the mid-1920's on the basis of the August ice content. This extent was close to 8.2 million square kilometers. Figure 3 shows that by the mid-1950's the extent had decreased to 7.6 million square kilometers. It must also be noted that the correlation coefficients characterizing the closeness of the correlation between the mean annual area of the ice and its area in other months were approximately the same as for August. This makes it possible, with a greater assurance than before, to apply the conclusions drawn on the basis of seasonal or monthly data concerning prolonged tendencies in the development of the ice cover to the entire year period.

The striving to examine the sea ice cover as a whole for the Arctic Ocean or for the entire hemisphere inevitably results in a loss of part of the valuable information: the volume of the useful material will be determined by the length of the shortest series of observations taken into account in reckoning total ice content. Nevertheless, comparing the data presented above on the change in the area of polar sea ice in the Arctic Ocean, the preliminary estimates of the total quantity of polar sea ice in the northern hemisphere made at the Arctic and Antarctic Scientific Research Institute and similar data published by Sanderson [26] and Walsh [29], we discover that all these materials indicate that a general characteristic of the development of the arctic ice cover during recent years was its contraction.

BIBLIOGRAPHY

1. Borzenkova, I. I., Vinnikov, K. Ya., Spirina, L. P., Stekhnovskiy, D. I., "Change in Air Temperature in the Northern Hemisphere During the Period 1881-1975," METEOROLOGIYA I GIDROLOGIYA (Meteorology and Hydrology), No 7, 1976.

2. Budyko, M. I., Vinnikov, K. Ya., "Global Warming," METEOROLOGIYA I GIDROLOGIYA, No 7, 1976.

3. Vize, V. B., OSNOVY DOLGOSROCHNYKH LEDOVYKH PROGNOZOV DLYA ARKTICHESKIKH MOREY (Principles of Long-Range Ice Forecasts for Arctic Seas), Moscow, Izd-vo Glavsevmorputi, 1944.

4. Vinnikov, K. Ya., "On the Problem of the Method for Obtaining and Interpreting Data on Changes in Air Surface Temperature in the Northern Hemisphere During the Period 1881-1975," METEOROLOGIYA I GIDROLOGIYA, No 9, 1977.

5. Gruza, G. V., Ran'kova, E. Ya., DANNYYE O STRUKTURE I IZMENCHIVOSTI KLIMATA. TEMPERATURA VOZDUKHA NA UROVNE MORYA. SEVERNOYE POLUSHARIYE (Data on the Structure and Variability of Climate. Air Temperature at Sea Level. Northern Hemisphere), Obninsk, 1979.

6. Zakharov, V. F., "Cooling of the Arctic and Ice Cover of Arctic Seas," TRUDY AANII (Transactions of the Arctic and Antarctic Scientific Research Institute), Vol 337, 1976.

7. Zakharov, V. F., Strokina, L. A., "Recent Changes of the Ice Cover of the Arctic Ocean," METEOROLOGIYA I GIDROLOGIYA, No 7, 1978.

8. KARTY OTKLONENIY TEMPERATURY VOZDUKHA OT MNOGOLETNYKH SREDNIKH SEVERNOGO POLUSHARIYA (Maps of Deviations of Air Temperature from Long-Term Means for the Northern Hemisphere), Nos 1-4, GGO, 1960-1967.

9. Kirillov, A. A., Khromtsova, M. S., "Long-Term Variability of the Ice Content of the Greenland Sea and a Method for Its Prediction," TRUDY AANII, Vol 303, 1971.

10. Polyak, I. I., METODY ANALIZA SLUCHAYNYKH PROTSESSOV I POLEY V KLIMATOLOGII (Methods for Analysis of Random Processes and Fields in Climatology), Leningrad, Gidrometeoizdat, 1979.

11. Rubinshteyn, Ye. S., STRUKTURA KOLEBANIY TEMPERATURY VOZDUKHA NA SEVERNOM POLUSHARII (Structure of Variations of Air Temperature in the Northern Hemisphere), Part I, 1973, Part II, 1977, Leningrad, Gidrometeoizdat.

12. SINOPTICHESKIY BYULLETEN'. SEVERNOYE POLUSHARIYE (Synoptic Bulletin. Northern Hemisphere), 1961-1978, Gidromettsentr SSSR-VNIIGMI-MTsD, Obninsk.

13. Spirina, L. P., "Secular Variation of Mean Air Temperature in the Northern Hemisphere," METEOROLOGIYA I GIDROLOGIYA, No 1, 1962.

14. Angell, J. K., Korshover, J., "Estimate of the Global Change in Temperature, Surface to 100 mb, Between 1958 and 1975," MON. WEATHER REV., Vol 105, No 4, 1977.

15. Angell, J. K., Korshover, J., "Global Temperature Variation, Surface-100 mb: an Update Into 1977," MON. WEATHER REV., Vol 106, No 6, 1978.

16. Barnett, T. P., "Estimating Variability of Surface Air Temperature in the Northern Hemisphere," MON. WEATHER. REV., Vol 106, No 9, 1978.

17. Brinkman, W. A. R., "Surface Temperature Trend for the Northern Hemisphere Updated," QUATERN. RES., Vol 6, 1976.

18. Callendar, G. S., "Temperature Fluctuations and Trends Over the Earth," QUART. J. ROY. METEOROL. SOC., Vol 87, No 371, 1961.

19. Harley, W. S., "Trends and Variations of Mean Temperature in the Lower Troposphere," MON. WEATHER REV., Vol 106, No 3, 1978.

20. Kukla, G. J., Angell, J. K., Korshover, J., Dronia, H., Hoshiai, M., Namias, J., Rodewald, M., Yamamoto, R., Iwashima, T., "New Data on Climatic Trends," NATURE, Vol 270, No 5638, 1977.

21. Landsberg, H. E., Groveman, B. S., Hakkarinen, I. M., "A Simple Method for Approximating the Annual Temperature of the Northern Hemisphere," GEOPHYS. RES. LETTERS, Vol 5, No 6, 1978.

22. Mitchell, J. M., "Recent Secular Changes of Global Temperature," ANNALS OF THE NEW YORK ACADEMY OF SCI., Vol 95, Article 1, 1961.

23. Mitchell, J. M., "On the Worldwide Pattern of Secular Temperature Change. Changes of Climate," ARID ZONE RESEARCH, XX, UNESCO, Paris, 1963.

24. Oort, A. H., "Structure of Atmospheric Variability on a Global Scale," SYMPOSIUM ON THE STRUCTURE OF THE PRESENT CLIMATE AND ITS VARIABILITY, Leningrad, USSR, 1977.

25. Painting, D. J., "A Study of Some Aspects of the Climate of the Northern Hemisphere in Recent Years," METEOROL. OFFICE SCIENTIFIC PAPER, No 35, London, Her Majesty's Stationery Office, 1977.

26. Sanderson, R. M., "Changes in the Area of Arctic Sea Ice 1966 to 1974," METEOROL. MAGAZ., Vol 104, No 1240, 1975.

27. Starr, V. P., Oort, A. H., "Five-Year Climatic Trend for the Northern Hemisphere," NATURE, Vol 242, No 5396, 1973.

28. Walsh, J. E., "The Incorporation of Ice Station Data into a Study of Recent Arctic Temperature Fluctuations," MON. WEATHER REV., Vol 105, No 12, 1977.

29. Walsh, J. E., Johnson, C. M., "An Analysis of Arctic Sea Ice Fluctuations 1953-1977," J. PHYS. OCEANOGR., Vol 9, No 3, 1979.

30. Willett, H. C., "On the Present Climatic Variation. Centenary Proceedings. Roy. Meteorol. Soc., 1950.

31. Willett, H. C., "Do Recent Climatic Fluctuations Portend an Imminent Ice Age?" GEOPHYS. INT., Vol 14, No 4, 1974.

32. Yamamoto, R., Iwashima, T., Hoshiai, M., "Change of the Surface Air Temperature Averaged Over the Northern Hemisphere and Large Volcanic Eruptions During the Years 1951-1952," J. METEOROL. SOC. JAPAN, Vol 53, No 6, 1975.

UDC 551.509.3

SOME RESULTS OF JOINT SOVIET-POLISH INVESTIGATIONS IN THE FIELD OF NUMERICAL SHORT-RANGE FORECASTING OF METEOROLOGICAL ELEMENTS

Moscow METEOROLOGIYA I GIDROLOGIYA in Russian No 6, Jun 80 pp 18-26

[Article by Candidates of Physical and Mathematical Sciences B. M. Il'in and L. V. Rukhovets, Doctor J. Parfiniewicz, G. A. Kobyshev and J. Nemec, Main Geophysical Observatory and Institute of Meteorology and Water Management Polish People's Republic, submitted for publication 30 October 1979]

[Text]

Abstract: A study was made of problems relating to improvement of a model of short-range numerical forecasting used by the Main Geophysical Observatory. These improvements are a result of joint investigations carried out at the Main Geophysical Observatory and at the Institute of Meteorology and Water Management by way of bilateral cooperation between the USSR State Committee on Hydrometeorology and the Hydrometeorological Service of the Polish People's Republic. The article gives a brief description of a new three-parameter model. Test results indicated that the success of pressure field predictions for 24 and 48 hours under the new model is substantially higher than when using the Main Geophysical Observatory model.

Investigations carried out at the present time within the framework of direct cooperation between the USSR State Committee on Hydrometeorology and the Hydrometeorological Service of the Polish People's Republic, in addition to other work, provide for joint work in the field of numerical short-range weather forecasting. Some of this work is related to improvement of the short-range forecasting model developed at the Main Geophysical Observatory, employed in the routine practice of some prognostic centers of the USSR State Committee on Hydrometeorology. This same model is the operational model used by the forecasting service of the Polish People's Republic.

Without dwelling in detail on a description of the Main Geophysical Observatory model [1], we will note only its principal features. Two fundamental ideas were used in the model. The first of these (belonging to M. I. Yudin) is use of the base of eigenfunctions of a linearized differential operator of a prognostic equation jointly with the base of empirical orthogonal functions. This idea served as the basis for the quasigeostrophic forecasting model with few parameters developed in [6]. Recently this same idea was used in [5] in developing a model with few parameters in full equations.

Beginning in 1964 a model with few parameters has been used in the routine practice of the Northwestern Administration of the Hydrometeorological Service ([3]). The second idea (belonging to I. Z. Lutfulin), serving as the basis for the Main Geophysical Observatory model, is the use of data on the three-hour surface pressure trends for the purpose of refining the surface field forecast. This idea was used in [2] for creating first a two-level model of a forecast and then for forecasting the surface field in a model with few parameters. Such a combined model already for more than 10 years has been used in the operational practice of the Northwestern Administration of the Hydrometeorological Service, and in recent years, after some improvements made by A. B. Simanovskiy, this model has been included in the BTGMTs (Baltic Territorial Hydrometeorological Center), Murmansk and some other administrations of the State Committee on Hydrometeorology. Since 1974 the Main Geophysical Observatory model has been used in the operational practice of the Institute of Meteorology and Water Management of the Polish People's Republic.

In 1978 the Central Asian Regional Scientific Research Hydrometeorological Institute carried out comparative tests of a number of models used in the operational practice of the State Committee on Hydrometeorology [4]. These tests indicated that the Main Geophysical Observatory model gives better results than other models in the prediction of the surface field. With respect to the quality of forecasts of high-altitude charts, here it is difficult to give preference to any one model; several models have virtually identical evaluations for the probable success of forecasts. At the same time, the Main Geophysical Observatory model is extremely economical both with respect to computation time and with respect to the volume of the necessary computer memory. This is attributable to the fact that the Main Geophysical Observatory model involves the use of two parameters and for computation of the predicted fields at six levels in the atmosphere it is necessary to have approximately an equal memory and computation time as in a similar two-level model. Accordingly, the Main Geophysical Observatory model can be used at forecasting centers not having high-capacity electronic computers. In particular, it is easy to use with the M-220 and Minsk-32 electronic computers.

However, for centers having higher-capacity electronic computers (such as the BESM-6) the economy factor is no longer so significant. However, the use of only two parameters for the purpose of economy is naturally reflected in the accuracy of the resulting forecasts. Accordingly, in the joint investigations made at the Main Geophysical Observatory and the Institute of Meteorology and Water Management specialists have developed a three-parameter model [8, 9]. In this model a third parameter has been added; like the other two it is an eigenfunction (vector) of a linearized operator, differentiated in the vertical coordinate, entering into the prognostic equation. In addition, as in the two-parameter Main Geophysical Observatory model, the right-hand sides of the prognostic equation, expressing the nonlinear terms, are represented by empirical orthogonal functions. The changeover from the eigenfunctions of the differential operator to empirical orthogonal functions is based on the least squares method with use of information on the vertical statistical structure. It can be assumed that this changeover stage introduces definite errors into the results. Accordingly, it was decided that in the model no use be made of the base of empirical orthogonal functions and that a model would be formulated which makes use only of the eigenfunctions of the mentioned differential operator.

As the initial equations of the model we will use the equations for vorticity and heat influx in quasigeostrophic and adiabatic approximations:

$$\nabla^2 q + lA_{\Omega} = l^2 \frac{\partial \omega}{\partial \zeta}, \tag{1}$$

$$\zeta \frac{\partial q}{\partial \zeta} + RA_T + \frac{d^2 l}{\zeta} \omega = 0. \tag{2}$$

Here Φ is geopotential,

$$\zeta = \frac{p}{p_0},$$

p is pressure, p_0 is standard pressure at the earth,

$$\omega = \frac{dq}{dt}, \qquad q = \frac{d\zeta}{dt},$$

$l = 2\Omega \sin\varphi$ is the Coriolis parameter,

$$d^2 = \frac{(\gamma_a - \gamma) R^2 T}{g l^2}$$

is the statistical stability parameter, being a function only of the vertical coordinate, T is temperature, R is the gas constant,

$$A_{\Omega} = \frac{1}{l^2} J\left(\Phi, \Delta\Phi + \frac{l^2}{2}\right); \quad A_T = \frac{1}{Rl} J\left(\Phi, \zeta \frac{\partial \Phi}{\partial \zeta}\right);$$

$$\nabla^2 = \Delta = \frac{\partial^2}{\partial x^2} + \frac{\partial^2}{\partial y^2}; \quad J(A, B) = \frac{\partial A}{\partial x} \frac{\partial B}{\partial y} - \frac{\partial B}{\partial x} \frac{\partial A}{\partial y}.$$

The vertical boundary conditions are:

$$\omega = 0 \quad \text{when} \quad \zeta = 0, \tag{3}$$

$$\omega = \frac{p}{p_0} q - \frac{g \rho}{p_0} w_{\text{error}} \quad \text{when} \quad \eta = 1 - \delta, \tag{4}$$

where ρ is air density, δ is the thickness of the boundary layer, w_{error} is the vertical velocity at the upper boundary of the boundary layer.

After replacement of the vertical derivatives by finite differences in a system of equally spaced points of intersection with the interval $\Delta\zeta = 0.075$ ($\zeta_{1/2} = 0$, $\zeta_1 = 0.075$, $\zeta_{1\,1/2} = 0.15$, $\zeta_2 = 0.225$, $\zeta_{2\,1/2} = 0.3$, ..., $\zeta_7 = 0.975$) and use of the Fourier method we obtain a system of equations for the eigenvectors

$$\dot{X}_i = \sum_{k=1}^{7} x_{ik} q_k;$$

$$\tau^2 \dot{X}_i + \lambda_i X_i = F_i \quad (i = 1, 2, \ldots, 7). \tag{5}$$

Here

$$F_i = \sum_{j=1}^{6} \alpha_T^i\left(\zeta_{j+\frac{1}{2}}\right) RA_T\left(\zeta_{j+\frac{1}{2}}\right) + \sum_{j=1}^{7} \alpha_\Omega^i(\zeta_j)\ lA_\Omega(\zeta_j) - \frac{8 g \rho l^2}{0{,}45\, p_0} w_{error}, \tag{6}$$

where

$$\alpha_T^i\left(\zeta_{j+\frac{1}{2}}\right) = -\frac{j}{2 d^2_{j+\frac{1}{2}}} x_{ij} + \frac{j}{2 d^2_{j+\frac{1}{2}}} x_{ij+1} \quad \text{for } j = 1, 2, 3, 4;$$

$$\alpha_T^i(\zeta_{5\,1/2}) = 5\,(x_{i6} - x_{i5} - x_{i7}\,3)/d^2_{5\,1/2};$$

$$\alpha_T^i(\zeta_{6\,1/2}) = 2\,(8\,x_{i7} - 3\,x_{i6} - x_{i7})/d^2_{6\,1/2};$$

$$\alpha_\Omega^i(\zeta_j) = -x_{ij} \quad \text{for } j = 1, 2, \ldots, 7;$$

λ_i are the eigenvalues, x_{ij} are the components of the eigenvectors, represented in Table 1, $d_{j+1/2}$ are the values of the statistical stability parameter in the layer (ζ_j, ζ_{j+1}), computed on the basis of climatic data. These values, taken from [6], are cited in the last column of Table 1.

The values of the coefficients $\alpha_T^i(\zeta_{i+1/2})$ are given in Table 2.

In order to obtain the initial values of the X_i parameters, using the values of the heights of the isobaric surfaces 200, 300, 500, 700, 850 and 1000 mb, we employ information on the statistical structure of the vertical geopotential profiles.

Table 1

Values of Components of Eigenvectors x_{ij}, Eigenvalues λ_i and Statistical Stability Parameter $d^2_{j+1/2}$

Уровень, мб Level, mb	x_{1j}	x_{2j}	x_{3j}	x_{4j}	x_{5j}	x_{6j}	x_{7j}	$d^2_{j+\frac{1}{2}} \times 10^{-12}$ м^{2}
75	0,517	0,846	0,146	−0,016	−0,001	−0,000	−0,000	
225	0,409	−0,094	−0,854	0,334	0,078	−0,014	0,001	1,3
375	0,380	−0,223	−0,111	−0,695	−0,569	0,199	−0,023	0,8
525	0,368	−0,248	0,127	−0,354	0,576	−0,632	0,136	0,5
675	0,358	−0,257	0,264	0,091	0,443	0,712	−0,435	0,6
975	0,125	−0,095	0,129	0,19[illegible]	−0,208	−0,227	−0,461	0,8
$-\lambda_i \cdot 10^{12}$ м$^{-2}$	0,161	0,8[illegible]	5,251	16,217	41,937	80,402	132,585	1,3

Table 2

Values of Coefficients $a^i_T\left(\zeta_{j-\frac{1}{2}}\right) \cdot 10^{12}$ м$^{-2}$

i	$\zeta_{j+\frac{1}{2}}$					
	150	300	450	600	750	900
1	−0,083	−0.072	−0,072	−0.067	−0,067	−0,065
2	−0,723	−0,323	−0,150	−0,060	−0,015	−0,028
3	−0,769	1,858	1,428	0,913	0,450	0.037
4	0,269	−0,573	2,046	2,967	2,079	0,420
5	0,061	−1,618	6,870	−0,887	−0,423	−1,338
6	−0,011	0,533	−4,986	8,960	−0,283	−2,917
7	0,001	−0,060	0,954	−3,807	8,485	−9,932

Table 3 gives the factors for conversion from the geopotential values for the mentioned isobaric surfaces for conversion to the X_i values obtained by the least squares method.

For conversion from the X_i values to the geopotential values at standard levels an inverse matrix is employed. This conversion is accomplished at the end of the forecast for obtaining the prognostic values at standard levels.

On the right-hand sides of (6) the vertical derivatives are represented by finite differences, after which in place of Φ_i, entering under the signs of the horizontal differential operators, we introduce the X_j values with the coefficients cited in Table 3. We will limit ourselves to the first three vectors (corresponding to the three minimum eigenvalues).

Finally, the difference equations in a grid with a 300-km interval, serving for determination of the three parameters $\dot{X}_1$, $\dot{X}_2$, $\dot{X}_3$, assume the following form:

$$
\begin{aligned}
\Delta_4 \dot{X}_1 - 1{,}449 \cdot 10^{-2} \dot{X}_1 = \frac{10^{-9}}{l} (&0{,}206\, J_6 (X_1, X_2) - \\
&-0{,}258\, J_6 (X_1, X_3) + 0{,}634\, J_6 (X_2, X_3) - \\
&-1{,}067\, J_6 (X_1, \Delta_8 X_1) - 0{,}169\, J_6 (X_1, \Delta_8 X_2) + \\
&+0{,}024\, J_6 (X_1, \Delta_8 X_3) - 1{,}207\, J_6 (X_2, \Delta_8 X_2) - \\
&-0{,}169\, J_6 (X_2, \Delta_8 X_1) - 0{,}066\, J_6 (X_2, \Delta_8 X_3) + \\
&+0{,}024\, J_6 (X_3, \Delta_8 X_1) - 0{,}066\, J_6 (X_3, \Delta_8 X_2) - \\
&-1{,}028\, J_6 (X_3, \Delta_8 X_3)) - \frac{0{,}028}{l^2} J_6 (X_1, l^2) + \\
&+10^{-3} (-0{,}028\, \Delta_8 X_1 + 0{,}062\, \Delta_8 X_2 - 0{,}085\, \Delta_8 X_3);
\end{aligned}
$$

$$
\begin{aligned}
\Delta_4 \dot{X}_2 - 7{,}704 \cdot 10^{-2} \dot{X}_2 = \frac{10^{-9}}{l} (&1{,}824\, J_6 (X_1, X_2) + \\
&+0{,}622\, J_6 (X_1, X_3) + 3{,}703\, J_6 (X_2, X_3) - \\
&-0{,}169\, J_6 (X_1, \Delta_8 X_1) - 1{,}207\, J_6 (X_1, \Delta_8 X_2) - \\
&-0{,}066\, J_6 (X_1, \Delta_8 X_3) - 1{,}207\, J_6 (X_2, \Delta_8 X_1) - \\
&-1{,}367\, J_6 (X_2, \Delta_8 X_2) - 0{,}383\, J_6 (X_2, \Delta_8 X_3) - 0{,}066\, J_6 (X_3, \Delta_8 X_1) - \\
&-0{,}383\, J_6 (X_3, \Delta_8 X_2) + 0{,}303\, J_6 (X_3, \Delta_8 X_3)) - \frac{0{,}028}{l^2} J_6 (X_2, l^2) + \\
&+10^{-3} (0{,}062\, \Delta_8 X_1 - 0{,}047\, \Delta_8 X_2 + 0{,}064\, \Delta_8 X_3);
\end{aligned}
$$

$$
\begin{aligned}
\Delta_4 \dot{X}_3 - 4{,}726 \cdot 10^{-1} \dot{X}_3 = \frac{10^{-9}}{l} (&-0{,}012\, J_6 (X_1, X_2) + \\
&+11{,}848\, J_6 (X_1, X_3) - 3{,}213\, J_6 (X_2, X_3) + 0{,}024\, J_6 (X_1, \Delta_8 X_1) - \\
&-0{,}066\, J_6 (X_1, \Delta_8 X_2) - 1{,}028\, J_6 (X_1, \Delta_8 X_3) - 0{,}066\, J_6 (X_2, \Delta_8 X_1) - \\
&-0{,}383\, J_6 (X_2, \Delta_8 X_2) + 0{,}303\, J_6 (X_2, \Delta_8 X_3) - 1{,}028\, J_6 (X_3, \Delta_8 X_1) + \\
&+0{,}303\, J_6 (X_3, \Delta_8 X_2) + 1{,}388\, J_6 (X_3, \Delta_8 X_3)) - \frac{0{,}028}{l^2} J_6 (X_3, l^2) + \\
&+10^{-3} (-0{,}084\, \Delta_8 X_1 + 0{,}064\, \Delta_8 X_2 - 0{,}087\, \Delta_8 X_3).
\end{aligned}
$$

Table 3

Matrix for Conversion from Heights of Isobaric Surfaces H_j to Vectors X_i

X_i	Level, mb (Уровень, мб) 200	300	500	700	850	1000
X_1	0,668	0,323	0,426	0,474	0,339	0,095
X_2	0,542	−0,149	−0,485	−0,338	−0,254	−0,073
X_3	0,510	−0,296	0,064	0,328	0,332	0,099
X_4	0,229	−0,292	−0,575	0,075	0,434	0,147
X_5	0,056	−0,293	0,252	0,457	−0,315	0,159
X_6	0,010	0,106	−0,277	0,402	−0,093	−0,173
X_7	0,001	−0,012	0,022	0,167	0,500	−0,352

Here Δ_4, Δ_8, J_6 are difference operators:

$$\Delta_4 a_{i,j} = a_{i,j-1} + a_{i,j+1} + a_{i+1,j} + a_{i-1,j} - 4a_{i,j};$$

$$\Delta_8 a_{ij} = 8\,(a_{i,j-1} + a_{i+1,j} + a_{i,j+1} + a_{i-1,j} +$$

$$+ a_{i-1,j-1} + a_{i+1,j-1} + a_{i+1,j+1} - a_{i-1,j+1} - 8a_{i,j});$$

$$J_6(A, B) = \left(\frac{\partial A}{\partial x}\right)_6 \cdot \left(\frac{\partial B}{\partial y}\right)_6 - \left(\frac{\partial B}{\partial x}\right)_6 \cdot \left(\frac{\partial A}{\partial y}\right)_6,$$

$$\left(\frac{\partial A_{i,j}}{\partial x}\right)_6 = A_{i+1,j-1} - A_{i-1,j-1} + 2\,(A_{i+1,j} - A_{i-1,j}) +$$

$$+ A_{i+1,j+1} - A_{i-1,j+1};$$

$$\left(\frac{\partial A_{i,j}}{\partial y}\right)_6 = A_{i-1,j-1} - A_{i-1,j+1} + 2\,(A_{i,j-1} - A_{i,j+1}) + A_{i+1,j-1} - A_{i+1,j+1}.$$

The problem is solved in time intervals (by the central differences method). The sums of the changes during the forecast time δX_1, δX_2, δX_3 are added with the corresponding weights to the initial geopotential fields for obtaining the prognostic fields.

The H_{1000} field is predicted using the already mentioned method [2] by transfer of the field of surface pressure trends. We note that the $\dot{X}_1$, $\dot{X}_2$, $\dot{X}_3$ fields are corrected in each time interval using the determined $\partial H_{1000}/\partial t$ values. Tests of the model indicated that in general the model gives a fictitious increase in the geopotential values (spurious anticyclogenesis). In order to eliminate this shortcoming it was postulated that the sum of the positive and negative changes should be equal to zero in each interval. Thus, we have the equation

$$(1+\alpha)\,\Sigma_+ + (1-\alpha)\,\Sigma_- = 0,$$

where Σ_+, Σ_- are the sums of the positive and negative changes respectively and α is the correcting value. Hence

$$\alpha = -(\Sigma_+ + \Sigma_-)/(\Sigma_+ - \Sigma_-).$$

The mentioned procedure of "balancing" the changes is applied in each time interval to the $\dot{X}_1$, $\dot{X}_2$, $\dot{X}_3$ values.

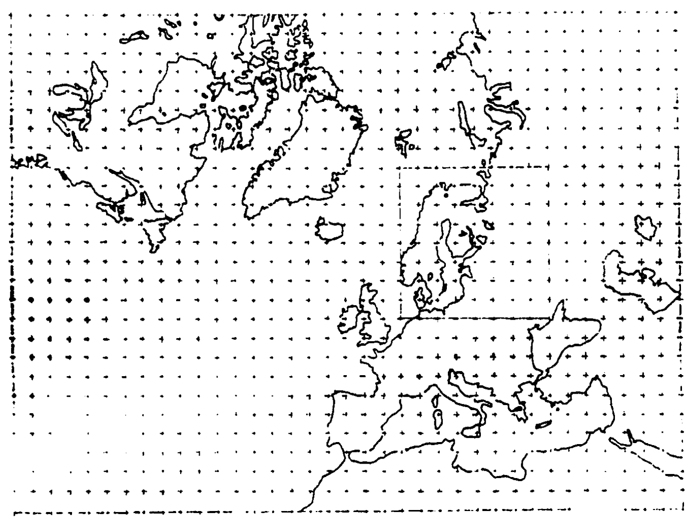

Fig. 1. Prognostic grid and region for evaluating forecasts (inner square 9 x 9 points of intersection).

Table 4

Mean Evaluations of Forecasts for 24 and 48 Hours According to Operational Two-Parameter Model of Main Geophysical Observatory (I) and Three-Parameter Model (II)

Срок Time	ОО RE		КК CC		ρ		S		η		Уровень Level
	I	II	I	II	I	II	I	II	I	II	
24 ч hours	0,67	0,62	0,71	0,75	0,57	0,59	0,53	0,48	0,72	0,71	1000
	0,74	0,70	0,67	0,70	0,51	0,55	0,51	0,47	0,50	0,75	850
	0,75	0,64	0,67	0,76	0,49	0,59	0,46	0,40	0,52	0,76	700
	0,72	0,63	0,71	0,78	0,53	0,62	0,46	0,40	0,56	0,68	500
	0,73	0,63	0,68	0,77	0,53	0,60	0,50	0,45	0,66	0,71	300
	0,74	0,71	0,66	0,73	0,49	0,56	0,49	0,48	0,71	1,02	200
48 ч	0,83	0,81	0,58	0,59	0,42	0,47	0,75	0,70	0,75	0,82	1000
	0,84	0,85	0,56	0,59	0,39	0,45	0,69	0,64	0,63	0,90	850
	0,85	0,80	0,58	0,67	0,38	0,46	0,62	0,55	0,70	0,90	700
	0,84	0,75	0,62	0,71	0,42	0,49	0,59	0,52	0,76	0,80	500
	0,89	0,75	0,62	0,70	0,41	0,50	0,62	0,66	0,90	0,81	300
	0,91	0,88	0,63	0,68	0,40	0,46	0,59	0,57	0,97	1,11	200

Notes: RE -- relative forecasting error; CC -- correlation coefficient between prognostic and actual changes; ρ evaluation of probable success of prediction of sign of changes; S -- error in probable success of gradient forecasting; η -- ratio of absolute prognostic variability to actual variability.

The archives of objective analyses obtained under operational conditions, available at the Main Geophysical Observatory, was used for checking the quality of forecasts using the described three-parameter model. The data present in the archives belong to the period 1973-1975 (approximately half to the winter season and half to the summer season) and make it possible to compute and evaluate 36 forecasts for 24 hours and 31 forecasts for 48 hours. These data were used in computing and evaluating forecasts using a three-parameter model and were compared with operational forecasts using the two-parameter model of the Main Geophysical Observatory.

The figure shows the territory of the forecast and the region for which the evaluations was made. The evaluations were made for the points of intersection of a 9 x 9 grid using the results of objective analysis. The results of these comparisons (statistical evaluations) are given in Table 4. These results indicate that in the case of a 24-hour forecast all the evaluations, and in the case of a 48-hour forecast -- the overwhelming majority of evaluations using a three-parameter model, are better than when using the operational model of the Main Geophysical Observatory. A circumstance of particular importance is that in a three-parameter model there is a considerable increase in the prognostic variability (η value) at all levels other than the ground level. The latter circumstance is attributable to the fact that in both models the surface chart forecast is essentially made using one and the same method. However, an improvement of the evaluations at this level is associated with the inverse influence of improved forecasts aloft on the AT_{1000} forecast.

It was of interest to compare evaluations made using other hydrodynamic models with synoptic forecasts. Source [7] gives the results of comparisons of operational forecasts prepared by the weathermen of the USSR Hydrometeorological Center and also obtained using the quasigeostrophic model formulated by S. L. Belousov (USSR Hydrometeorological Center), using a model with full equations formulated by V. P. Dymnikov, G. R. Kontarev (Computation Center Siberian Department USSR Academy of Sciences and West Siberian Regional Scientific Research Hydrometeorological Institute), using the A. N. Mertsalov synoptic-hydrodynamic model and by the National Meteorological Center (United States). Evaluations of 34 forecasts are cited; these relate to the period March-May 1976.

Since the sample used in [7] does not coincide with that which was used in this study, it goes without saying that it is impossible to draw far-reaching conclusions from a comparison of the evaluations cited in [7] and evaluations made using a three-parameter model. However, some idea about the possibilities of these models is possible on the basis of such a comparison. Table 5 gives evaluations for those levels (ground, 500 mb) for which comparisons are possible. In discussing the diversity of the samples we should also mention that forecasts by the method used at the United States National Meteorological Center were obtained using a more complete volume of initial information than what was used in other models given in Table 5.

Table 5

Mean Evaluations of Forecasts for 24 Hours

Метод 1	ОО 2		КК 3		ρ		S		η	
	земля 4	500 мб 5	земля 4	500 мб 5	земля	500 мб	земля	500 мб	земля	500 мб
6 Синоптический, Гидрометцентр СССР	0,75	—	0,72	—	0,51	—	0,49	—	0,93	—
7 А. Н. Мерцалова	0,70	—	0,73	—	0,54	—	0,50	—	0,82	—
8 С. Л. Белоусова	0,85	0,67	0,65	0,62	0,41	0,42	0,55	0,45	0,94	0,59
9 В. П. Дымникова,	0,93	0,72	0,69	0,68	0,33	0,51	0,53	0,43	0,98	0,996
10 Г. Р. Контарева										
11 НМЦ США	0,64	0,57	0,80	0,74	0,56	0,53	0,46	0,38	0,90	0,94
12 Схема II (ГГО, ИМВХ)	0,62	0,63	0,75	0,78	0,59	0,62	0,48	0,40	0,71	0,68

KEY:

1. Method
2. RE
3. CC
4. Ground
5. mb
6. Synoptic, USSR Hydrometeorological Center
7. A. N. Mertsalov
8. S. L. Belousov
9. V. P. Dymnikov
10. G. R. Kontarev
11. United States National Meteorological Center
12. Model II
    (Main Geophysical Observatory, Institute of Meteorology and Water Management)

BIBLIOGRAPHY

1. Bushkova, T. A., et al., "Description of a Numerical Analysis and Forecasting Model Routinely Used at the Northwestern Administration of the Hydrometeorological Service," TRUDY GGO (Transactions of the Main Geophysical Observatory), No 353, 1975.

2. Il'in, B. M., "One Model for Predicting the Pressure Field at the Ground," TRUDY GGO (Transactions of the Main Geophysical Observatory), No 226, 1968.

3. Il'in, B. M., Orlova, L. S., Rukhovets, L. V., "Geopotential Model With Few Parameters and its Routine Testing," METEOROLOGIYA I GIDROLOGIYA (Meteorology and Hydrology), No 10, 1967.

4. Martem'yanov, V. I., et al., "Results of Testing of Models of Short-Range Hydrodynamic Forecasting of the Pressure Field Over the Territory of the Central Asiatic Region," METEOROLOGIYA I GIDROLOGIYA (Meteorology and Hydrology), No 11, 1978.

5. Marchuk, G. I., Penenko, V. V., Protasov, A. V., "Model of Atmospheric Dynamics of the Spectral-Difference Type With Few Parameters," METEOROLOGIYA I GIDROLOGIYA, No 1, 1978.

6. Rukhovets, L. V., "Multilevel Model of Forecasting of the Geopotential Field Based on a Small Number of Parameters," TRUDY GGO, No 151, 1964.

7. Ugryumov, A. I., et al., "Comparative Evaluation of Regional Models of Numerical Forecasting of the Pressure Field for 24 and 36 Hours," GIDROMETTSENTR SSSR. INFORMATSIONNYY SBORNIK (USSR Hydrometeorological Center. Informative Collection of Articles), No 6, 1978.

8. Parfiniewicz, J., Ruchoves, Z., "Koncepcja wielopoziomowego modelu prognozy geopotencjaly opartege na trzech parametrach," PRZEG. GEOFIZ., 1977.

9. Parfiniewicz, J., "Obiektiwizacja sistemu meteorologicznych prognoz krotkoterminowych IMGW," MAT SESJI NAUKOWEJ, IMGW, Warszawa, 1979.

UDC 551.(543.1+509.314)

CORRECTION OF THE INITIAL FIELD OF SURFACE PRESSURE TRENDS IN NUMERICAL PREDICTION OF PRESSURE FIELD

Moscow METEOROLOGIYA I GIDROLOGIYA in Russian No 6, Jun 80 pp 27-32

[Article by A. A. Mulyukov, Central Asian Regional Hydrometeorological Scientific Research Institute, submitted for publication 17 December 1979]

[Text]

Abstract: It is proposed that the initial field of surface pressure trends during a definite observation time be corrected by means of subtracting the corresponding systematic values at the same observation time. The effectiveness of the three variants for the correction of the initial pressure trends is checked by means of a comparison of the mean evaluations of the quality of pressure forecasts at sea level using a quasigeostrophic model. The results indicate the desirability of using the proposed method for correction of the initial pressure trends in models for numerical forecasting of the pressure field.

The initial field of surface pressure trends is used in many modern numerical models of short-range forecasting of the pressure field [1-5, 8, 11, 12]. In [4] it serves for "adjusting" prognostic equations for describing the transpiring atmospheric process. In [1-3, 5, 8, 11] the pressure trend, determined at some distance from the point of forecasting with a definite weight, is used as one of the independent components of the local pressure change. In [12] the initial field of pressure trends is used for dynamic assimilation of the initial information. However, the measured value of the three-hour pressure trend cannot always reflect the change in pressure caused by a change in circulatory processes since it contains terms governed by the periodic diurnal variation of pressure and the distortion associated with the location of the stations at some height above sea level.

In the objective analysis of the field of trends an interpolation error is also added which is dependent primarily on the density of the network of synoptic stations. Among the above-mentioned forecasting models only in one

[5, 8] has there been a correction introduced to the pressure trends for the purpose of excluding the pressure change as a result of diurnal variation. The magnitude of the correction is determined using an empirical formula in dependence on the surface pressure Laplacian, and also in dependence on season of the year [6-8]. In addition, in [6] the value of the correction to the pressure trends was obtained in dependence on the degree of cloud coverage, but such a correction is nevertheless not introduced in the model in [8].

Below we propose another approach to determination of the corrections to surface pressure trends for their use in numerical prognostic models. It is proposed that the result of objective analysis of the pressure trend q_{oa} at some point on the map be represented in the form of the sum of three components: systematic q_s, dynamic q_d and the random errors δq, that is

$$q_{oa} = q_s + q_d + \delta q. \tag{1}$$

The q_s component includes: pressure change caused by the diurnal variation, systematic measurement errors and the mean (in time) error in objective analysis, changing from point to point; q_d is the sought-for component, which must be used in numerical forecasting models. In δq, in addition to the random errors in measuring, coding and transmission through communication channels, not detected by checking, it is possible as well to include the variable part of the error in objective analysis due to irregularity in the receipt of communications from synoptic stations.

In order to discriminate q_s we apply to equation (1) the procedure of averaging for n q_{oa} records at a definite observation time (for example, at 0300 Moscow time). Then the second and third terms on the right side of the equation will tend to zero with an increase in n. Hence $q_s \approx \overline{q}_{oa}$.

The figure shows maps of the mean values and dispersions of the results of objective analysis of pressure trends at the observation times 0300 and 1500 hours at the points of intersection of a regular grid 26 x 37 points with a 300-km interval, applicable in numerical short-range forecasting of the pressure field at the Central Asian Regional Scientific Research Hydrometeorological Institute. The maps were obtained using 120 records (n = 120) from archival material for the periods: 8 January - 6 February, 1-30 April, 8 July - 6 August, 1-30 October 1977.

On both maps there is a decrease in the absolute $\overline{q}_{oa}$ values with an increase in geographic latitude approximately from 30 to 90°N. To the south of 30° there is again a decrease in the $\overline{q}_{oa}$ values. The latter finding is attributable to the fact that the stations situated in the tropical zone ($\varphi < 32°$) report on the change in pressure during a 24-hour period, as a result of which there is exclusion of the change in pressure caused by the intradiurnal variation. In these cases the model of objective analysis of surface trends used at the Central Asian Regional Scientific Research

Table 1

Diurnal Variation of Pressure Trend at Tashkent During Period of Observation December 1968 - November 1969

Сезон 1	Высота над уровнем моря, м 2	3 Синоптические сроки наблюдения, ч							
		00	03	06	09	12	15	18	21
4 Зима	477	−0,20	−0,15	+0,30	+0,44	−0,78	+0,16	+0,33	−0,10
	0	−0,09	−0,04	+0,29	−0,31	−1,24	+0,41	+0,89	+0,09
5 Весна	477	−0,58	−0,05	+0,69	+0,17	−0,66	−0,22	+0,46	+0,19
	0	−0,31	+0,05	+0,32	−0,48	−1,08	−0,10	+1,04	−0,56
6 Лето	477	−0,44	−0,15	−0,85	+0,16	−0,47	−0,58	+0,15	−0,18
	0	−0,07	−0,32	−0,10	−0,66	−0,78	−0,64	+0,98	+0,95
7 Осень	477	−0,33	−0,09	+0,64	−0,34	−0,78	−0,08	+0,47	−0,17
	0	−0,27	−0,10	−0,55	−0,79	−1,22	+0,05	+1,37	+0,41
8 Год	477	−0,39	−0,03	−0,62	0,28	−0,67	−0,18	+0,35	+0,02
	0	0,19	−0,06	−0,27	−0,56	1,08	−0,07	+1,07	+0,50

KEY:
1. Season
2. Elevation above sea level, m
3. Synoptic observation times, hours
4. Winter
5. Spring
6. Summer
7. Autumn
8. Year

Hydrometeorological Institute [10] provides for the division of the trends by 8.

The dispersion of the results of objective analysis of pressure trends increases with latitude to 70°N and then somewhat decreases toward the north pole.

The rather mottled distribution of $\bar{q}_{oa}$ foci, most frequently localized over seas and lowlands (see Fig. 1), is attributable to the different elevation of stations above sea level. At meteorological stations the trends are computed from barometer readings at the station level [9]. In objective analysis this trend, without changes, is related to sea level. Table 1 illustrates the discrepancy in the trend values for two variants of its determination: according to barometer readings at station elevation (477 m) and barometer readings reduced to sea level in one and the same series of observations from December 1968 through November 1969 at the meteorological

Table 2

Mean Evaluations of Forecasts of Surface Pressure Field According to 1977 Archival Data

Варианты определения поправок 1	По исходным данным за 03 ч 2				По исходным данным за 15 ч 3			
	ε	r	ρ	S_1	ε	r	ρ	S_1
4 Прогнозы на 12 ч								
8 Без поправок	0,80	0,58	0,70	0,62	1,36	0,43	0,54	0,63
9 При $n=2$	0,86	0,55	0,66	0,62	0,92	0,46	0,63	0,64
При $n=30$	0,78	0,62	0,70	0,59	0,85	0,57	0,69	0,61
При $n=120$	0,82	0,59	0,68	0,59	0,90	0,52	0,67	0,62
5 Прогнозы на 24 ч								
Без поправок	0,83	0,06	0,72	0,69	1,54	0,57	0,65	0,72
При $n=2$	0,84	0,60	0,69	0,73	0,91	0,57	0,67	0,75
При $n=30$	0,78	0,67	0,73	0,68	0,87	0,67	0'72	0,70
При $n=120$	0,82	0,66	0,73	0,68	0,94	0,65	0,71	0,71
6 Прогнозы на 36 ч								
10 Без поправок	0,92	0,60	0,68	0,79	1,83	0,45	0,53	0,83
При $n=2$	0,85	0,61	0,69	0,82	0,92	0,55	0,67	0,84
При $n=30$	0,88	0,62	0,69	0,79	0,95	0,60	0,70	0,80
При $n=120$	0,94	0,60	0,67	0,79	1,06	0,55	0,68	0,81
7 Прогнозы на 48 ч								
Без поправок	1,06	0,56	0,68	0,84	2,03	0,47	0,60	0,88
При $n=2$	0,91	0,57	0,69	0,88	0,99	0,56	0,68	0,88
При $n=30$	0,99	0,56	0,68	0,86	1,10	0,56	0,68	0,87
При $n=120$	1,04	0,55	0,68	0,86	1,20	0,53	0,67	0,87

KEY:
1. Variants of determination of corrections
2. Using initial data for 0300 hours
3. Using initial data for 1500 hours
4. Forecasts for 12 hours
5. Forecasts for 24 hours
6. Forecasts for 36 hours
7. Forecasts for 48 hours
8. Without corrections
9. With...

station Tashkent (observatory). Data from TM-1 tables were used. Table 1 reveals a distinct difference of both the amplitudes and phases of change in the pressure trend in the diurnal variation already for a small elevation. Many synoptic stations in the figure near the q_{oa} foci are situated considerably higher above sea level than Tashkent.

Table 3

Mean Evaluations of Forecasts of Surface Pressure Field According to 1979 Operational Data

Варианты определения поправок 1	По исходным данным за 03 ч 2				По исходным данным за 15 ч 3			
	ε	r	ρ	S_1	ε	r	ρ	S_1
4 Прогнозы на 12 ч								
8 Без поправок	—	—	—	—	1,28	0,51	0,55	0,62
9 При $n=30$	0,77	0,62	0,70	0,58	0,82	0,62	0,70	0,60
5 Прогнозы на 24 ч								
Без поправок	—	—	—	—	1,42	0,59	0,66	0,71
При $n=30$	0,78	0,70	0,73	0,67	0,86	0,68	0,72	0,70
6 Прогнозы на 36 ч								
Без поправок	—	—	—	—	1,71	0,50	0,55	0,83
При $n=30$	0,88	0,62	0,68	0,79	0,94	0,62	0,70	0,82
7 Прогнозы на 48 ч								
Без поправок	—	—	—	—	1,86	0,48	0,62	0,89
При $n=30$	1.00	0,57	0,67	0,86	1,08	0,57	0,68	0,88

10 Примечание. Использовались поправки $\bar{q}_{0a}$, полученные на материале 1977 г.

KEY:

1. Variants of determination of corrections
2. Using initial data for 0300 hours
3. Using initial data for 1500 hours
4. Forecasts for 12 hours
5. Forecasts for 24 hours
6. Forecasts for 36 hours
7. Forecasts for 48 hours
8. Without corrections
9. With
10. Note. The corrections $\bar{q}_{oa}$ obtained using data for 1977 were used.

The introduction of corrections to pressure trends in the model of numerical forecasting of the pressure field in our case essentially involves subtraction of the values $q_s \approx \bar{q}_{oa}$ from the current results of objective analysis of pressure trends at the corresponding points.

The effectiveness of correction of the initial field of pressure trends was determined by a comparison of the mean evaluations of the quality of 112 forecasts on the basis of initial data for 0300 hours and 112 forecasts on the basis of initial data for 1500 hours using the same archival material which was used in obtaining the q_{oa} fields in the figure. The forecasts were computed using the model in [1]. We tested 3 variants of correction of the initial fields of pressure trends in which the corrections $q_s \approx q_{oa}$ were computed using a different number of cases: n = 2, n = 30, n = 120. With n = 2 the correction of the current results of objective analysis of the trends (a_{cor}^{today}) was reduced to performance of the operations using the formula

$$q_{cor}^{today} = q_{oa}^{today} - 0.5\ (q_{oa}^{today} + q_{oa}^{yesterday}) = 0.5\ (q_{oa}^{today} - q_{oa}^{yesterday}).$$

In the variant n = 30 from the trends for each date of one season we subtracted one and the same q_{oa} values, computed for 30 dates of this same season. In the variant n = 120 from the trends for each date for the entire archives we computed one and the same q_{oa} values whose isolines are shown in the figure.

Table 2 gives mean evaluations of the quality of forecasts computed with the use of the initial fields of trends without their prior correction and with three variants of the introduction of corrections. This table gives the values of the relative error in the forecast ε, the correlation coefficient r between the prognostic and actual changes, the ratio of the number of coincidences of the sign of the prognostic and actual changes to the total number of points in the evaluation field ρ and the error in forecasting of the gradients S_1. The evaluations of the forecasts were obtained relative to the results of objective analysis for a forecasting region of 16 x 20 points with a 300-km interval. The greatest improvement in the mean evaluations of the quality of the forecasts for 12 and 24 hours is observed when the corrections introduced to the initial q_{oa} trends were obtained for 30 cases and to 36- and 48-hour forecasts -- when q_{oa} were obtained using 2 cases. The correction of the initial trends at 1500 hours leads to a more considerable effect in comparison with correction at 0300 hours. In this case the forecasts for 12-36 hours which are clearly unsatisfactory with respect to forecasting errors (ε = 1.36-1.83) become acceptable (ε = 0.85-0.95).

Taking into account the fact that the correction of the initial pressure trends at the observation time 0300 hours with the use of the corrections q_{oa} with n = 2 somewhat reduces the quality of the forecasts for 12 and 24 hours and the use of the corrections q_{oa} with n = 30 improves the quality of the forecasts in all cases, it is desirable to use the last variant for making corrections.

Beginning in October 1978 the correction of the initial pressure trends for the observation times 0300 and 1500 hours by the proposed method was included in the operational forecasting model [1]. In the course of each season as the corrections to the pressure trends we used the q_{oa} field obtained from one of the four months in the archives for 1977 corresponding to the particular season. An exception was the winter season, when the q_{oa}

field obtained using material for October 1977 was used for corrections.

Using independent operational data it was of interest to check the stability of the considerable effect from correction of the initial trends for the observation time 1500 hours, which was noted using archival data for 1977. For this purpose for the observation time 1500 hours we organized calculations of two variants of a prediction of the field of surface pressure: with and without correction of the initial pressure trends in operational and nonoperational regimes respectively.

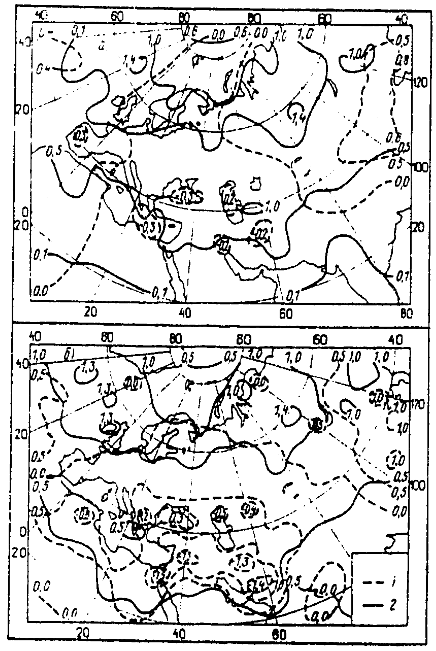

Fig. 1. Maps of the distribution of the mean values (1) of the results of objective analysis of pressure trends and their dispersions (2). a) observation time 0300 hours, b) observation time 1500 hours.

For a more objective comparison of the evaluations of forecasts of the surface pressure field on the basis of materials for 1977 and 1979 Table 3 gives mean evaluations of forecasts only for January, April, July and October 1979 (a total of 114 cases). Evaluations of the quality of the forecasts, computed on the basis of independent operational material for 1979, differ little from the corresponding evaluations of forecasts computed on the basis of archival data for 1977, although the fields of corrections $\bar{q}_{oa}$ are separated by two years with respect to the time of their preparation and the operational initial data. This fact characterizes a rather high stability (in time) of the fields of corrections $\bar{q}_{oa}$ for the initial pressure trends.

APPROVED FOR RELEASE: 2007/02/08: CIA-RDP82-00850R000300030024-9

Thus, it appears possible to correct the initial field of surface pressure trends with adequate effectiveness by means of subtracting from it the field of systematic $\bar{q}_{oa}$ values obtained on the basis of past archival material in a rather small volume, in our example -- with 30 cases in each season. The use of $\bar{q}_{oa}$ values based on "moving" archives for the last 30 days as corrections would possibly give a still greater effect, but this would complicate the procedures for operational numerical computations.

BIBLIOGRAPHY

1. Dolmatov, B. K., Martem'yanov, V. I., Mulyukov, A. A., "Numerical Prediction of Pressure at Sea Level With Allowance for the Surface Pressure Trend," METEOROLOGIYA I GIDROLOGIYA (Meteorology and Hydrology), No 10, 1978.

2. Dubov, A. S., Il'in, B. M., "Allowance for Pressure Trends in Hydrodynamic Forecasts," METEOROLOGIYA I GIDROLOGIYA, No 11, 1971.

3. Il'in, B. M., "One Model for Predicting the Pressure Field at the Earth's Surface," TRUDY GGO (Transactions of the Main Geophysical Observatory), No 226, 1968.

4. Lutfulin, I. Z., NOVYYE METODY PREDVYCHISLENIYA METEOROLOGICHESKIKH POLEY (New Methods for Precomputing Meteorological Fields), Leningrad, Gidrometeoizdat, 1966.

5. Mertsalov, A. N., "Prediction of the Pressure Field in the Lower Layer of the Atmosphere," TRUDY GIDROMETTSENTRA SSSR (Transactions of the USSR Hydrometeorological Center), No 57, 1969.

6. Mertsalov, A. N., "Corrections to the Surface Pressure Trend for its Diurnal Variation," TRUDY GIDROMETTSENTRA SSSR, No 68, 1970.

7. Mertsalov, A. N., "Allowance for the Diurnal Variation of Pressure Trends During Winter," TRUDY GIDROMETTSENTRA SSSR, No 82, 1971.

8. Mertsalov, A. N., "Numerical Synoptic-Hydrodynamic Forecasts of the Surface Pressure Field for 24 Hours in Advance Using a Simplified Model," TRUDY GIDROMETTSENTRA SSSR, No 129, 1974.

9. NASTAVLENIYE GIDROMETEOROLOGICHESKIM STANTSIYAM I POSTAM (Instructions for Hydrometeorological Stations and Posts), No 3, Part I, Leningrad, Gidrometeoizdat, 1969.

10. Bagrov, A. N., Belousov, S. L., Artanova, A. K., Tarnopol'skiy, A. G., "Operational Model for Objective Analysis of Surface Meteorological Fields in the Northern Hemisphere for a Rectangular Grid With a Variable Interval," TRUDY GIDROMETTSENTRA SSSR, No 123, 1974.

11. Bushkova, T. A., et al., "Description of a Numerical Analysis Model in Routine Use at the Northwestern Administration of the Hydrometeorological Service," TRUDY GGO (Transactions of the Main Geophysical Observatory), No 353, 1975.

12. Spectorman, A. D., Fuks-Rabinovich, M. S., "Use of Information on Surface Pressure Trends in the Dynamic Assimilation of Initial Fields for a Regional Prognostic Model," TRUDY GIDROMETTSENTRA SSSR, No 212, 1978.

UDC 551.577.22

METHOD FOR INDIRECT COMPUTATION OF THE MEAN LONG-TERM PRECIPITATION DURATION VALUES

Moscow METEOROLOGIYA I GIDROLOGIYA in Russian No 6, Jun 80 pp 33-37

[Article by Candidate of Geographical Sciences E. G. Bogdanova, Main Geophysical Observatory, submitted for publication 21 November 1979]

[Text]

Abstract: The author proposes a computation formula which makes it possible to compute the mean long-term monthly and annual duration of precipitation on the basis of its correlation with the characteristics of air temperature and humidity and the number of days with precipitation. The accuracy of the computed monthly and annual durations of precipitation is ±(30-35)% and ±(20-25)%.

The duration of precipitation is a climatic characteristic which for its direct determination requires extremely careful continuous observations. The automatic recorders which have long been in use for registry of the quantity and duration of precipitation as a rule give values for both which are too low -- especially when the precipitation is of a low intensity. This fact is well known and it always must be taken into account when using pluviographic data on the duration of precipitation. In addition, pluviographs register only liquid precipitation. In general, there are no reliable automatic recorders of solid precipitation which are suitable for use in a mass meteorological network and the source of information on the duration of precipitation is exclusively visual observations. The processing of such observations for obtaining the mean long-term characteristics of precipitation is extremely time-consuming and the series of observations are frequently short and nonuniform. Accordingly, information on the duration of precipitation is very limited in the reference literature.

The duration of precipitation is best represented for the territory of the USSR. In the SPRAVOCHNIK PO KLIMATU SSSR [6] information is given for 475 stations on the mean long-term (for a period from 20 to 30 years and the maximum during this period) monthly duration of precipitation and also maps of the annual duration of precipitation for the territories of most of the administrations of the Hydrometeorological Service. In addition, the duration of liquid precipitation in the territory of the USSR was investigated in detail in a monograph by A. N. Lebedev [4].

With respect to foreign territories, systematic data on the duration of precipitation are virtually lacking for such areas.

For the first time an indirect method for computing the duration of precipitation was proposed as early as 1880 by Köppen, who made the assumption that the ratio of the number of observation times with precipitation during a month to the total number of times when precipitation is measured is equal to the ratio of the total monthly duration of precipitation to the number of hours per month, that is:

$$\tau = \frac{n}{m} T, \tag{1}$$

where τ is the duration of precipitation per month, T is the number of hours per month (that is, 24 x 30 or 24 x 31), n is the number of observation times with the falling of precipitation per month, m is the total number of times when precipitation is measured during this same month.

Thus, the Köppen formula determines the mean long-term monthly duration of precipitation only in dependence on the number of observation times with precipitation (since the relationship between the number of hours per month and the total number of times when precipitation is measured during the month is a constant value for a given number of precipitation measurements during a 24-hour period).

Formula (1) is still used extensively in climatological computations and its accuracy has been repeatedly evaluated [4]. In most cases it was satisfactory to all intents and purposes. Difficulties arise only due to the circumstance that in by no means all cases is it possible to find information on the number of times with precipitation. This information is not published in yearbooks, its extraction from current monthly publications is extremely time consuming, and is virtually impossible for extensive regions and prolonged periods.

In 1958 Bontron proposed several other empirical formulas for indirect determination of the duration of precipitation [4]. These formulas give more precise results than formula (1), but their application requires a knowledge of the number of rains and the mean duration of individual rains, which is already extremely difficult when mass computations are involved.

After investigating the duration of rains in the territory of the USSR and having extensive observational data from the network of meteorological stations, A. N. Lebedev proposed still another refined empirical formula for determining the mean long-term duration of rains [4]. The formula has the form

$$\tau = 6\frac{m-k}{m-n}\,n, \qquad (2)$$

where k is the number of rains per month; the remaining notations are the same as in formula (1).

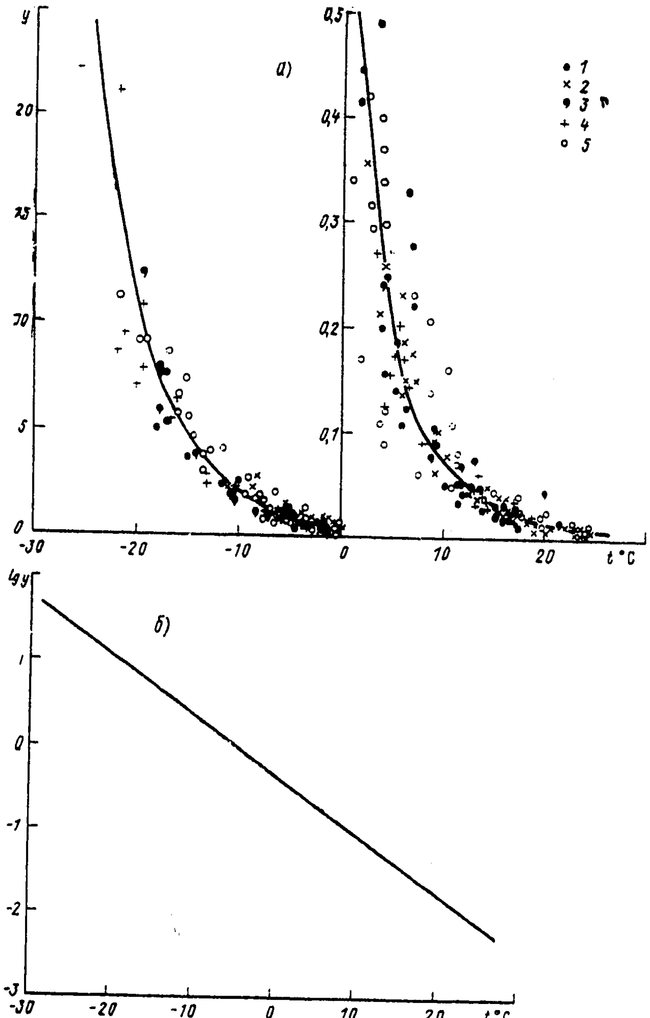

Fig. 1. Curve of the dependence between the mean long-term duration of precipitation during the month (τ) and temperature and air humidity characteristics (t, r, e) and the number of days with precipitation during the month (D). a) in ordinary, b) in semilogarithmic coordinates, 1) Northern European USSR, Baltic states; 2) Center and South of European USSR, Ukraine; 3) Far East, Primor'ye; 4) Siberia, Yakutia; 5) Central Asia (including high mountains), Kazakhstan

Monograph [4] gives a table which on the basis of data for 100 stations in the USSR gives the results of comparison of computations made using all the mentioned formulas (Köppen, Bontron and Lebedev) and the results of visual observations for the warm season of the year. The comparison convincingly demonstrates the superior accuracy of formula (2) over the others, but once again, for its application it is necessary to have information on the number of times with precipitation and on the number of individual rains. However, as already stated, there is either very little such information or none at all. And for a number of scientific and practical problems it is necessary to have data on the duration of precipitation over extensive territories -- as extensive as continents and the land as a whole. In order to satisfy this requirement it is necessary to have a method for indirect computation of the duration of precipitation which is based on the use of those meteorological elements on which the data are most complete and represented most extensively in the world reference literature. We used air temperature and relative humidity as such elements in seeking a method for indirect computation of the duration of precipitation, the number of days with precipitation was also used. The initial materials were the data published in the SPRAVOCHNIK PO KLIMATU SSSR [6] on the mean long-term monthly duration of precipitation (τ), the number of days with precipitation (D), temperature (t), relative (r) and absolute (e) humidity at 22 stations in the Soviet Union. On the basis of these data an attempt was made to establish a correlation between the mean duration of precipitation on a day with precipitation (τ/D), on the one hand, and air temperature and humidity, on the other. Figure 1a shows the constructed correlation graph in the coordinates

$$y = \frac{\tau}{D^{1.5}} \frac{100}{e^2 (100 - r)}$$

(ordinate) and t (abscissa), where e is in mb, r is in % and t is in °C. Each point on the graph corresponds to an individual month for a particular station. The mean curve was drawn through the centers of gravity of the entire set of points in 2°-intervals of the t value. The different symbols on the graph denote data for physiographic regions differing greatly with respect to the regime of falling of precipitation. Their systematic deviations from the mean curve on the graph are extremely small.

Figure 1b shows this same dependence, but in semilogarithmic coordinates. The dependence was linear, which made it possible to determine its parameters without difficulty, as well as its statistical characteristics. The correlation coefficient between the lg y and t values was 0.99 and the standard deviation of the experimental points from the correlation line was $\sigma_{\lg y} = \pm 0.13$.

The formula for determining the τ value in accordance with the graph in Fig. 1b has the form

$$\tau = 0{,}01\ D^{1.5}\ e^2\ (100 - r)\ 10^{[illegible]}, \qquad (3)$$

where τ is the mean long-term monthly duration of falling of precipitation (in hours); D is the mean number of days with precipitation during the month; e is absolute air humidity, mb; r is relative humidity, %; t is air temperature, °C, the mean long-term values during this same month; α and β are constants; $\alpha = -0.355$, $\beta = -0.0699$.

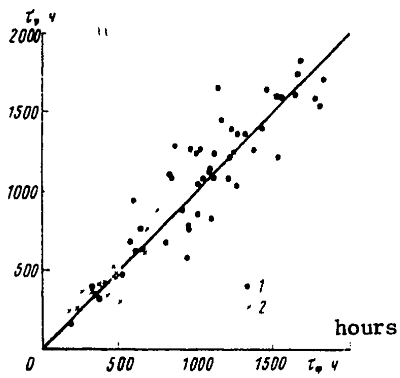

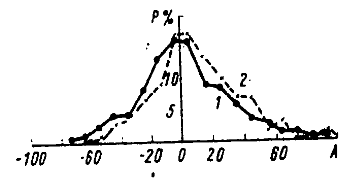

Fig. 2. Comparison of actual τ_{act} and computed τ_{comp} values of annual precipitation duration. 1) USSR, 2) Indonesia

Fig. 3. Probability distribution curves P% of monthly values $A = \tau_{comp} - \tau_{act}/\tau_{act}$ 100% in 10% intervals of these values. 1) USSR; 2) Indonesia

It should be noted that in different publications the number of days with precipitation means different things. Depending on the accuracy with which precipitation is measured in different countries and the form in which these data are published, this may refer either to the number of days with a quantity of precipitation $\geqslant 0.1$ mm or $\geqslant 0.01''$, that is, $\geqslant 0.25$ mm, or even $\geqslant 1.0$ mm. In formula (3) the value $D_{\geqslant 0.1\ mm}$ is used and when employing other D values they must first be reduced to the necessary value. The method for performing such a reduction is given in [1].

Formula (3) was checked for the purpose of determining the accuracy of the τ values computed from it; this was done on the basis of independent material using data from 54 stations in the USSR not employed in constructing the graph in Fig. 1. In addition, the formula was checked using data for 18 stations in Indonesia, which publishes information on the duration of precipitation registered using a pluviograph [3]. Since the precipitation in this region is usually very heavy, its duration according to pluviograph data virtually does not differ from the visual observations and it can be used for the checking of formula (3). Unfortunately, it was impossible to find any other published data on the duration of precipitation and therefore we had to be content only with the mentioned data.

Figure 2 shows the results of comparison of the actual τ_{act} and computed (using formula (3)) τ_{comp} annual durations of precipitation for both the Soviet Union and Indonesia. The standard deviation between τ_{act} and τ_{comp} in this case should be characterized by the value

$$\sigma_\tau = \sqrt{\frac{\Sigma\left(\frac{\tau_p - \tau_\phi}{\tau_\phi}\,100\right)^2}{n-1}}, \tag{4}$$

which for the USSR was equal to ±21%, and for Indonesia -- ±24%. The somewhat greater σ_τ value for Indonesia is attributable to the limited statistical sample and the lesser accuracy of the initial parameters -- the numbers of days with precipitation and the air humidity characteristics.

The accuracy in computing the monthly values of the duration of precipitation is characterized by Fig. 3, which gives the probability distribution curves for the values A = τ_{comp} - τ_{act}/ τ_{act} 100%, computed for each month for the same stations in the USSR and Indonesia. (It is infeasible to construct such curves for the annual τ_{comp} values due to the smallness of the sample.) The curves presented in Fig. 3 indicate that the error in computing the monthly values of the duration of precipitation using formula (3) in 70% of the cases is not more than 30% both for the USSR and for Indonesia.

Thus, formula (3) makes it possible to obtain the computed values of the mean long-term monthly and annual durations of precipitation with an accuracy of ±30% and ±(20-25)%, having data only on the number of days with precipitation, on air temperature and humidity, and in case of necessity -- also on the precipitation sum. These data are represented sufficiently completely in the world reference literature for the entire territory of the land (except, perhaps, for Antarctica). Accordingly, it seems possible to compute the monthly and annual durations of precipitation and map them on a planetary scale. In addition, after obtaining maps of the duration of precipitation and after constructing a world map of the annual sums of precipitation [5], for the first time it will be possible to obtain a map of the mean annual intensity of precipitation for the entire territory of the land.

BIBLIOGRAPHY

1. Bogdanova, E. G., "Computation of the Number of Days With Precipitation of Different Gradations," TRUDY GGO (Transactions of the Main Geophysical Observatory), No 404, 1978.

2. Drozdov, O. A., "Duration of the Falling of Precipitation as a Climatic Characteristic," TRUDY 2-go VSESOYUZNOGO GEOGRAFICHESKOGO S"YEZDA (Transactions of the Second All-Union Geographical Congress), Vol 2, Moscow, Geografizdat, 1948.

3. KLIMATICHESKIY SPRAVOCHNIK ZARUBEZHNOY AZII (Climatic Handbook of Foreign Asia), Leningrad, Gidrometeoizdat, 1974.

4. Lebedev, A. N., PRODOLZHITEL'NOST' DOZHDEY NA TERRITORII SSSR (Duration of Precipitation Over the Territory of the USSR), Leningrad, Gidrometeoizdat, 1964.

5. MIROVOY VODNYY BALANS I VODNYYE RESURSY ZEMLI (World Water Balance and the Earth's Water Resources), Leningrad, Gidrometeoizdat, 1974.

6. SPRAVOCHNIK PO KLIMATU SSSR. CH. II I IV, VYP 1-34 (Handbook of USSR Climate. Parts II and IV, Nos 1-34), Leningrad, Gidrometeoizdat, 1965-1970.

APPROVED FOR RELEASE: 2007/02/08: CIA-RDP82-00850R000300030024-9

UDC 551.513.1

MODEL INVESTIGATION OF THE GLOBAL MEAN ZONAL THERMAL REGIME OF THE EARTH'S ATMOSPHERE

Moscow METEOROLOGIYA I GIDROLOGIYA in Russian No 6, Jun 80 pp 38-48

[Article by Doctor of Physical and Mathematical Sciences I. L. Karol' and V. A. Frol'kis, Main Geophysical Observatory, submitted for publication 24 September 1979]

[Text]

Abstract: The article presents a semiempirical simplified model of the thermal regime of the atmosphere belonging to the Budyko-Sellers class of models. A study is made of the relative influence of the northern and southern hemispheres and the effect of exclusion of horizontal transfer. An allowance is made for the change in the vertical distribution of temperature and the latitudinal change in the temperature of ice formation and their influence on the model regime. Numerical experiments were carried out for studying the effect of a change in the solar constant on a model climatic system.

1. In the investigations of changes in climate carried out at the present time by use of so-called semiempirical models, based on the equations for heat balance of the earth - atmosphere system, a study is usually made of the thermal regime of one isolated hemisphere (usually the northern hemisphere) and no allowance is made for interaction between the northern and southern hemispheres [2, 10, 11, 13]. However, the differences in the mean characteristics of the radiation and dynamic factors forming the climate of these hemispheres and the relationship of their temperature distributions (deviation of the mean annual thermal equator from the geographic equator) are well known. Accordingly, it is important to take into account this difference of the hemispheres in the parameters of a model and include the thermal relationship between the hemispheres in the model, and also trace how this difference in the reaction of the model thermal regime is reflected in the change of an external factor (the solar constant S_0).

In this article we present some results of such an investigation for a variant of a model close to the Sellers-North model [10, 11, 13] in which use was made of several meridional distributions of radiation factors which differ somewhat from one another. The response of a model temperature regime to these differences is examined, as well as the effect of the influence of the meridional temperature gradient in the atmosphere at the mean level T on the intensity of heat transfer between the tropical and polar zones. For evaluating the role of this heat transfer we computed the distributions of radiation-equilibrium temperature with the exclusion of heat transfer, which are compared with the principal distributions with these same values of the solar constant S_0. An attempt was also made to take into account the influence exerted on the model regime by another inverse relationship: the dependence of T and the temperature of the surface layer of the atmosphere T_0 on T, reflecting the change in the vertical distribution of temperature and not taken into account, for example, in [3].

2. Following [3], we will use the heat balance equation at the level z

$$\frac{\partial}{\partial z}(H+F) = -c_p \rho \nabla (K \nabla T') + r, \tag{1}$$

where H and F are the vertical macroturbulent and radiant heat fluxes (positive, if directed upward), c_p = 0.24 cal/(g·°C) is the heat capacity of the air at a constant pressure, ρ [g/m^3] is air density, K[m^2/sec] is the coefficient of macroturbulent thermal conductivity in the horizontal plane, ∇ is the two-dimensional first-order operator, T' is air temperature, r is the flux of latent heat.

Equation (1) describes the steady mean annual temperature distribution. The heat transfer is parameterized by macroturbulent heat exchange.

Following [3], we integrate (1) for the entire thickness of the atmosphere:

$$(H+F)_{z=\infty} - (H+F)_{z=0} = \nabla(\gamma \nabla T) + R_1, \tag{2}$$

where

$$T = \frac{1}{p_0}\int_0^{p_0} T'\,dp \tag{3}$$

is the temperature of a vertical column of the atmosphere of a unit cross section averaged for pressure; p_0 = 1000 mb is surface pressure,

$$R_1 = \int_0^{\infty} r\,dz, \quad \gamma = c_p p_0 K/g, \quad g = 9.8\ \text{m}^2/\text{sec} \tag{4}$$

$$D = (H+F)_{z=0} - (H+F)_{z=\infty} + R_1$$

is the total heat influx to a vertical column of the atmosphere of a unit cross section.

We will express $(H+F)_{z=0}$ through the heat balance equation for the underlying surface:

$$(H+F)_{z=0}+R_2+G=0, \tag{5}$$

where G is the flux of "evident" and R_2 is the flux of latent heat into the soil. At the upper boundary of the atmosphere

$$(H)_{z=\infty}=0 \tag{6}$$

and there is satisfaction of the radiation balance of the earth-atmosphere system

$$-(F)_{z=\infty}=S(1-\alpha_p)-I, \tag{7}$$

where S is the flux of solar radiation at the upper boundary of the atmosphere, I is the flux of outgoing long-wave radiation, α_p is the albedo of the earth-atmosphere system.

Substituting (5)-(7) into (4), we finally obtain

$$\nabla(\gamma\nabla T)=-D,\quad D=S(1-\alpha_p)-I+(R_1-R_2)-G. \tag{8}$$

Henceforth we will assume that all the fields are zonally homogeneous. The outgoing thermal radiation I, according to Budyko [2], is a bilinear function of the surface temperature T_0 (in °C) and the tenths of effective cloud cover n.

$$I=I_0'+\beta' T_0,\quad I_0'=\alpha_1-\alpha_2 n,\quad \beta'=b_1-b_2 n, \tag{9}$$

where n is cloud cover in fractions of unity (in tenths), a_1, a_2, b_1, b_2 are empirical coefficients.

3. In order to relate the temperature T in (8), approximately coinciding with the temperature of the 500-mb surface, with T being the mean for a vertical column of the atmosphere, and the surface temperature T_0 in formula (9), we obtain the empirical relationship between T and $T_q = T_0 - T$ for different latitudes [4].

We will examine two variants of this relationship. In the first $T_{q1} = T_0(\varphi) - T(\varphi)$ is determined from mean zonal climatic data [5-7]. It is regarded as an empirical function and is not dependent on external parameters. It is possible to use T_{q1} for computations of modern climate, but with a change of any external parameters such T_{q1} values can substantially distort the T changes. In the second variant we will represent T_{q2} in the form

$$T_{q2}=T_0-T=g_1 T+g_2. \tag{10}$$

where g_1 and g_2 are determined from a linear regression equation on the basis of these same data on T_0 and T. This equation was derived for the entire northern hemisphere and separately for the zone from the equator to 60°S. In Antarctica the high level of the surface does not make it possible to include the local values for the southern hemisphere T_0 - T and T in the general correlation.

The following values of the coefficients in (10) were obtained:

$$g_1 = 0.57/0.127; \; g_2 = 37.76/33.03 + q(\varphi),$$

where the numerator applies to the northern hemisphere and the denominator applies to the southern hemisphere, $q(\varphi)$ is an empirical function equal to zero to the north of 60°S, whereas to the south of 60°S $q(\varphi)$ is selected in such a way that with the present-day value of the solar constant S_0 formula (10) is satisfied everywhere in the southern hemisphere, that is

$$q(\varphi) = (T_0 - T) - (g_1 T - g_2), \; 60° \text{ S} < \varphi < 90°\text{S.}, \tag{11}$$

where T_0 and T are the climatic temperature values [5, 7]. T_{q2} approximately takes into account the influence of the inverse relationship between the averaged temperature T of a vertical column of air and the surface air temperature T_0.

The mechanism of this inverse relationship is particularly significant in those experiments where the changes in T are considerable.

Substituting (10) and (11) into (9), we obtain

$$I = I_0 + \beta T, \quad \beta = \begin{cases} \beta' \\ \beta' + g_1 \end{cases}, \quad I_0 = I_0' + \begin{cases} \beta' T_{c1} \\ \beta' g_2 \end{cases}, \tag{12}$$

where the upper line applies to the variant T_{q1} and the lower line to the variant T_{q2}.

The mean zonal albedo of the earth-atmosphere system α_p is respresented in accordance with Budyko and Cess [2, 8] in the form

$$\alpha_p = \alpha_c n + \alpha_s (1 - n), \tag{13}$$

where α_c is the albedo of clouds, α_s is the albedo of the earth-atmosphere system in the case of a cloudless sky.

We introduce the dependence of α_c on solar zenith angle ζ and on α_c [8, 9] in the form

$$\alpha_c = A_1 + A_2 \alpha_s - A_3 \cos \zeta, \tag{14}$$

where A_1, A_2, A_3 are dimensionless empirical coefficients and the dependence of α_s on temperature, as in the Budyko and North models [2, 10, 11], is

$$\alpha_s = \begin{cases} \alpha_i & , \quad T_0 < T_i \\ (\alpha_i + \alpha_0)/2, & T_0 = T_i \\ \alpha_0 & , \quad T_0 > T_i, \end{cases} \tag{15}$$

where α_i, α_0 is the albedo of the earth—atmosphere system in the cases of surfaces with and without a snow and ice covered surface, T_i is the temperature of the surface air at which the surface is covered with ice and snow.

The mean zonal α_0 and α_i values are represented in the form

$$\alpha_0 = \alpha_{0L} P_L + \alpha_{0W} (1 - P_L), \quad \alpha_i = \alpha_{iL} P_L + \alpha_{iW} (1 - P_L). \tag{16}$$

α_{0L}, α_{iL}, α_{0W}, α_{iW} are the α_0 and α_i values for the land and ocean respectively, P_L is the latitudinal distribution of the fraction of the area of the land to the area of the zonal "belt."

In a steady mean annual zonal homogeneous atmosphere R_1 and R_2 compensate one another and the heat flux to the underlying surface is $G = 0$.

4. As a result, the considered thermal regime of a zonally homogeneous, vertically averaged atmosphere is described by the equation

$$\nabla (\gamma \nabla T) = -S\,[1 - \alpha_p (T_0, n)] + I_0 (n) + \beta (n)\,T, \tag{17}$$

where α_p, I_0, β are determined from expressions (10)-(16). The coefficient K, entering into γ, is determined from the condition: temperature $T_0(\varphi)$ at the latitudes of the boundaries φ_N and φ_S of the northern and southern polar caps should assume values $T_i(\varphi)$.

$$T_0(\varphi_N) = T_i(\varphi_N), \; T_0(\varphi_S) = T_i(\varphi_S). \tag{18}$$

With the present-day level of the solar constant S_0 we have approximately $\varphi_N = 72°N$ and $\varphi_S = 60°S$. As follows from (10) and (11), $T_0(\varphi)$ is related to $T(\varphi)$ by the formula

$$T_0(\varphi) = \begin{cases} T(\varphi) + T_{q1}(\varphi), & T_{q1} \\ (1 + g_1)\,T(\varphi) + g_2 \cdot T_{q2}. \end{cases} \tag{19}$$

The coefficient $K = (K_N, K_S)$ is considered constant within the limits of each of the hemispheres and its values will be determined below.

We will examine two variants of the $T_i(\varphi)$ values. In the first variant $T_{i\,1}(\varphi)$ = const in the limits of each of the hemispheres and is equal to -10°C in the northern hemisphere [2] and -1.9°C in the southern hemisphere, that is, the temperature of ocean freezing. In the second variant $T_{i\,2}(\varphi)$ is a variable and approximately takes into account that the surface air temperature at which a snow-ice cover is formed changes with latitude.

$$T_{i2}(\varphi) = \begin{cases} -10 & P_L(\varphi) \geq 0{,}3 \\ -1{,}9 - 81\,(P_L(\varphi) - 0{,}2), & 0{,}2 \leq P_L(\varphi) \leq 0{,}3 \\ -1{,}9 & ,\ P_L(\varphi) \leq 0{,}2. \end{cases}$$

If interlatitudinal heat transfer is neglected, the thermal conductivity coefficient in (17) will be equal to zero and the thermal regime of the earth - atmosphere system is determined only by radiant equilibrium from the heat balance equation (17). Then we have

$$T_0(\varphi) = \frac{S\,[1 - \alpha_p\,(T_0,\ n)] - I_0\,(n)}{\beta\,(n)}. \tag{20}$$

In this study we make use only of the data from Cess, obtained as a result of processing of satellite measurements with the following values of the empirical coefficients in (9) and (14) [8, 9]: a_1 = 257/262; a_2 = 91/81 (W/m^2); b_1 = 1.63/1.64; b_2 = 0.11/0.09 (W/(m^2·°C)); A_1 = 0.641/0.691; A_2 = 0.258/0.219; A_3 = 0.494/0.619. Here the numerator applies to the northern hemisphere and the denominator to the southern hemisphere, whereas in (16): $\alpha_{0\,L}$ = 0.43/0.275; $\alpha_{0\,W}$ = 0.43/0.103; $\alpha_{i\,L}$ = 0.43; $\alpha_{i\,W}$ = 0.43. The numerator applies to Antarctica, where it is assumed that to the south of 64°S the continental ice does not thaw; the denominator applies to the remaining part of the earth's surface. For example, the author of [12] gives other values of the coefficients a_1, a_2, b_1, b_2. However, with the use of a cloud cover value equal to 0.5 different values of the coefficients in (9) give close results. The cloud cover value is assumed to be constant within the limits of the hemisphere and is equal to n_N = 0.51 in the northern hemisphere and n_S in the southern hemisphere [8]. The latitudinal variation of the solar radiation flux was taken from [8] for a value of the solar constant S_0 = 1360 W/m^2.

5. The temperature T(x) of the considered thermal regime is determined from the zonally homogeneous equation (17). Since the coefficients γ and β are constant within the limits of each of the hemispheres, it is possible to find T(x) for each of them and "splice" them at the equator for the thermally interacting hemispheres.

Using a Green's function of the differential operator

$$\frac{d}{dx}(1-x^2)\frac{d}{dx}-\varepsilon_j,$$

the conditions of continuity and limitation on temperature and the heat flux within the limits of a hemisphere, and also the equality of the flux at the poles to zero

$$\sqrt{1-x^2}\frac{dT}{dx}=0 \quad \text{when } x = \pm 1,$$

from (17) we obtain

$$T_N(x)=\int_0^1 G_N(x, y)[S(1-\alpha_p)-I_0]\,dy+C_N P_N(x), \quad 0\leqslant x\leqslant 1,$$

$$T_S(x)=\int_{-1}^0 G_S(x, y)[S(1-\alpha_p)-I_0]\,dy+C_S P_S(-x), -1\leqslant x\leqslant 0. \tag{21}$$

Here

$$G_j(x, y)=\frac{R^2}{\gamma_j W_j}\begin{cases}P_j(x)\,P_j(-y), & y<x\\ P_j(-x)\,P_j(y), & y>x,\end{cases}$$

$$P_j(x)=P_{\nu_j}(x),\ P_j(-x)=P_{\nu_j}(-x)$$

are linearly independent Legendre functions of the first kind [1]

$$x=\sin\varphi,\ \nu_j=-1/2+i\psi_j,\ \psi_j=\sqrt{\varepsilon_j-0{,}25},\quad \varepsilon_j=\beta_j R^2/\gamma_j,\quad W_j=(2/\pi)\,\mathrm{ch}\,(\pi\psi_j),$$

$R = 6.37\cdot10^8$ cm is the earth's radius, C_j is an arbitrary integration constant which is determined from the conditions at the equator, j = N, S is the index for the northern or the southern hemisphere, π = 3.14159.

We will examine two types of conditions at the equator.

The condition G is for thermally interacting hemispheres:

$$T_N(x)=T_S(x),\quad \gamma_N\sqrt{1-x^2}\frac{dT_N(x)}{dx}=$$

$$=\gamma_S\sqrt{1-x^2}\frac{dT_S(x)}{dx}, \quad \text{when } x = 0. \tag{22}$$

The condition H is for thermally isolated hemispheres:

$$\sqrt{1-x^2}\frac{dT_N(x)}{dx}=0,\quad \sqrt{1-x^2}\frac{dT_S(x)}{dx}=0, \quad \text{when } x = 0. \tag{23}$$

The condition H is used in the Budyko and North models [2, 10, 11].

As follows from (13)-(15), α_p in expression (20) is dependent on a continuously distributed temperature $T_0(\varphi)$. If we determine the latitudes φ_N and φ_S of the boundaries of the "polar caps," for which (18) is satisfied, in (20) α_p is a function of the argument φ and the parameters

φ_N and φ_S, that is, in place of (15) we have

$$\alpha_S = \begin{cases} \alpha_l & , \ \varphi < \varphi_S \ \text{or} \ \varphi > \varphi_N \\ (\alpha_l + \alpha_0)/2, & \varphi = \varphi_S \ \text{or} \ \varphi = \varphi_N \\ \alpha_0 & , \ \varphi_S < \varphi < \varphi_N. \end{cases} \tag{24}$$

In the model it is assumed that the boundaries of the polar caps with the present-day values of the solar constant and other parameters are known. Substituting (19), (21) and (24) into (18), we obtain a system of two transcendental equations, from which, as it can be shown, it is possible to make an unambiguous determination of the coefficient of macroturbulent thermal conductivity $K = (K_N, K_S)$. Substituting the determined K values into (21), taking (19) and (24) into account, we find the $T_0(\varphi)$ profile corresponding to the present-day value of the external parameters. Then, investigating the changes of the thermal regime with variation of the solar constant or other external parameters, the thermal conductivity coefficient K can be considered either constant or variable in a known way. Substituting known K into (21), which, in turn, is substituted into (18) and (19), we obtain two transcendental equations for the perturbed values φ'_N and φ'_S. After determining φ'_N and φ'_S and substituting them into (24), from (19) and (21) we find the perturbed temperature profile $T_0'(\varphi)$.

$T_0(\varphi)$ is similarly determined in the absence of ordered heat transfer. Expressions (20) and (24) are substituted into (18). By solving the derived system of two transcendental equations, we find φ_N and φ_S. Substituting the determined φ_N and φ_S values into (20), we determine the surface temperature $T_0(\varphi)$, corresponding to the radiation equilibrium with selected values of the external parameters. However, condition (18), used for obtaining a solution of equations (17), is not unique. The φ_N and φ_S values can be a solution; these are determined by the condition

$$\varphi_N = \varphi_S = 0 \qquad \text{when} \quad T_0(\varphi) < T_l(\varphi), \tag{25}$$

$$\varphi_N = 90°\text{N.}, \quad \varphi_S = 90°\text{S} \qquad \text{when} \quad T_0(\varphi) > T_l(\varphi).$$

The roots of all the considered transcendental equations are determined numerically by the successive approximations method.

6. The numbers of the different model variants for which the computations were made and the value of the fitted parameter -- the coefficient of macroturbulent exchange $K = (K_N, K_S)$ (in $10^6 m^2/sec$) -- are given in Table 1.

The mean annual zonal profiles of surface temperature T_0 for variants 1, 2, 4, 5 are given in Fig. 1. The discrepancy between variants 1 and 2 in the equatorial latitudes is attributable to the different conditions at the equator. The heat insulation of the equator in the condition H leads to an excessive accumulation of heat in the northern hemisphere in comparison with the southern hemisphere, and in the condition G the excess heat from the northern hemisphere is transported into the southern hemisphere. Accordingly, in the equatorial latitudes of the southern hemisphere it is warmer in variant 1 than in variant 2. Figure 1 shows that the conditions at the equator do not exert an influence on the temperate and polar latitudes. The difference between variants 4 and 5 from variants 1 and 2 is attributable to the inaccuracy of parameterization when using the function $T_{q\ 2}$, especially in the northern hemisphere. In the equatorial latitudes T_0 in variants 4 and 5 is similar to T_0 in variants 1 and 2. The break in the T_0 profile in variant 4 is a result of the "discontinuity" of the function $T_{q\ 2}$ at the equator. As a comparison, Fig. 1 shows the climatic values T_0 from [5-7], which are denoted with the letter k.

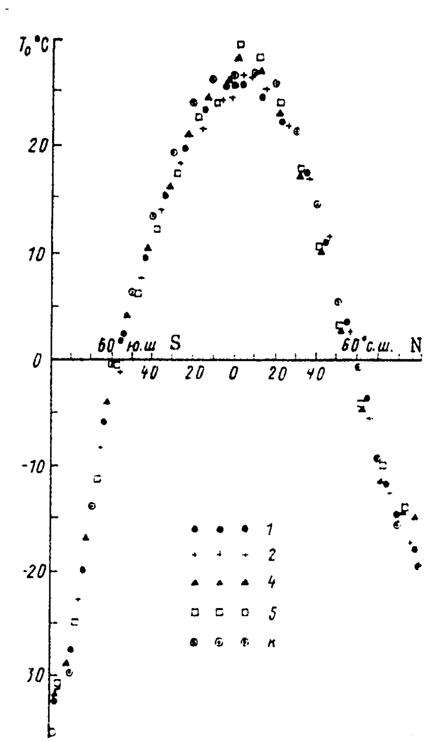

Fig. 1. Mean annual mean zonal surface air temperature T_0.

Table 1

Variants of Model and Corresponding K_N and K_S Values

1 Вариант модели	2 Условие G T_{q1}	2 Условие G T_{q2}	3 Условие H T_{q1}	3 Условие H T_{q2}	4 Условие термического равновесия
T_{i1}	1	4	2	5	8
T_{i2}	3	6	7	—	
K_N	4,09	3,70	3,97	3,70	0
K_S	3,57	3,50	3.70	3.61	0

KEY:

1. Variant of model
2. Condition G
3. Condition H
4. Condition of thermal equilibrium

Note. With use of the variants $T_{i\ 1}$ or $T_{i\ 2}$ the values of the corresponding coefficients K_N and K_S coincide because for present-day φ_N and φ_S values the variants $T_{i\ 1}(\varphi)$ and $T_{i\ 2}(\varphi)$ coincide.

Table 2

Change in Solar Constant in Percent With Complete Thawing of Ice Cover of the Northern Hemisphere $\Delta S'$, With Formation of "White Earth" $\Delta S''$ With Corresponding φ_N and φ_S Values for Different Variants

	Model variant / Вариант модели 1	2	3	4	5	6	7	8
$\Delta S'$ %	4.5	4,5	9,5	1,2	0.9	8,6	9,5	11,5
$\Delta S''$ % N	−6	−12,5 / 4,5	−6	−7	−12 / 3,5	−7	−12,5 / −4,5	−27 / −23
φ_N °с. ш. / φ_S °ю. ш. S	54	34 / 34	54 / 34	43 / 29	26 / 37	43 / 29	34 / 34	0 / 0

KEY:

1. Variant of model
2. N/S

Note. In variants 2, 5, 7, 8 the $\Delta S''$ value in the numerator corresponds to the northern hemisphere and the $\Delta S''$ value in the denominator corresponds to the southern hemisphere.

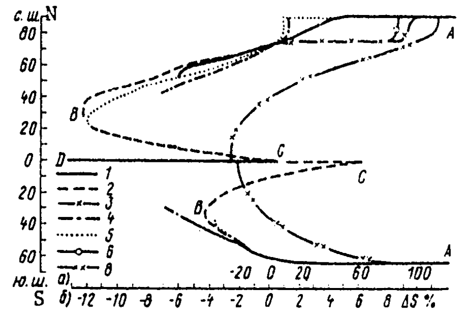

Fig. 2. Boundaries of polar ice caps with different values of solar constant. The figures correspond to the numbers of the variants. The scale a relates to variant 8, scale b to all the remaining variants.

The boundaries of the northern and southern polar caps for different values of the solar constant are shown in Fig. 2.

We will denote the deviation from S_0 in percent as ΔS and we will examine experiments with an increase in S ($\Delta S > 0$). Variants 1 and 2, and also variants 3 and 7 coincide. This indicates that the considered difference in the thermal condition at the equator exerts no influence on the area of the ice polar caps. The horizontal segment on the curve in variants 3 and 6 and such a high ΔS value at which there is a complete melting of the ice cover in the northern hemisphere are attributable to the fact that with the advance of the boundary of the polar cap poleward there is a marked increase in the melting temperature of the ice. In the pole region the ice cap consists of sea ice which in contrast to continental ice melts at a higher mean annual temperature. Therefore, quite high ΔS values are necessary in order to heat sea ice to the necessary temperature $T_{i\ 2}$. This process corresponds to the horizontal segment of the curve in variants 3 and 6. In variants 4 and 5 the total melting of the north polar cap occurs even with small ΔS, which is a result of the effect of the inverse relationship $T_{q\ 2}$, whose mechanism is considered below. The $\Delta S'$ values at which there is complete melting of the ice cover of the northern hemisphere are given in Table 2. In all variants the boundary of the ice in the southern hemisphere cannot advance beyond 64°S, since in the model it is assumed that continental ice in Antarctica does not melt with any ΔS values. For this reason all the variants in the southern hemisphere coincide.

Now we will examine experiments with a decrease in the solar constant ($\Delta S < 0$). Variants 1 and 3, and also variants 2 and 7 coincide since $T_{i\ 1}(\varphi)$ and $T_{i\ 2}(\varphi)$ differ only to the north of 72°N. The difference in variants 1 and 2 is attributable to the fact that with advance of the polar ice equatorward the thermal condition at the equator becomes significant. As was stated above, in variant 2 in the northern hemisphere in the equatorial latitudes it is warmer than in variant 1; therefore, in Fig. 2 the curve for variant 2 lies higher than the curve for variant 1. In the southern hemisphere the reverse phenomenon is observed. A similar picture is observed in variants 4 and 5. With a decrease in ΔS to the value ΔS", $\Delta S > S"$ the area of the ice polar caps increases smoothly. With $\Delta S <$ Δ S" there is a jumplike total glaciation of the earth. Table 2 gives the Δ S" values and the corresponding limiting latitudes of the boundaries of the ice caps.

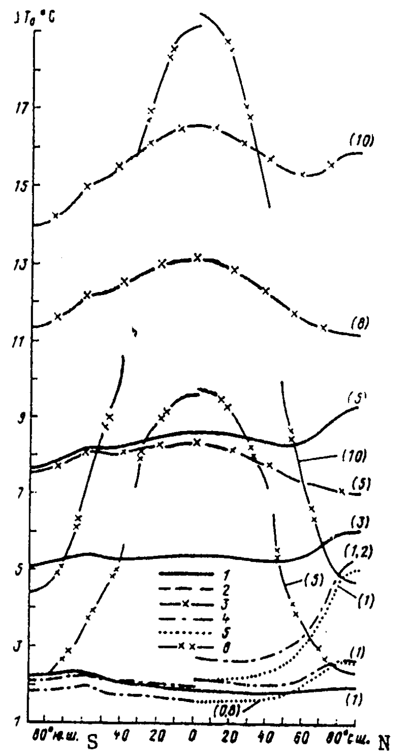

Fig. 3. Changes in the mean annual mean zonal air surface temperature T_0 with an increase in the solar constant. The figures in parentheses are the Δ S values in percent; the figures without parentheses are the numbers of the variants.

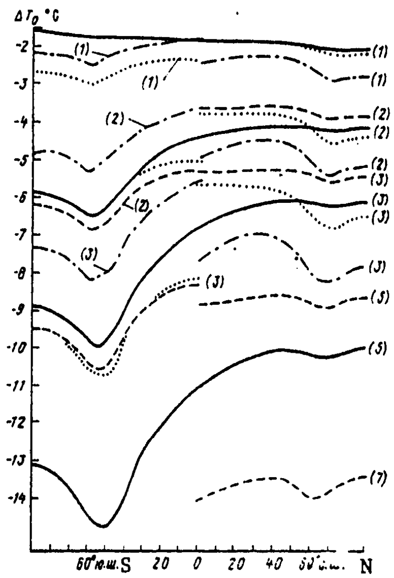

Fig. 4. Changes in the mean annual mean zonal air temperature with a change in the solar constant. The notations are the same as in Fig. 3.

In variant 2 the segment of the curve between the points A and B corresponds to a stable state of the climate; the segment between the points B and C corresponds to an unstable state of the climate. An unstable state was also described by North and Budyko [2, 10, 11]. An unstable state is characterized by an increase in the area of the ice cover with an increase in ΔS.

The existence of an unstable state in variants 2, 5, 7, also noted in other studies [3, 10, 11], and its absence in variants 1, 3, 4, 6, evidently is attributable to the thermal insulation of the equator. A similar situation arises in variants 4 and 5. All the considered model variants allow the existence of still another stable climatic state -- a "white earth" state which corresponds to condition (25), and Fig. 2 shows the line between the points C and D. The "white earth" state was also obtained in [2, 10, 11]. In variant 2 an unstable state and a "white earth" arise with one and the same ΔS value. The "white earth" in all variants exists with any values $\Delta S < 1\%$, with the exception of variants 2, 5, 7, where in the southern hemisphere the "white earth" exists with $\Delta S < 6\%$, which is attributable to the high T value.

Figure 2 also shows the boundaries of the northern and southern polar caps for variant 8 of thermal equilibrium with different ΔS values. With $\Delta S = 0$ $\varphi_N = 40°N$, $\varphi_S = 37°S$; a "white earth" exists with $\Delta S < -20\%$. The break at the equator is attributable to the "discontinuity" in the parameterization of $T_{i\ 1}$, I_0 and β.

7. The latitudinal profiles of the temperature change ΔT_0 corresponding to a change in the solar constant by the value ΔS are shown in Fig. 3 for $\Delta S > 0$ and in Fig. 4 for $\Delta S < 0$.

With $\Delta S > 0$ ΔT_0 in variants 1 and 2, 3 and 7 coincide, which indicates a nondependence of the change in the thermal regime when $\Delta S > 0$ on the conditions at the equator. At the equator the quantity of arriving solar radiation is greater than at the poles and due to the lower α_S values it is absorbed more effectively. Accordingly, in variant 8 of thermal equilibrium the maximum increase in absorbed radiation occurs at the equator, which leads to greater ΔT_0 values. In the territory where the ice cover melts a marked decrease in albedo leads to an increase in absorbed solar radiation and ΔT_0. In Fig. 4 we have denoted only the boundaries corresponding to a marked increase in ΔT_0 due to the melting of ice because the ΔT_0 values themselves do not fit into the format of the figure. It is convenient to trace the influence of ordered horizontal transfer in a comparison of variants 8 and 3 with ΔS = 5 and 10%. As Fig. 2 shows, with this ΔS the ice boundary in variant 3 does not change and accordingly its movement exerts no influence on the ΔT_0 profile. Horizontal transfer redistributes T_0 and leads to a decrease in the ΔT_0 values at the equator and an increase in ΔT_0 at the poles. The effect of movement of the boundary of the north polar cap is traced in a comparison of the ΔT_0 profiles with different ΔS for one and the same variant and also in a comparison of variants 1 and 3 with $\Delta S = 5\%$. The melting of the polar cap will result in a stronger increase in the absorption of solar radiation and accordingly heating in the polar regions than in the equatorial regions.

A similar result was obtained by Budyko in [2]. An exception is variant 3 with $\Delta S = 10\%$. This is attributable to the fact that with such a high ΔS value the increase in the absorption of solar radiation in the equatorial zone is greater than in the polar zone, despite the melting of the polar ice. The inverse relationship ("feedback") effect between T_0 and T is traced in a comparison of variants 1 and 4, 2 and 5. An increase in T in variants 4 and 5 will lead to an additional increase in T_0 in accordance with (19). This effect will be manifested most strongly at the poles, where ΔT is maximum, and in the equatorial zone ΔT_0 is constant in latitude. The difference between the ΔT_0 values at the north pole and at the equator is about 10°C. Budyko [2] and Manabe and Wetherold [14] obtained a similar picture, but with a different ΔS value as a result of use of a different parameterization. The break in the T_0 profile at the equator is attributable to the discontinuity of the $T_{q\ 2}$ function, but $T(\varphi)$ is continuous. At the south pole there are no sharp changes in ΔT_0 because the ice boundary remains virtually constant.

With $\Delta S < 0$ ΔT_0 of variants 1 and 2 with $\Delta S = -1\%$ still coincide, but with $\Delta S < -1\%$ they differ, since with advance of the boundary of the ice cover equatorward the equatorial thermal conditions begin to exert an effect. Variants 1 and 3, 2 and 7 coincide, since in the temperate latitudes $T_{i\ 1}(\varphi) = T_{i\ 2}(\varphi)$. In all variants the most significant changes occur in the southern hemisphere, where the ocean is covered with ice considerably more rapidly than the land in the northern hemisphere. For this same reason the $T_{q\ 2}$ effect is manifested for the most part in the southern hemisphere.

8. Thus, our investigation indicated the importance of the influence of the southern hemisphere, changes in the vertical distribution of atmospheric temperature, and also allowance for the variability of the temperature of ice formation at different latitudes in modeling of the thermal regime of the earth - atmosphere system and its variations.

BIBLIOGRAPHY

1. Beytmen, G., Erdeyn, A., VYSSHIYE TRANSTSENDENTNYYE FUNKTSII (Higher Transcendental Functions), Vol I, Moscow, 1973.

2. Budyko, M. I., IZMENENIYE KLIMATA (Climatic Change), Leningrad, Gidrometeoizdat, 1974.

3. Gandin, L. S., et al., "Influence of Changes in External Parameters on the Thermal Regime of the Atmosphere," TRUDY GGO (Transactions of the Main Geophysical Observatory), No 315, 1973.

4. Kagan, R. L., Vinnikov, K. Ya., "Stipulation of Heat Influxes in Numerical Experiments Using a Thermotropic Model," TRUDY GGO, No 256, 1970.

5. Rubinshteyn, Ye. S., "Mean Latitudinal Air Temperatures on the Earth and Their Relationship to Climatic Change," TRUDY GGO, No 269, 1970.

6. Khanevskaya, I. V., TEMPERATURNYY REZHIM SVOBODNOY ATMOSFERY NAD SEVERNYM POLUSHARIYEM (Temperature Regime of the Free Atmosphere Over the Northern Hemisphere), Leningrad, Gidrometeoizdat, 1968.

7. Khanevskaya, I. V., Bushkanets, G. S., "General Patterns of Spatial Distribution of Temperature in the Free Atmosphere of the Southern Hemisphere," TRUDY NIIAK (Transactions of the Scientific Research Institute of Aeroclimatology), No 80, 1972.

8. Cess, R. D., "Climate Change: An Appraisal of Atmospheric Feedback Mechanisms Employing Zonal Climatology," J. ATMOS. SCI., Vol 33, No 10, 1976.

9. Lian, M. S., Cess, R. D., "Energy Balance Climate Models: A Reappraisal of Ice-Albedo Feedback," J. ATMOS. SCI., Vol 34, No 7, 1977.

10. North, G. R., "Analytical Solution to a Simple Climate Model With Diffusive Heat Transport," J. ATMOS. SCI., Vol 32, No 7, 1975.

11. North, G. R., "Theory of Energy-Balance Climate Models," J. ATMOS. SCI., Vol 32, No 11, 1975.

12. Ramanathan, V., "Radiative Transfer Within the Earth's Troposphere and Stratosphere: A Simplified Radiative-Convective Model," J. ATMOS. SCI., Vol 33, No 7, 1976.

13. Sellers, W. D., "A New Global Climatic Model," J. APPL. METEOROL., Vol 12, No 2, 1973.

14. Smagorinsky, J., "Global Atmospheric Modeling and the Numerical Simulation of Climate," WEATHER MODIFICATION, edited by W. N. Hess, John Wiley and Sons, N. Y., 1974.

UDC 551.512.2

APPLICATION OF THE TEACHING MODEL METHOD IN AN INVESTIGATION OF THE MOTION OF A TROPICAL CYCLONE

Moscow METEOROLOGIYA I GIDROLOGIYA in Russian No 6, Jun 80 pp 49-56

[Article by T. B. Rostkova and Candidate of Physical and Mathematical Sciences A. Ye. Ordanovich, Moscow State University, submitted for publication 30 October 1979]

[Text]

Abstract: A determination of the parameters characterizing a tropical cyclone (TC) and the medium surrounding it on the basis of available observations is of great interest for subsequent prediction of the motion of TC. In this connection the authors propose application of the teaching model method to the investigation of cyclone trajectories. The method is essentially as follows. In order to determine the earlier unknown parameters of the system of equations describing the motion of a TC use is made of its trajectory, known up to some moment in time. With the receipt of new data the values of the parameters are corrected, which makes it possible to take their nonstationary state into account. The teaching model method is tested in the example of motion of a cyclone in linear pressure fields with latitudinal and meridional arrangement of the isohypses.

A study of the dependence of the trajectory of a tropical cyclone (TC) on different parameters characterizing both the cyclone itself and the medium surrounding it, as well as the determination of these parameters on the basis of available observations, is of great interest for subsequent prediction of the motion of a TC.

As is well known, existing methods for predicting the trajectories of TC can be divided into two large classes: statistical and hydrodynamic methods. Statistical forecasting methods [2] generalize already accumulated experimental data on the basis of some a priori assumptions concerning the nature of motion of TC.

These methods, in essence, do not make it possible to investigate the influence of parameters of TC and the surrounding medium on the trajectory under new nonstandard conditions without preliminary accumulation of the corresponding statistical material. In this case it is better to use hydrodynamic methods which are based on use of the equations of hydrodynamics which are somehow simplified [1]. A solution of these equations with some values of the parameters obtained from observations gives the TC trajectory. The principal merit of hydrodynamic methods is the possibility for investigating the dependence of the cyclone trajectory on the parameters of the corresponding equations. However, many parameters, such as the extent and intensity of the TC, are unknown to us in advance and can change considerably during its evolution. Moreover, some characteristics of tropical cyclones (such as the drag coefficient, see [3-5, 8]) can be obtained as a result of direct meteorological observations.

In this connection it is proposed that the teaching model method be applied in an investigation of a TC trajectory [7]. Essentially, in this method for determining the earlier unknown parameters of the system of equations describing the motion of a cyclone use is made of its trajectory, known up to some moment in time. The resulting values of the parameters can be used in forecasting. Some parameters can be stipulated a priori, which makes it possible to investigate the dependence of the prognostic trajectory on them. As a merit of the method we should note that the receipt of new data on the motion of a TC makes it possible to correct the parameters, improving their evaluation and taking into account a possible nonstationary state.

This article is devoted to an exposition of the teaching model method applicable to an investigation of the trajectories of tropical cyclones and testing of this method for some model situations.

Now we will examine the essence of the method in greater detail. Assume that there is an object whose state is described by the vector $\overline{Y}(t)$ when it is acted upon by the controlling effects vector $\overline{X}(t)$. The $\overline{X}(t)$ vector is determined in the time interval $0 \leqslant t \leqslant T$ and the values of the $\overline{Y}(t)$ vector are known at some definite moments in time t_i within this interval. In this case the $\Delta t_i = t_{i+1} - t_i$ value is not mandatorily a constant, but

$$\sum_{i=1}^{\Lambda} \Delta t_i = T.$$

As a model of the object we use the system of differential equations

$$\dot{\overline{Y}}(t) = f(\overline{X}(t),\ \overline{Y}(t), \overline{c}), \tag{1}$$

where $\overline{X}(t)$ is the vector of external effects known from measurements, $\overline{Y}(t)$ is the vector of state of the model, similar in structure to the vector of state of the investigated object $\overline{Y}(t)$, $\overline{c}$ is the still unknown vector of coefficients -- the parameters of the model.

Some of these parameters can be stipulated a priori; the others must be determined and are selected in such a way that the vectors of state of the model and investigated object are close. For this purpose we form the "mismatch" vector

$$\bar{\varepsilon}(t_i) = \bar{Y}(t_i) - \hat{\bar{Y}}(t_i)$$

for those moments in time t_i for which the state of the object is known and we form some functional $J[\bar{\varepsilon}(t_i), \bar{c}]$ in such a way that it has a minimum when

$$\bar{\varepsilon}(t_i) = 0. \tag{2}$$

Since the $\bar{Y}(t_i)$ vector is dependent on $\bar{c}$, accordingly the vector $\bar{\varepsilon}(t_i)$ and the functional $J[\bar{\varepsilon}(t_i), \bar{c}]$ are functions of the $\bar{c}$ vector. In this case the minimum of the functional $J[\bar{\varepsilon}(t_i), \bar{c}]$ with a change in the vector of the parameters $\bar{c}$ can serve as a criterion of the closeness of the state of the model $\bar{Y}(t_i)$ and the object $\hat{Y}(t_i)$. The components of the vector c, guaranteeing the minimum of the functional J, will be considered parameters of the system.

We will examine the solution $\bar{Y}(t_i)$ of the system of equations (1) with the known vector $\bar{X}(t_i)$, the coinciding initial states of the system and object $\bar{Y}(t_1 = 0) = \hat{Y}(t_1 = 0)$ and some arbitrary initial value of the vector of parameters $\bar{c}_1$ (see figure). In this case the components of the mismatch vector $\bar{\varepsilon}(t_i)$ can differ greatly from zero. In order to find the optimum value of the c^* vector we use the condition of the minimum of the function

$$\nabla_{\bar{c}} J[\bar{\varepsilon}(t_i), \bar{c}] = 0. \tag{3}$$

Equation (3) as a rule is not solved analytically. In such a case it is necessary to use one of the algorithms of the successive approximations method, for example [7].

$$\bar{c}_{n+1} = \bar{c}_n - \gamma\nabla_{\bar{c}} J[\bar{\varepsilon}(t_i), \bar{c}_n], \tag{4}$$

where γ is a matrix stipulating the values of the intervals in different coordinates, n is the number of the interval.

The new value of the vector $\bar{c}_{n+1}$ which is obtained is used again for obtaining the vector $Y(t_i)$; we compute $\bar{\varepsilon}(t_i)$, then $\nabla_{\bar{c}} J[\bar{\varepsilon}(t_i), \bar{c}]$, etc. The process is continued until the difference between the two successive values of the c vector attains a stipulated accuracy. The resulting optimum vector $\bar{c}^*$ can then be used for predicting the state of the system at the time $t_{i+1} \bar{\lambda} T + \Delta t_i$. If in this case new data are received on the state of the object $\hat{Y}(t_{i+1})$ (the vector $\bar{X}(t_i)$ as before is considered known) the teaching model method makes it possible to correct the value of the c^* vector using the same procedure, but as a zero approximation we now use the value of the $\vec{c}^{\,*}$ vector obtained for the preceding time interval.

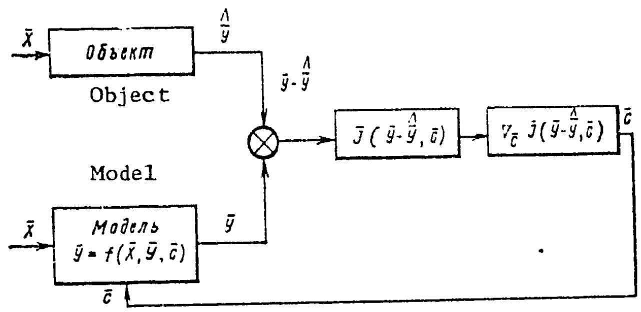

Fig. 1. Diagram of operation of teaching model method.

KEY:
1. Object
2. Model

In application to a tropical cyclone as the components of the $\bar{X}(t)$ vector we can use the known values of the forces acting on the tropical cyclone or the characteristics of the meteorological fields; as the vectors $\bar{Y}(t_i)$ and $\bar{Y}(t_i)$ it is possible to use the coordinates of the center of the cyclone known experimentally and computed from the model; as the components of the $\bar{c}$ vector it is possible to use different parameters, such as the extent and intensity of the tropical cyclone, the friction and drag coefficients, etc. In addition, the components of the $\bar{c}$ vector can be the parameters characterizing the surrounding medium, such as the coefficients of expansion of the field of isobaric heights of the steering current into a series.

We will examine the functioning of the teaching model method in the specific example of determination of the parameters of a tropical cyclone moving in a linear stationary pressure field. Following I. G. Sitnikov [6], we will assume that its motion conforms to the equations

$$\begin{cases} \dot{x} = -\frac{g}{l} m^2 \frac{\partial H(t)}{\partial y} - \alpha m^2 \frac{\partial}{\partial y}\left(m^2 \frac{g}{l} \Delta H(t) + l\right) \\ \dot{y} = \frac{g}{l} m^2 \frac{\partial H(t)}{\partial x} + \alpha m^2 \frac{\partial}{\partial x}\left(m^2 \frac{g}{l} \Delta H(t) + l\right), \end{cases} \quad (5)$$

where x,y are the coordinates of the center of the TC, H(t) is the height of the isobaric surface of the steering current at the level 500 mb at the center of the TC, m is the parameter of distortion of a cylindrical cartographic surface, l is the Coriolis parameter, g is the acceleration of free falling, α is a parameter proportional to the square of the radius of the TC.

All the derivatives are taken at the point of the center of the TC. The origin of coordinates is situated at the point of intersection of the equator with the meridian 120°E; the OX-axis is directed eastward along the equator, the OY-axis is directed northward along the meridian. The first terms in equations (5) describe the motion of the cyclone under the influence of the steering current; the second describe motion as a result of interaction of the fields of the current and cyclone; the third describe the motion caused by the Rossby effect. The equations contain only the parameter characterizing the extent of the tropical cyclone.

The external field H(t) is considered stipulated. The method for describing this field and computing its derivatives for an arbitrary point constitutes an individual complex problem. Usually in working with hydrodynamic methods the H(t) field and its derivatives are determined by numerical methods at the points of intersection of a grid covering a large area, but for use of the teaching model method it is more convenient to have an analytical stipulation of the field because system (5), as will be seen from the text which follows, must be differentiated for α. Accordingly, we will stipulate the H(t) field in the form of a third-degree polynomial relative to the coordinates x, y of the center of the TC:

$$H(t) = H_1(t) + H_2(t)x + H_3(t)y + H_4(t)x^2 + H_5(t)xy + H_6(t)y^2 + H_7(t)x^3 + H_8(t)x^2y + H_9(t)xy^2 + H_{10}(t)y^3. \quad (6)$$

Here the coefficients H(t) are computed by the multiple linear regression method [1]. For this purpose the field values $H(t_i)$ at ten points with known coordinates situated around the center of the TC at a distance from 700 to 1,000 km from it are read from the pressure pattern map at each moment in time t_i. It is dangerous to place these points closer to the center of the tropical cyclone, since at small distances the field of the cyclone itself will substantially distort the steering current field. It makes no sense to place them at a greater distance because the data at points at a distance of more than 1,000 km from one another correlate poorly with one another [1]. The values of the H parameter, and also the coordinates for each of the ten points, are substituted into equation (6) and thus we have a system of ten equations for determining the ten coefficients $H_j(t_i)$. In order to take into account the temporal variability of these coefficients the H(t) values for one and the same points are read at the two successive moments in time t_i and t_{i+1}. A system of linear equations is solved for each of these moments and the $H_j(t_{j+1})$ values are determined. Then we use linear interpolation

$$H_j(t) = \frac{H_j(t_{i+1}) - H_j(t_i)}{t_{i+1} - t_i}\, t + H_j(t_i),$$

where $t_i \leqslant t \leqslant t_{i+1}$.

Now we will examine the sense of all the parameters entering into system (5) from the teaching model method in greater detail and we will indicate ways to solve it. The expansion coefficients of the $H_j(t)$ field will be considered components of the controlling effects

$$\overline{X}(t) = \{H_1(t), H_2(t), \ldots, H_{10}(t)\}.$$

The components of the vectors of state $\hat{Y}(t_i)$ and $\bar{Y}(t_i)$ will be the coordinates of the center of the TC read from the map and computed using the model:

$$\hat{Y}(t_i) = \{\hat{x}(t_i), \hat{y}(t_i)\},$$

$$\bar{Y}(t_i) = \{x(t_i), y(t_i)\}.$$

The trajectory read from the map will be called the standard trajectory and the coordinates corresponding to it $\hat{x}(t_i)$, $\hat{y}(t_i)$ will be called the standard coordinates. The c vector in this case is replaced by the scalar α because system (5) does not contain any other parameters of the TC. As the functional J we take the standard deviation of the computed coordinates of the center of the TC -- x, y -- from the standard coordinates:

$$J = \sum_{i=1}^{N} [(x(t_i) - \hat{x}(t_i))^2 + (y(t_i) - \hat{y}(t_i))^2]. \tag{7}$$

The α parameter will be determined using the Newton algorithm [7]:

$$\alpha_{n+1} = \alpha_n - \gamma \frac{\partial J}{\partial \alpha}(x, y, \alpha_n), \tag{8}$$

where $\gamma = \left(\frac{\partial^2 J}{\partial \alpha^2}\right)^{-1}$.

In order to determine the derivatives $\partial J/\partial\alpha$ and $\partial^2 J/\partial\alpha^2$ it is necessary to know the derivatives of the coordinates of the center of the cyclone x and y relative to α. The following procedure is used for their computation. System (5) is differentiated twice for α; the derived new equations are joined to the former equations and we solve a system of six equations with six unknowns x, y,

$$\frac{\partial x}{\partial \alpha}, \quad \frac{\partial y}{\partial \alpha}, \quad \frac{\partial^2 x}{\partial \alpha^2}, \quad \frac{\partial^2 y}{\partial \alpha^2}.$$

The standard coordinates are stipulated with an interval of one day. Thus, the standard trajectory is constructed using points whose number is equal to the number of days of life of the TC. The model is constructed in such a way that the identification, that is, the determination of the optimum parameter α^*, is accomplished first using two points. A prediction of the trajectory for 24 hours is given for the determined α^* value; then this value is used as the initial value for identification on the basis of three points, etc. The value of the α^*_n parameter is deemed to be optimum if computation of the next α_{n+1} value gives a radius of the cyclone r_{n+1} differing from the preceding value by not more than 10 km.

As indicated above, the functioning of the teaching model method is considered in model problems of the motion of a TC in a linear pressure field. A computer experiment was carried out for the linear field H(t), stipulated by the formula

$$H(t) = H_1(t) + H_2(t)x + H_3(t)y.$$

The isohypses of such a field are straight lines. The gradient $\partial H(t)/\partial y = 2$ m/degree $= 1.805 \cdot 10^{-5}$ was stipulated for a stationary field with a latitudinal arrangement of isohypses. Such a field was constructed graphically; then, in accordance with the method described above, we make a survey of the data and the coefficients $H_1(t), \ldots, H_{10}(t_i)$ are computed by solution of a linear system of ten equations. In this case the $H_1(t_i)$ value is equal to $5.86 \cdot 10^{-3}$, the values $H_3(t_i) = \partial H(t_i)/\partial y$ fall in the range from $1.940 \cdot 10^{-5}$ to $1.947 \cdot 10^{-5}$ and all the remaining coefficients are close to zero.

Table 1

Errors in Identification and Prediction for Motion of TC in Fields With Latitudinal (Left) and Meridional (Right) Arrangement of Isohypses

№	Δx м	Δy м	$\Delta R_{и}$ м 1	$\Delta R_{п}$ м 2	Δx м	Δy м	$\Delta R_{и}$ м 1	$\Delta R_{п}$ м 2
2	5,59	17,4	18,3	21	$1.46 \cdot 10^{-4}$	523	523	502
3	10	16,4	21,3	86,6	$4.37 \cdot 10^{-5}$	565	565	322
4	24	24,8	36	160	$6.31 \cdot 10^{-5}$	487	487	321
5	37,3	56,8	68,9	239	$8 \cdot 10^{-5}$	507	507	1550
6	53,6	69,2	92,7	214	$9{,}6 \cdot 10^{-5}$	419	419	1600
7	63,8	61,3	101	380	$1.14 \cdot 10^{-4}$	404	404	1830
8	99,6	55,6	130	441	$5{,}68 \cdot 10^{-4}$	953	953	794
9	125	50	148	334	$1.47 \cdot 10^{-4}$	863	863	101

KEY:
1. Identification
2. Prediction

As the standard trajectory we used the motion of a TC along latitude 10° with a velocity of 30.8 km/hour. The selected initial value of the radius was 300 km, which corresponded to a value $\alpha(t_1 = 0) = 6.1354 \cdot 10^3$ km^2. It is clear that with this stipulation of the field the α parameter enters only into the first equation of system (5); however, along the OY-axis the velocity with zero initial conditions is equal to zero. We will evaluate the terms in this equation, taking into account that

$$\frac{\partial l}{\partial y} \approx 2 \cdot 10^{-11} (c \cdot м)^{-1}, \quad m = 9{,}38 \cdot 10^{-2}, \quad \alpha = \left(\frac{r}{3.83}\right)^2,$$

$$\frac{\partial H(t_i)}{\partial y} = 1.94 \cdot 10^{-5}.$$

The first term, representing the velocity of the steering current, is equal to 23.71 km/hour; the third, expressing the Rossby effect for a cyclone with the radius r = 300 km, is equal to 4.13 km/hour. Thus, the velocity of the TC for this case is equal to 27.84 km/hour, that is, is too low in comparison with the standard value (30.8 km/hour). As indicated above, the identification was made first using the first two points of the standard trajectory. In this case the functional J (formula (7)) contains two terms (N = 2), of which the first is equal to zero, since the coordinates of the first points of the standard and computed trajectories coincide. After two intervals, according to the Newton algorithm (8), the cyclone radius changed up to 1,174 km. Since a uniform motion was selected as the standard and the field was stationary, with identification on the basis of three, four, etc. points with the choice as an initial approximation $\alpha(t_1 = 0)$ of a value corresponding to the radius r = 1,174 km, the radius of the TC did not experience further change. The Rossby effect for this case gives a velocity increment of approximately 6.7 km/hour. The mean identification errors for the coordinates are

$$\Delta x = \frac{1}{N}\sum_{i=1}^{N}|x(t_i) - \hat{x}(t_i)|, \quad \Delta y = \frac{1}{N}\sum_{i=1}^{N}|y(t_i) - \hat{y}(t_i)|,$$

and also for the radius-vector $\Delta R_1 = \frac{1}{N}\sum_{i=1}^{N}|R(t_i) - \hat{R}(t_i)|$,

drawn from the origin of coordinates at the center of the TC, are given in the left part of the table. Here N is the number of points used in identification,

$\Delta R_1 = \frac{1}{N}\sum_{i=1}^{N}|R(t_{i+1}) - \dot{R}(t_{i+1})|$ is the error in a 24-hour prediction. In existing models the errors in determining the radius-vector are 200-300 km for 24 hours. The small error obtained for this model is associated primarily with stipulation of a simple field and a suitable standard trajectory.

In computing the motion of a TC in a stationary field with a meridional arrangement of the isohypses and a stipulated gradient $H_2 = \partial H(t)/\partial x$ = 2.14 m/degree as the initial value of the cyclone radius we used the same value r = 300 km. In this case the standard trajectory was a precise solution of system (5) for r = 900 km. The field coefficients $H_j(t_i)$ were not computed for this case, but were simply stipulated numerically. As in the preceding case, for identification it was sufficient to use two intervals in the Newton algorithm, after which the radius attained 900.5 km and then did not change. The identification and prediction errors are given in the right part of the table. It can be seen that the greatest contribution to the identification error is from the error along the OY-axis. The value of this error agrees with the accuracy in stipulation of points on the standard trajectory, which is equal to 1 km. The error along the OX-axis is substantially smaller due to the identification. The substantial difference in the errors Δx between the two considered cases is attributable to the fact that in the second case the H(t) field is stipulated precisely, whereas in the first case it is computed using a system of linear equations, which introduces an additional error.

The standard trajectory was "spoiled" for the purpose of complicating the problem. The form of the trajectory remained as before, but motion along it was stipulated with a velocity exceeding the precise velocity, or not attaining the precise velocity. Due to an inexact survey from the graph of standard coordinates $x(t_i)$; $y(t_i)$ the form of the trajectory was slightly distorted. The results of computation of the radius of the TC and the identification errors indicated that the radius values for a "rapid" cyclone were exaggerated, whereas for a "slow" cyclone they were too low in comparison with the value r = 900 km, which agrees well with the qualitative picture of motion. In a stationary pressure field with a meridional arrangement of the steering current, giving the principal contribution to the motion of a TC, a constant velocity is directed along the OY-axis. It can be seen from equations (5) that the y-component of cyclone velocity is not dependent on cyclone extent, whereas the value of the x-component is governed by the Rossby effect. Accordingly, the total velocity of the TC is also essentially dependent on it. The influence of the Rossby effect on cyclone motion increases with an increase in its extent, which results in an increase in velocity. Vice versa, in order for a cyclone to move at a greater velocity it must have greater dimensions. The principal contribution to the identification error ΔR_1 as before is from the y-component. It is easy to see that the distortion of the standard trajectory led to a substantial increase in errors. It therefore follows that a considerable part of the errors in computing the trajectories can be attributed to the fact that the selected equations of motion do not take into account all the factors acting on the TC.

Thus, in this study we have demonstrated the possibility of using the teaching model method for determining TC parameters which cannot be measured directly but which are necessary for predicting its trajectory. The computer experiments described in the article are of independent interest because they make it possible to determine the parameters of the TC during its motion in simple pressure fields of the Trades zone type.

BIBLIOGRAPHY

1. Belov, P. N., CHISLENNYYE METODY PROGNOZA POGODY (Numerical Weather Forecasting Methods), Leningrad, Gidrometeoizdat, 1975.

2. Gruza, G. V., Gres'ko, P. D., STATISTICHESKIYE METODY PROGNOZA PEREMESHCHENIYA TROPICHESKIKH TSIKLONOV ATLANTICHESKOGO OKEANA (Statistical Methods for Predicting the Movement of Tropical Cyclones in the Atlantic Ocean), Leningrad, Gidrometeoizdat, 1977.

3. Nesterova, A. V., Nesterov, A. V., "One Model of Motion of a Tropical Cyclone." In press.

4. Pavlov, N. I., "Correlation Between the Intensity and Nature of Motion of Typhoons and the Thermal Regime of the Surface Layer of the Ocean," TAYFUN-75 (Typhoon-75), Vol 2, Leningrad, Gidrometeoizdat, 1978.

5. Purganskiy, V. S., "Method for Computing the Trajectory of Motion of Convective Eddies of Great Intensity," TRUDY TsAO (Transactions of the Central Aerological Observatory), No 75, 1967.

6. Sitnikov, I. G., "Experience in Numerical Forecasting of the Trajectories of Tropical Cyclones in the Republic of Cuba," TRUDY GIDROMETTSENTRA SSSR (Transactions of the USSR Hydrometeorological Center), No 29, 1968.

7. Tsypkin, Ya. Z., ADAPTATSIYA I OBUCHENIYE V AVTOMATICHESKIKH SISTEMAKH (Adaptation and Teaching in Automatic Systems), Moscow, Nauka, 1968.

8. Kuo, H. L., "Motions of Vortices and Circulating Cylinder in Shear Flow with Friction," J. ATMOS. SCI., Vol 26, No 3, 1969.

UDC 551.509.6

POSSIBLE MECHANISMS OF ICE FORMATION ON SILVER IODIDE PARTICLES IN A DIFFUSION CHAMBER AND IN A FOG CHAMBER

Moscow METEOROLOGIYA I GIDROLOGIYA in Russian No 6, Jun 80 pp 57-63

[Article by Candidate of Chemical Sciences B. Z. Gorbunov, N. A. Kakutkina, Candidate of Technical Sciences K. P. Kutsenogiy, N. M. Pshenichnikov, Institute of Chemical Kinetics and Combustion, submitted for publication 19 September 1979]

[Text]

Abstract: The authors have ascertained the dependence of the fraction of silver iodide particles forming ice crystals on supersaturation for different temperatures in the chamber and particle sizes. The possible mechanisms of ice formation on silver iodide particles in a diffusion chamber and in a fog chamber are analyzed.

The process of formation of ice crystals in a supercooled fog has still not been fully studied. The formation of ice on aerosol particles in dependence on environmental conditions and the properties of the particles themselves can transpire with different mechanisms [9]. With different ice formation mechanisms supersaturation exerts a different influence on the probability of appearance of ice crystals [8]. This makes it possible to obtain information on the mechanism of ice formation by investigating the dependence of the ice-forming activity on supersaturation.

A great many studies [6, 7, 11, 12, 14] have been devoted to investigation of the influence of supersaturation on the ice-forming activity. However, as indicated in [4], due to an incorrect procedure in ascertaining the volume effect the results of these investigations can be greatly distorted. In addition, in these studies the investigation of the influence of supersaturation was made in a narrow range of temperatures and particle sizes.

In this article, using the method described in [4], we investigate the dependence of the ice-forming activity of silver iodide particles on supersaturation in a broad range of temperatures and particle sizes. An analysis of the possible mechanism of ice formation on silver iodide particles is made on the basis of these data.

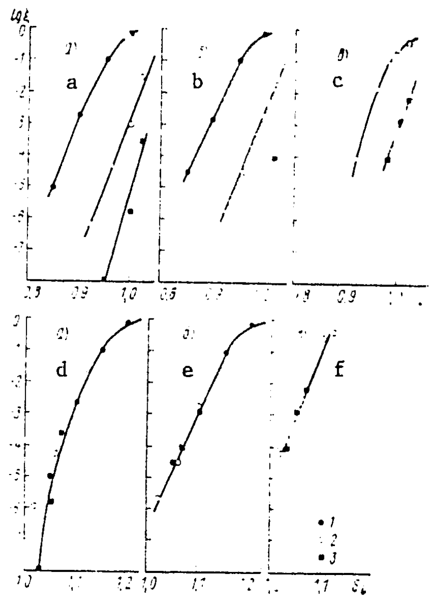

Fig. 1. Dependence of fraction of AgI particles on supersaturation relative to water (at top) and ice (at bottom). a) R_3 = 250 A, b) R_3 = 380 A, c) R_3 = 640 A. 1) T = -20°C, 2) T = -10°C, 3) T = -5°C.

An investigation of the influence of supersaturation was made using thermocondensation aerosols of silver iodide [1]. The value of the ice-forming activity of aerosols was characterized by the fraction of active particles ξ and was determined as the ratio of the number of ice particles forming in a sample to the number of aerosol particles in it [1].

Typical dependences of the fraction of active particles on supersaturation relative to water (S_w) are shown in the upper part of Fig. 1. With any mean cubic radius of silver iodide particles (R_3) and temperature (T) an increase in S_w leads to a marked increase in ξ. With a decrease in temperature with a constant S_w ξ also increases.

In the lower part of Fig. 1 these very same curves were reconstructed in dependence on supersaturation relative to ice. It is a remarkable fact that all the points for temperatures -5, -10 and -20°C fit onto one monotonic curve for each particle size. The deviation of points from the curve does not exceed the errors in the experimental determination of ξ. Qualitatively this same result was obtained in a study by Huffman [11]. However, quantitatively the results published by Huffman differ from those obtained in our study. In [11] the slope of the curve of the dependence of the probability of formation of a crystal on S_i is equal to 4-4.5 for a thermocondensation aerosol of silver iodide. This is considerably less than in our study, in which the slope is equal to 7-9. An inaccuracy in making allowance for the depletion effect is the reason for the weaker dependence of ice-forming activity on supersaturation obtained in [11] relative to that obtained in our study.

Data on the dependence of the ice-forming activity on supersaturation make it possible to detect the most probable mechanisms of ice formation. In the diffusion chamber the ice crystals can be generated on aerosol particles by means of the following principal mechanisms:
-- sublimation;
-- condensation on a water droplet particle with its subsequent freezing;
-- adsorption on a particle of a polymolecular film with subsequent freezing.

Depending on what is obtained as a result of interaction between the aerosol particle and water vapor -- an ice nucleus, liquid droplet or adsorbed film, vapor pressure exerts a different influence on the probability of generation of a crystal. Accordingly, by analyzing the dependence of ξ on supersaturation conclusions can be drawn on exactly how the formation of crystals comes about.

The nature of the dependence of ξ on supersaturation during sublimation and condensation with subsequent freezing is known [8]. However, it is not clear how supersaturation should exert an influence on the probability of the formation of ice by means of adsorption with subsequent freezing. In a general case this dependence can be very complex. Vapor pressure should exert an influence both on the first stage in the process -- adsorption of the film, and on the second -- its freezing. With a change in pressure there is a change in the equilibrium thickness of the film [5]. This, in turn, can result in a change in the properties of the film, such as the specific free energy at the ice nucleus- film interface. In addition, at low vapor pressures the ice nucleus may not be completely covered with the film. All this greatly complicates computation of the expressions for the dependence of the probability of ice formation by means of adsorption with subsequent freezing on supersaturation. However, with some simple assumptions this dependence can be derived.

We will assume that a quite thick film has been adsorbed on the particles so that the ice nucleus of critical size is completely immersed in it. Also assume that the specific free energy at the ice nucleus - film interface does not change with distance from the backing to the film surface and is equal to σ_{ia}. We will write the change in free energy ΔG during the formation of an ice nucleus in the adsorbed film:

$$\Delta G = (\mu_i - \mu_a)\ V_i n_i + A_{ia}\sigma_{ia} - A_{ci}(\sigma_{ca} - \sigma_{ci})\ m. \qquad (1)$$

Here V is volume, A is the surface, μ is the chemical potential; the subscripts i, a and c apply to ice, the adsorbed film and the backing respectively.

In accordance with [8]

$$\mu_i = kT \ln P_i, \tag{2}$$

where P_i is the pressure of the saturated vapor over the plane surface of the ice.

The adsorbed film is in thermodynamic equilibrium with the vapor at the pressure P, different for different film thicknesses [5]. Accordingly, the chemical potential of the molecules in the adsorbed film must be equal to the chemical potential of the molecules in the vapor:

$$\mu_a = kT \ln P. \tag{3}$$

Substituting (2) and (3) into (1) and expressing V and A through the radius of the dome-shaped nucleus, for the critical radius of the ice nucleus we obtain [8]

$$r^* = \frac{2\sigma_{ia}}{n_i kT \ln (P/P_i)}.$$

The work of formation of a critical ice nucleus ΔG^* is equal to

$$\Delta G^* = \frac{16\pi}{3} \frac{\sigma_{ia}^3 f(m, x)}{(n_i kT \ln (P/P_i))^2},$$

where $x = R/r^*$, R is the radius of the aerosol particle. This expression is almost identical to the expression for the work of formation of a critical ice nucleus by sublimation. In this case the only difference is that the quantity of specific free energy at the ice-vapor interface σ_{iv} is replaced by the specific free energy at the ice-film discontinuity σ_{ia}. Thus, in the formation of ice by the freezing of the adsorbed polymolecular film supersaturation also exerts an influence on the probability of ice formation, as in the sublimation mechanism. However, the r^* values and the work of formation of a critical ice nucleus in the case of freezing of the film should be considerably less than in the case of sublimation, since $\sigma_{ia} < \sigma_{iv}$.

Knowing the theoretical dependences on supersaturation for all possible ice formation mechanisms, we will attempt, after analyzing the experimental dependences, to determine by what mechanism the ice is formed on the silver iodide particles.

First we will examine the mechanism of condensation with subsequent freezing of a droplet. The nature of the influence of supersaturation in the formation of ice by this mechanism is dependent on what stage of the process is slower -- the stage of vapor condensation or the stage of freezing of a droplet. When the stage of droplet freezing is limited in time the probability of ice formation in general must not be dependent on vapor pressure [8]. The experiment shows that ξ is dependent on pressure (Fig. 1). Therefore, if ice formation occurs in accordance with the condensation mechanism with subsequent droplet freezing, it is only possible to limit the vapor condensation stage. In this case the problem of ice nucleation is directly theoretically dependent only on the supersaturation relative to water and only indirectly through the pressure of saturated vapor -- on temperature. This means that the curves for the dependence of ξ on S_w for different temperatures must fit on a single curve for each particle size. Figure 1 shows that this is not so. Each temperature has its $\xi - S_w$ curve. It can therefore be concluded that the formation of ice on silver iodide particles does not occur in accordance with the mechanism of condensation with subsequent freezing.

In the case of ice nucleation by means of sublimation or freezing of an adsorbed film the probability is directly dependent only on the supersaturation relative to ice. In other words, the $\xi - S_i$ curves for different temperatures must fit on a single curve. This is observed experimentally (Fig. 1). Thus, an analysis of the dependence on supersaturation indicates that the formation of ice on silver iodide particles in a diffusion chamber occurs either in accordance with the sublimation mechanism or by means of adsorption with the subsequent freezing of a film.

We note that usually an unambiguous conclusion is drawn concerning the sublimation mechanism of ice formation on the basis of dependences of the type shown in Fig. 1. As was demonstrated above, this, in general, is not true.

Experimental dependences of ice-forming activity on supersaturation do not make it possible to ascertain by which of two mechanisms ice is formed on silver iodide particles: sublimation or adsorption with subsequent freezing of the film. However, there are data in the literature on the adsorption of water on silver iodide which support the latter. For example, the formation of a polymolecular quasifluid film was observed on AgI particles with a radius of about 1 μm [5]. For example, with -3°C and $S_w = 1.00$ the film thickness was 100 A. Moreover, phenomena were also observed which the author of [5] interpreted as the nucleation of ice in these films. In addition, the following fact supports adsorption with subsequent freezing. It was discovered in a comparison of the theory for sublimation with experimental data that the radii of AgI particles forming ice crystals are less than the minimum possible radii for the sublimation process, that is, the activity of AgI particles is greater than the limiting value for the sublimation mechanism [10]. This indicates that ice is not formed on AgI particles in accordance with the sublimation mechanism. As was indicated above, the maximum ice-forming activity in the mechanism of adsorption with subsequent freezing is greater than in the sublimation mechanism. Accordingly, if it is assumed that the ice is formed by means of freezing of an adsorbed film, the contradiction between theory and experimental data discovered in [10] is eliminated. This information, together with data on the influence of supersaturation on ice-forming activity, gives basis for assuming that the formation of ice in a diffusion chamber on silver iodide particles occurs in accordance with the mechanism of adsorption with subsequent freezing of a film.

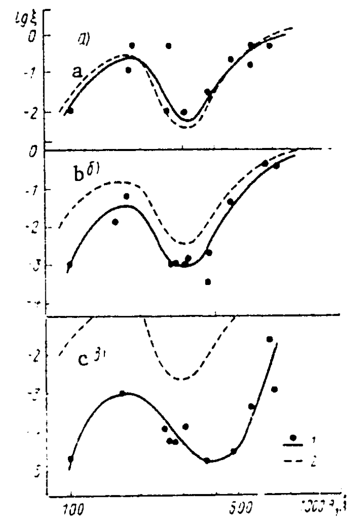

Fig. 2. Dependence of fraction of active AgI particles on mean cubic radius of particles at a temperature -10°C. 1) dependences obtained in a diffusion chamber with supersaturation: a) $S_w = 1.02$, b) $S_w = 1.00$, c) $S_w = 0.96$, 2) dependence obtained in a fog chamber [2].

Table 1

Fractions of Silver Iodide Particles Measured in Fog Chamber or in Diffusion Chamber With Supersaturation Relative to Water S = 1.02

		R, Å 70	200	380	640	700
$T = -20°$ C	lg ξ $S_w = 1.02$	−0.3	−0.2	0	0	0
	lg ξ в камере тумана*	−0.5	−0.2	0	0	−0.1
$T = -5°$ C	lg ξ $S_w = 1.02$	−6.3	−[illegible].5	−4.2	−2.7	−3.3
	lg ξ в камере тумана*	−6.3	−3.4	−5	−2	−2.6

* In fog chamber

Data on the mechanism of ice formation in a diffusion chamber make it possible to obtain information on the process of ice formation under conditions closer to those in clouds -- in a fog chamber. For this purpose we will compare the dependence of ξ on the mean cubic radius of the particles R_3, obtained in a diffusion chamber and in a fog chamber.

Figure 2 shows that the $\xi(R_3)$ curve, obtained in a diffusion chamber with $T = -10°C$ and $S_w = 1.02$, in the entire range of sizes coincides with the curve for a fog chamber at this same temperature. With $S_w = 1.00$ there is also a fair coincidence: the difference in the ξ values measured in a diffusion chamber with $S_w = 1.00$ and a fog chamber almost nowhere exceeds the error in determining $\lg \xi$, equal to 0.4 [4]. However, the averaged curve, drawn through the experimental points, for the diffusion chamber lies somewhat lower than for the fog chamber. The experimental points obtained for the diffusion chamber with $S_w = 0.96$ fall far lower than the dependence $\xi(R_3)$ for a fog chamber. The difference is from 1 to 2.5 orders of magnitude ξ for different R_3.

The nature of the dependence of ξ on R_3 in all cases is the same. In particular, in all the dependences with R_3 = 300-400 A there is a minimum. As was demonstrated before, the reason for the nonmonotonic dependence of ξ on R_3 is the change in the crystalline structure of AgI particles with a change in their radius [3].

At other temperatures the dependence of ξ on R_3 was not determined in detail in the diffusion chamber. However, the ξ values were determined at different supersaturations for several R_3 values. Parallely for these same aerosols we determined the ξ values in the fog chamber. It was found that with -5 and -20°C, the same as at -10°C, the ξ values measured in a diffusion chamber with $S_w = 1.02$, coincide within the limits of experimental error with those measured in a fog chamber (see Table 1). Thus, in the entire temperature range from -5 to -20°C the dependence of ξ on R_3, measured in a fog chamber, coincides with that measured in a diffusion chamber with a supersaturation over water $S_w = 1.02 \pm 0.02$.

Two conclusions follow from a comparison of data from the cloud and diffusion chambers. First, an agreement of the dependences of ξ on R_3 obtained in the diffusion chamber with S_w = 1.00-1.02 with those obtained in the fog chamber in the entire range of particle sizes indicates that in a fog chamber ice formation proceeds in accordance with the same mechanism as in a diffusion chamber. Second, the supersaturation value at which the ξ values coincide with those for the fog chamber is the effective supersaturation value in the fog chamber. Thus, S_w in the fog chamber is equal to 1.00-1.02. Such S_w values in a fog chamber are entirely natural. An S_w value slightly exceeding $S_w = 1$ can be attributed to the contribution of sectors near the evaporating fog droplets to the effective supersaturation. The estimated supersaturation value also shows that significant supersaturations do not arise in the used fog chamber with the admission of vapor. Accordingly, the ξ values obtained in the fog chamber must not differ greatly from those for a real cloud medium.

Thus, the dependences of the ice-forming activity of silver iodide aerosols on supersaturation were obtained at three temperatures and different mean particle sizes. An analysis of these dependences together with data in the literature makes it possible to assume that the formation of ice in both the diffusion chamber and in the fog chamber probably occurs by means of adsorption with subsequent freezing of the adsorbed film.

BIBLIOGRAPHY

1. Baklanov, A. M., Gol'dman, B. M., Gorbunov, B. Z., Kutsenogiy, K. P., Makarov, V. I., Sakharov, V. M., "New Apparatus for Investigating the Ice-Forming Activity of Aerosols," IZV. SO AN SSSR, KHIMIYA (News of the Siberian Department USSR Academy of Sciences, Chemistry), Vol 4, No 9, 1976.

2. Gorbunov, B. Z., Kakutkina, N. A., Kutsenogiy, K. P., Makarov, V. I., "Investigation of the Dependence of the Ice-Forming Activity of a Silver Iodide Aerosol on Dispersivity," IZV. AN SSSR, FIZIKA ATMOSFERY I OKEANA (News of the USSR Academy of Sciences, Physics of the Atmosphere and Ocean), Vol 12, No 12, 1976.

3. Gorbunov, B. Z., Kakutina, N. A., Kutsenogiy, K. P., Moroz, E. M., "Influence of the Size of Silver Iodide Particles on Their Crystalline Structure," KRISTALLOGRAFIYA (Crystallography), Vol 24, No 2, 1979.

4. Gorbunov, B. Z., Kakutkina, N. A., Kutsenogiy, K. P., Pshenichnikov, N. M., "Method for Determining Ice-Forming Activity in a Diffusion Chamber," in press.

5. Barchet, W. R., Corrin, M. L., "Water Vapor Adsorption by Pure Silver Iodide Above Ice Saturation," J. PHYS. CHEM., Vol 76, No 16, 1972.

6. Bolkom, J. E., Young, K. C., "Participant's Report. University of Arizona. Ice Nucleation Workshop, 1975," The Third Intern. Workshop on Ice Nucleus Measurements, Laramie, Wyoming, University of Wyoming, 1976.

7. Cooper, A., "Ice Nucleation Measurements Using a Stober Centrifuge," The Third Intern. Workshop on Ice Nucleus Measurements, Laramie, Wyoming, University of Wyoming, 1976.

8. Fletcher, N. H., THE PHYSICS OF RAINCLOUDS, Cambridge, Cambridge University Press, 1962.

9. Gokhale, N. R., "The Mechanics of Ice Nucleation Induced by AgI Particles in a Supercooled Cloud," PROCEED. 7th INTERN. CONF. ON CONDENSATION AND ICE NUCLEI, Prague, Vienna, 1969.

10. Gorbunov, B. Z., Kakutina, N. A., Koutzenogii, K. P., "Comparison of Experimental Data on Silver Iodide Ice-Forming Activity With the Theoretical Fletcher Models," ABSTRACTS OF THE 9th INTERNAT. CONF. ON ATMOSPHERIC AEROSOLS, CONDENSATION AND ICE NUCLEI, Galway, Ireland, 1977.

11. Huffman, P. J., "Supersaturation Dependence of Ice Nucleation by Deposition for Silver Iodide and Natural Aerosols," Report No AP108, College of Engineering, University of Wyoming, Laramie, 1973.

12. Jiusto, J. E., Lala, G. G., "Suny Diffusion Chamber Measurements and Related Analyses," The Third Intern. Workshop on Ice Nucleus Measurements, Laramie, Wyoming, University of Wyoming, 1976.

13. King, W. D., "Vapor Depletion in Processing Membrane Filters: the Effect of Chamber Parameters," J. APPL. METEOROL., Vol 17, No 10, 1978.

14. Meyer, D., Gravenhorst, G., "A Low Pressure Diffusion Chamber," The Third Intern. Workshop on Ice Nucleus Measurements, Laramie, Wyoming, University of Wyoming, 1976.

UDC 551.465.(47+531)(267)(677)

HORIZONTAL WATER CIRCULATION IN THE SOMALI REGION OF THE INDIAN OCEAN

Moscow METEOROLOGIYA I GIDROLOGIYA in Russian No 6, Jun 80 pp 64-73

[Article by Candidates of Geographical Sciences V. V. Pokudov, V. A. Golovastov and V. P. Tunegolovets, Far Eastern Regional Scientific Research Institute, submitted for publication 25 January 1980]

[Text]

Abstract: On the basis of data from observations made during the period of the international expeditions "Monsoon-77" and "MONEX-Summer" it is shown that a surface anticyclonic circulation occupies a thickness of 200 m. At the 400-m horizon there is a cyclonic circulation on whose western periphery there is transport of waters to the south along the Somali coast. Instrumental observations of currents reveal a multilayered structure of currents over the greater part of the Arabian Sea, including at the equator, where it is a four-layer structure. Inertial oscillations of current velocity have a maximum near 4°N and attain 60 cm/sec.

The detailed study of currents along the western boundaries of the Indian Ocean began relatively recently. This is associated with the detection of a substantial role of the Somali Current in the formation of macroscale deviations of weather over the northern part of the ocean, and in addition, over the entire Southeast Asia region [4].

New investigations carried out during the period of the major international expeditions "Monsoon-73," "Monsoon-77" and "MONEX-Summer" covered the region occupied directly by the Somali Current [2] and its oceanic countercurrent (Fig. 1).

Being a continuation of the South Trades Current, the Somali Current intersects the equator and continues northeastward along the shores of Africa. This is a cold current relative to the surrounding waters. Its development begins in the spring intermonsoonal season and is associated with the activation of cyclonic activity in the southern hemisphere, an intensification of the winds of the Southeast Trades and the velocities of the South Trades Current [3].

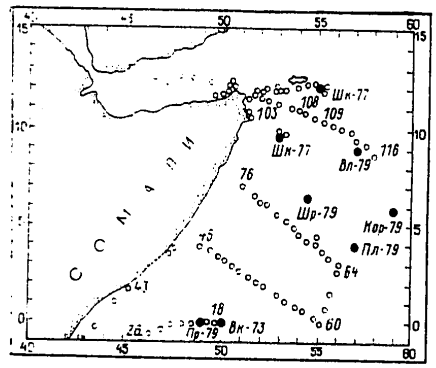

Fig. 1. Map of hydrological survey (stations 18-116; 23 May - 13 July 1977) and regions of placement of buoy stations in 1973, 197/ and 1979.
Шк -- scientific research ship "Yu. M. Shokal'skiy"
Вл -- scientific research weather ship "Volna"
Шр -- scientific research ship "Akademik Shirshov"
Kop -- scientific research ship "Akademik Korolev"
Пл -- scientific research weather ship "Priliv"
Пр -- scientific research weather ship "Priboy"
Bk -- scientific research ship "A. I. Voyeykov"

The first indications of the weak Somali Current to the north of 6°N are already manifested in March at the ocean surface; in April the current velocity attains 86 cm/sec [11]. In the season of the southwesterly monsoon the current velocity increases with transition from the southern to the northern hemisphere. At 4°S it attains values 140 cm/sec, 8°N -- 350 cm/sec. The width and depth of the current also increase from 80 km and 10 m at 4°S to 200 km and 200 m at 8°N [10].

Under the influence of bottom relief, shorelines and Coriolis force the Somali Current at 10-11°N turns eastward and then to the south, and merging with the flow coming from the northeast, forms a closed anticyclonic circulation whose center is situated at 8-9°N, 53°E. The eastern periphery of the mentioned circulation is also interpreted as the Somali Countercurrent with velocities up to 70 cm/sec in the north (9-11°N) and about 30 cm/sec in the south (2-3°N) [8].

A quite reliable picture with some new features of horizontal circulation of waters in the investigated region is given by maps of geostrophic currents (Fig. 2) computed on the basis of observations of the scientific research ship "Yu. M. Shokal'skiy" (May-July 1977) from 200 and 1,000 m (200 m is the lower boundary of the Somali Current [10], 1,000 m is the lower boundary of the main thermocline [3]).

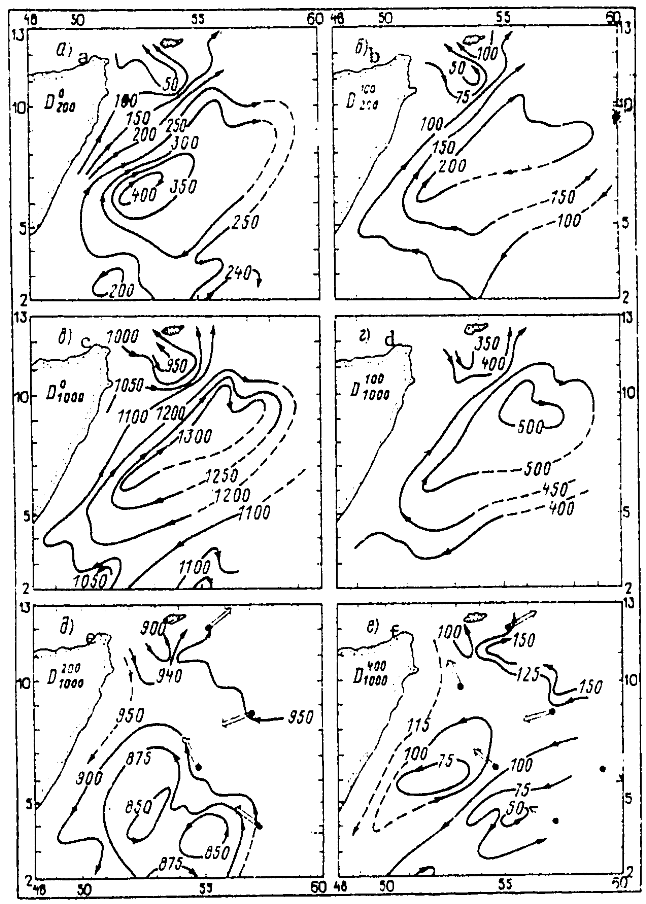

Fig. 2. Maps of geostrophic currents in the summer of 1977, computed from the surfaces 200 m (a, b) and 1,000 m (c, d, e, f) at the horizons: 0 m (a, c), 100 m (b, d), 200 m (e) and 400 m (f).

Figure 2a,b,c,d shows that regardless of the position of the reference surface the maps of circulation of waters at the surface and at the 100-m horizon are identical and in actuality constitute a local anticyclonic circulation. Unfortunately, observations during this period near the shores, where specifically the main flow of the Somali Current develops, were not made. Nevertheless, some of its characteristics can be investigated on the basis of the parameters of movement of waters and their structure at the eastern and northern (near Socotra Island) peripheries.

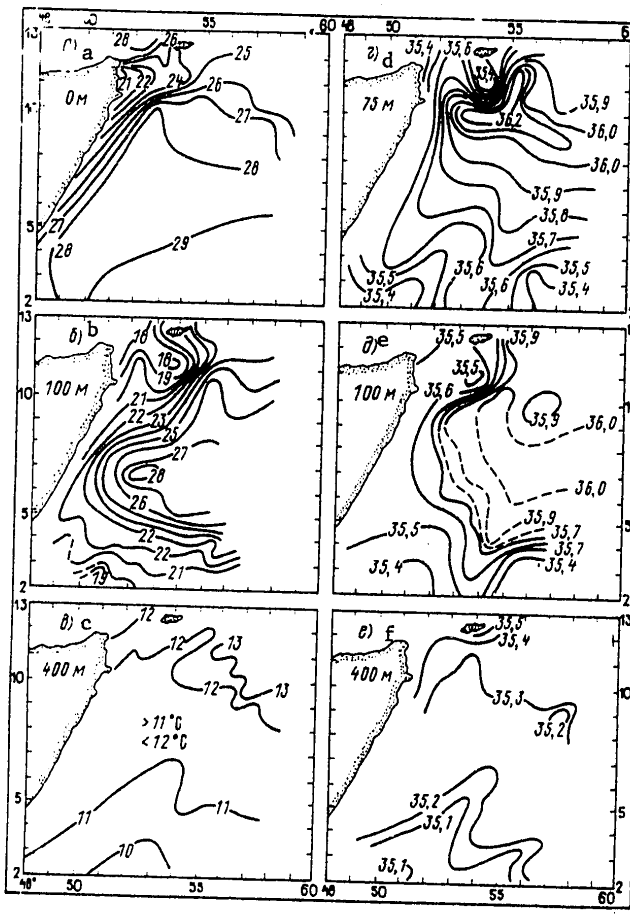

Fig. 3. Temperature distribution in May-July 1977 at horizons 0 (a), 10C (b), 400 m (c) and salinity at horizons 75 (d), 100 (e) and 400 m (f).

The above-mentioned anticyclonic circulation of waters on the maps of horizontal circulation is detected extremely clearly in the layer 0-100 m. As can be seen from the maps, the western periphery of this circulation is not the Somali Current, but a current running to the northeast parallel to the Somali Current. Figure 3a,b,d,e shows that the current on the western periphery of the circulation in this layer transports warmer and more saline waters than the Somali Current. The clearest differences in these currents are detected to the south of Socotra Island in the region 10-11° N, 54-56°E. Here the current on the western periphery of the circulation turns to the east and then to the south and southwest; in the region 3-5°N, 50-52°E it closes the considered circulation. To the south of Socotra Island it is also possible to trace the main flow of the Somali Current, whose easterly direction along 10°N (Fig. 2a,c) at the surface again changes to northeasterly, northerly and then passes to the east of Socotra Island. The existence of these two parallel currents is also confirmed by the horizontal distribution of temperature and salinity and their differences are represented especially clearly in the vertical structure of the waters (Fig. 4). The boundary separating these currents passes between stations 108 and 109, as is indicated by the great horizontal gradients of temperature and salinity. Between these stations the isohalines run vertically downward from the surface to a depth of 150 m.

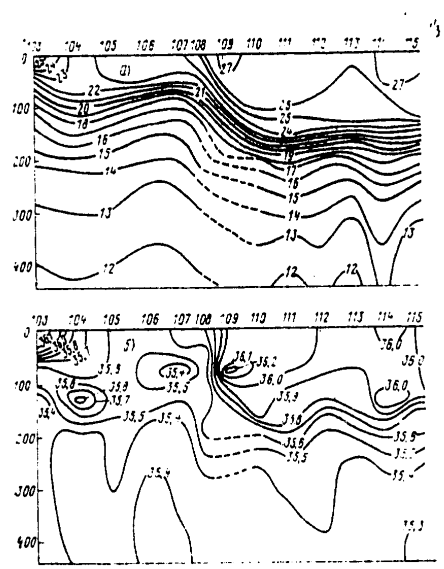

Fig. 4. Vertical distribution of temperature (a) and salinity (b) 10-13 July 1977 on section to south of Socotra Island.

This same Fig. 4 shows that the lower boundary of the upper isothermic layer in the Somali Current is situated at depths 40-50 m (temperatures 23.0-23.6°C), and in the other, warmer current (26.0-27.0°C) -- at depths 100-120 m. In addition, there is a marked difference of salinity at the "cores" of these currents: 35.40-35.50°/oo in the "core" of the Somali Current and

36.10-36.20°/oo in the current on the western periphery of the circulation (here this is already the northern periphery).

Differences in the structure of waters of these currents were also discovered on the basis of the distribution of dissolved oxygen. In the Somali Current (to station 108) the surface quasihomogeneous layer to a depth of 40-50 m contains 4.5-5.0 ml/liter of oxygen, and in the current on the western periphery of the circulation this layer with an oxygen content of 5.0-5.5 ml/liter occupies a depth of 100-120 m. In addition, the layer of maximum vertical gradients of dissolved oxygen under the Somali Current is situated at depths from 40 to 120 m, and under the adjacent current -- from 120 to 200 m.

The above-mentioned characteristics of the vertical distribution of hydrological elements confirm a significant upwelling of waters in the Somali Current to the south of Socotra Island which is evidently observed in the entire extent of this current.

Figure 4 shows that in the region of stations 114-115 there is also a "core" of increased salinity (more than 36°/oo), but already at greater depths, about 120-160 m. This, evidently, is in fact the very same flow of waters of the anticyclonic circulation, but here is has reached greater depths and now has a southerly and southwesterly direction (eastern periphery of the circulation).

A third detail of the circulation of waters in the surface layer of the investigated region is a local cyclonic eddy to the southeast of the strait between Socotra Island and Cape Guardafui (Somalia).

The waters emerging through the mentioned strait, flowing southeastward along the shores of Somalia, on their path encounter the flow of the Somali Current, turn northeastward and run parallel to this current; then at Socotra Island they divide into individual currents. Figure 4 shows that between stations 104 and 105 there is a boundary between the Somali Current and the flow of waters forming the considered cyclonic circulation. The salinity of the latter in the "core" of the flow at depths of 120-150 m is about 35.70-35.80°/oo; at the surface -- about 36.00-36.10°/oo.

Figure 2e,f shows that at the horizons 200 and 400 m the general pattern of the horizontal circulation of waters changes absolutely to the opposite, except for the strait between Socotra Island and Cape Guardafui, where the cyclonic eddy persists at all depths.

In the region of the anticyclonic eddy, which forms the character of circulation of waters in the surface layer, at depths beginning with the horizons 150-200 m it is easy to trace a "two-core" cyclonic eddy (Fig. 2e), which by the 400 m horizon is already divided into two independent, also cyclonic eddies. The waters of these eddies are relatively homogeneous (Fig. 3c,f). In the north of the investigated region the current at the horizons 200-400 m also had an opposite northwesterly direction.

An interesting peculiarity at the considered horizons 200 and 400 m is the absence of the Somali Current over the entire ocean area. Moreover, at these horizons indicators of the subsurface Somali Countercurrent appear at these horizons. This countercurrent is formed, for the most part, by the western periphery of the cyclonic circulation and apparently by the alongshore transport of waters in a southwesterly direction from the already considered strait. It follows from Fig. 2e, and also from the considered vertical distribution of hydrological elements, that the Somali Current does not even reach depths of 200 m.

The considered geostrophic circulation of waters quite reliably reflects the movement of waters over the entire area, but gives no idea concerning the current velocities and their temporal variability. This requires current observations. However, the organization of a network of autonomous buoy stations adequate for constructing a map of currents is virtually impossible even for such a small region.

In 1973, 1977 and 1979 the ships of the Far Eastern Scientific Research Hydrometeorological Institute in the investigated region occupied eight stations with a work duration from 7 to 12 days (Fig. 1). Although the observations were made at individual points, together with geostrophic maps they refine the true picture and help to give some quantitative estimates and current patterns.

In actuality, at all points in the first stationary polygon of the "MONEX-Summer" expedition the direction of the vectors of current velocities at the horizons 200 and 400 m, averaged for the observation period, coincided with the direction of the geostrophic flows which existed in May-July 1977 (Fig. 2e,f). The presence of a deep cyclonic circulation is evidently a characteristic feature of the deep circulation of waters in the Arabian Sea.

In the upper layers there was also some similarity in the direction of the geostrophic currents in 1977 and the averaged velocity vectors of the currents measured by instrumental methods in May 1979. This fact indicates a constancy of the characteristics of surface water circulation -- constant presence of an anticyclonic circulation of waters. Its existence is noted by all researchers; it is traced quite clearly even from satellite photographs [7, 8].

But the position of this surface anticyclonic circulation of waters, having a geostrophic nature, changes from year to year; it is evidently dependent on the intensity of the Somali Current. For example, in May 1979, in a year of anomalously weak development of the Somali Current, it was somewhat displaced eastward. The width of this flow on its western periphery was greater than in 1977 and the intensity of transport of waters was somewhat less (Fig. 5).

The first stationary polygon of "MONEX-Summer" was situated precisely at the center of the surface circulation of waters. The western and northern autonomous buoy stations were situated in the northeasterly flow and the eastern and southern buoy stations were situated in the southwesterly flow, constituting the surface Somali Countercurrent. The position of the current velocity vectors at the autonomous buoy stations rigorously corresponds to the direction of the geostrophic flows (Fig. 5).

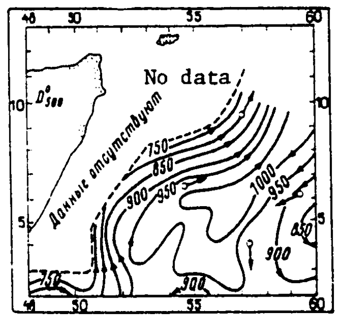

Fig. 5. Map of geostrophic currents in 1979 at the surface, computed from a depth of 500 m, and averaged vectors of residual currents at the 25-m horizon.

Here it should be noted that the direction of the velocity vector at a western point reflects the direction of the flow after 22 May 1979. Up to this time the transport of waters to all intents and purposes occurred in the reverse direction. This indicates that at the western periphery of the anticyclonic flow there was also its intensification due to intensification of the Somali Current, which, according to "MONEX-Summer" data, occurred during the period 20-22 May. Some traces of the variability of the structure of currents corresponding to this intensification were discovered in the surface Somali Countercurrent.

According to data from instrumental measurements of currents, the thickness of the layer occupied by the Somali surface countercurrent decreases from 150 m at 8°N to 75 m at the equator (Fig. 6). The velocity of transport of waters in its system at 6°16'N, 59°10'E in the layer 0-150 m varies from 35 to 19 cm/sec and at 4°N, 57°E it decreases to 15-22 cm/sec. But the current here occupies a layer of 75 cm (see Table 1).

It was extremely interesting that at 49°E the velocity of water transport in the layer 0-75 m across the equator in a southwesterly direction (and it can be interpreted as a continuation of the Somali Countercurrent) increases sharply in comparison with the extra-equatorial flow. Here it must be pointed out that the current in the surface layer in May 1979 was directed against the wind, whose velocity from 16 through 26 May increased from 5 to 10 m/sec.

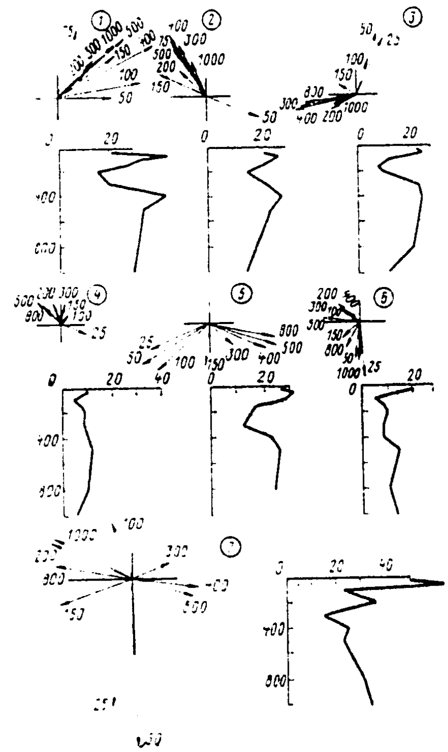

Fig. 6. Roses and curves of moduli of residual currents averaged during the period of observations. 1-7 -- numbers of observation points.

Equally surprising was the complete similarity of the current roses in the equatorial region at 49°E and 53°E in the layer 0-500 m. Observations at 53°E were already made in 1966 by Taft and Knauss [9] almost during the same period of the year. In both cases in the layer 0-75 m there was a southerly flow, in the layer 100-300 m -- westerly, deeper -- easterly flow. But the observations of 1979 made it possible to demonstrate that this easterly flow in the layer 700-1,000 m also is again replaced by a westerly flow with velocities 30-35 cm/sec (Fig. 6). However, these values characterize the mean diurnal flow velocity, whereas its instantaneous values in individual time intervals exceeded 50 cm/sec. Thus, at the equator in the region 49°E there was a four-layer structure of currents which is evidently characteristic for the period from March through June.

Such a pattern of the distribution of flows at autonomous buoy station points was obtained as a result of the averaging of current velocity over a quite prolonged time interval (7-12 days). The use of the mean daily

Components of Residual Currents

A № (см. рис. 6)	Судно, дата B	C Горизонты									
		25		50		75		100		150	
		v	u	v	u	v	u	v	u	v	u
1	НИС «Ю. М. Шокальский» 27 VI—08 VII 1977 г.	—	—	0	+21	−42	+12	+5	+32	+16	+23
2	НИС «Ю. М. Шокальский» 10—17 VI 1977 г.	—	—	−8*	+19*	+21	−14	—	—	+8	−19
3	ННСП «Волна» 7—29 V 1979 г	+22*	+10*	+25	+8	—	—	+12	+4	+4	−7
4	НИС «Академик Ширшов» 17—29 V 1979 г.	−4	+10	—	—	—	—	+3	+2	+7	+1
5	НИС «Академик Королев» 17—29 V 1979 г.	−10	−24	−16	−28	—	—	−18	−21	−17	−2
6	ННСП «Прилив» 17—29 V 1979 г.	−21	+1	−14	−2	—	—	+3	−5	−5	−7
7	ННСП «Прибой» 17—25 V 1979 г.	−50	−8	−66	+2	—	—	−21	−8	−10	−30

H * Осреднение меньше, чем за 7 суток

values (after filtering only of tidal oscillations of current velocity) does not give a complete idea concerning residual currents in the equatorial latitudes. At these latitudes the inertial oscillations of current velocity, occurring at any point in the world ocean, attain extremely high values. Both the period and the amplitude of the oscillations increase. The latter circumstance for the time being is completely inexplicable.

In the equatorial latitudes of the Indian Ocean fluctuations of current velocity are detected on the basis of the above-mentioned observations. Figure 7 shows the variability of the residual velocities of currents at different latitudes and depths at individual points of the first stationary polygon of "MONEX-Summer."

As in [1, 5], the represented variability of the residual currents occurs in circular orbits with rotation in a clockwise direction and with a period close to $2\pi/f$. The fluctuations of current velocity undoubtedly have an

Table 1

Averaged for Observation Periods

C Горизонты												D
200		300		400		500		800		1000		Координаты
v	u	v	u	v	u	v	u	v	u	v	u	
+10	+12	-14	+15	-20	-38	-23	26	—	—	-20	-22	12°00′ с. ш. E 55°14′ в. д. F
-10	-11	19	-11	-24	-15	+19	-13	—	—	-13	-7	09°43′ с. ш. 53°14′ в. д.
-3	-10	-4	-21	-4	25	+1	25	-3	-22	-4	-11	08°46′ с. ш. 57°01′ в. д.
+8	-3	8	-1	—	—	-8	-9	7	7	4	-2	06°28′ с. ш. 54°37′ в. д.
—	—	-8	+8	-10	+20	-9	-24	-6	+23		—	06°16′ с. ш. 59°10′ в. д.
-6	-8	-4	-6	+4	-7	-2	15	-9	-6	14	1	03°54′ с. ш. 57°11′ в. д.
14	-33	-6	11	3	-26	-6	+23	-7	31	-15	-31	00°01′ ю. ш. G 48°58′ в. д.

KEY:
- A) No (see Fig. 6)
- B) Ship, date
- C) Horizons
- D) Coordinates
- E) N
- F) E
- G) S
- H) Averaging for less than 7 days
- 1) Scientific research ship "Yu. M. Shokal'skiy"
- 2) Same
- 3) Scientific research weather ship "Volna"
- 4) Scientific research ship "Akademik Shirshov"
- 5) Scientific research ship "Akademik Korolev"
- 6) Scientific research weather ship "Priliv"
- 7) Scientific research weather ship "Priboy"

inertial nature. There is no doubt of this because with 24-hour averaging of the current velocity components the probable error in the readings of BPV current meters (and all the buoy stations registering the pertinent movements were outfitted specifically with these current meters), comparable with the amplitudes of the inertial oscillations, is of no practical significance [6].

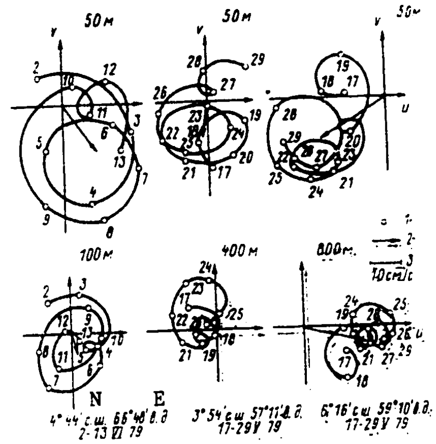

Fig. 7. Inertial oscillations of mean daily currents at individual points in the Indian Ocean. Near the density jump layer the maximum of the amplitude of the inertial oscillations of current velocity attains 60 cm/sec. Figure 7 shows that these oscillations can be interrupted for 24 hours or more, that is, they can be absent for a definite time interval.

Inertial oscillations of current velocity are characteristic for the entire layer from the surface to 1,000 m, that is, the layer in which instrumental observations were made. After the amplitude maximum in the thermocline layer they slowly attenuate and retain high values even at a depth of 1,000 m.

The amplitude of the inertial oscillations evidently is somehow dependent on the mean current velocity of the general flow, averaged over a quite prolonged time interval, taking in at least two or three cycles of rotation of a fluid particle in a circular orbit. It is also dependent on the stability and frequency of recurrence of the residual currents. Even at depths of 800-1,000 m with a mean current velocity of about 20 cm/sec during the observation period the amplitude of the inertial oscillations is commensurable with the current velocity with its frequency of recurrence within the limits of one direction from 30 to 40%. It becomes two or three times less with a frequency of recurrence of velocity from 50 to 80%. Here it is

ME)ROLOGY

18 SEPTEMBER 1980 NO. 6, JUNE 1980 2 OF 3

APPROVED FOR RELEASE: 2007/02/08: CIA-RDP82-00850R000300030024-9

interesting to note that the amplitude maximum was observed somewhat to the north of 4°N. Near this parallel within the confines of the Indian Ocean the water flows were least stable since the limit of propagation of zonal equatorial currents runs here and accordingly -- a zone of slightly stable flows.

Conclusions

1. The anticyclonic circulation of waters in the Arabian Sea occupies the surface 200-m layer.

2. In the subsurface and intermediate layers of the Arabian Sea to the south of Socotra Island there is an extensive two-centered cyclonic circulation. Its western periphery is possibly the deep Somali Countercurrent. To the east of the island it is possible to trace an anticyclonic circulation giving deep maxima of current velocity on the vertical distribution curve.

3. A vertical multilayer system of currents is the distinguishing characteristic of the Arabian Sea. The most consistent change in the signs of current velocities is traced in the equatorial region where, except for the surface layer, the currents have a zonal direction; in the layer 100-300 m water transport is to the westward, 300-600 m -- eastward, deeper -- again westward.

4. The amplitude of the inertial oscillations of current velocity in the equatorial latitudes of the Indian Ocean can exceed one knot. In order to obtain reliable data on the residual currents it is necessary to average the velocity values in a time interval which is a multiple of the period of the inertial oscillations and the period of the tidal currents.

BIBLIOGRAPHY

1. Brekhovskikh, L. M., et al., "Some Results of a Hydrophysical Experiment in a Polygon in the Tropical Atlantic." IZVESTIYA AN SSSR, FIZIKA ATMOSFERY I OKEANA (News of the USSR Academy of Sciences, Physics of the Atmosphere and Ocean), Vol 7, No 5, 1971.

2. Golovastov, V. A., "Oceanographic Investigations in the Experiment 'Monsoon-77'," METEOROLOGIYA I GIDROLOGIYA (Meteorology and Hydrology), No 9, 1978.

3. Golovastov, V. A., "Variability of the Heat Content of Waters in the Monsoonal Region of the Indian Ocean and the Factors Determining It," EKSPRESS-INFORMATSIYA. OKEANOLOGIYA (Express Information. Oceanology), No 3(46), 1978.

4. Golovastov, V. A., Tunegolovets, V. P., "Large-Scale Interaction Between the Ocean and the Atmosphere in the Example of the Pacific and Indian Oceans and the Problem of Long-Range Weather Forecasting (Review)," TRUDY DVNIGMI (Transactions of the Far Eastern Scientific Research Hydrometeorological Institute), No 87, in press.

5. Monin, A. S., Kamenkovich, V. M., Kort, V. G., IZMENCHIVOST' MIROVOGO OKEANA (Variability of the World Ocean), Leningrad, Gidrometeoizdat, 1974.

6. Rebayis, E. A., "Characteristic Motions of Anchored Buoy Stations and Their Influence on the Registry of Currents," TRUDY MEZHVEDOMSTVENNOY EKSPEDITSII TROPEKS-74 (Transactions of the Interdepartmental Expedition TROPEX-74), Volume II, OKEAN (The Ocean), 1976.

7. Tarasenko, V. M., "Investigation of the Somali Current," GIDROLOGIYA INDIYSKOGO OKEANA (Hydrology of the Indian Ocean), Moscow, Nauka, 1977.

8. Duing, W., "The Monsoon Regime of the Current in the Indian Ocean," E. W. Center Press, Honolulu, 1970.

9. Taft, B. A., Knauss, G. A., "The Equatorial Undercurrent of the Indian Ocean as Observed by the Lusiad Expedition," BULL. SCRIPPS INST. OCEANOGR., Univ. of California, Vol 9, 1967.

10. Swallow, G. J., Bruce, G. J., "Current Measurements Off the Somali Coast During the Southwest Monsoon of 1964," DEEP SEA RES., Vol 13 (5), 1966.

11. Wooster, W. S., Schoefer, M. B., Robinson, M. R., ATLAS OF THE ARABIAN SEA FOR FISHERY OCEANOGRAPHY, Univ. of California, 1967.

UDC 551.46.06:681.3.01+556

ONE METHOD FOR REPRESENTATION OF HYDROLOGICAL MAPS FOR ANALYSIS ON AN ELECTRONIC COMPUTER

Moscow METEOROLOGIYA I GIDROLOGIYA in Russian No 6, Jun 80 pp 74-77

[Article by L. P. Smirnykh, Institute of Automation and Process Control, Far Eastern Scientific Center USSR Academy of Sciences, submitted for publication 3 September 1979]

[Text]

Abstract: The author describes a method for representing hydrological maps in isotherms for analysis on an electronic computer. Each hydrological map is stipulated by a set of isotherms described by elements of the map coding grid. Methods are proposed for a comparative analysis of hydrological maps on an electronic computer, the results of which are quantitative or qualitative evaluations of changes in the position of individual isotherms or their sets. An archives of hydrological maps of the northwestern part of the surface of the Pacific Ocean has been created for such a representation, as well as a complex of programs for a YeS computer operational system for its processing with the use of graphic terminals. The use of the proposed method in commercial oceanography problems revealed its high promise and effectiveness.

In the processing of hydrological maps of surface temperatures of the ocean for the needs of commercial oceanography the problem arises of determining changes in the position of the isotherms of definite nominal temperatures during some observation period.

A direct comparative analysis of the isotherms for obtaining qualitative or quantitative evaluations of the change in their position is complex and time-consuming as a result of the specifics of plotting of hydrological maps (arbitrary configuration of isotherms, their nonuniform distribution over regions of the map, validity of the graphic description) and the great volume of information subject to simultaneous processing.

One of the possible means for solving the problem of a comparative analysis of the isotherms is the development of methods for transforming the initial description of a hydrological map into some other form in accordance with the conditions of the practical problem to be solved (representation), for which it is possible to use known comparison measures. In this case there is a need for automating some elements of processing of hydrological maps with the use of modern computers (graphic terminals).

Our objective is to construct a representation of hydrological maps with retention of a description in the form of isotherms for input and comparative analysis in an electronic computer. This representation must afford the possibility of comparison of individual isotherms and hydrological maps with one another with respect to the isotherms and also of obtaining evaluations of the results of the comparison.

In this article we propose that the maps be prepared in the form of a set of isotherms registered by a sequence of elements of the coding grid through which they pass. In this case with an accuracy to the dimensions of a grid element there is retention of the position of isotherms on the map. The concepts of regions of determination of isotherms, singularities and characteristics used in the preliminary analysis stage are introduced.

Algorithmic methods of comparative analysis of isotherms and isotherm maps based on different comparison measures are being developed. Methods for minimizing the initial representation of maps or groups of maps are considered.

The language of the theory of ratios is used for a formalization of descriptions of representations and algorithmic methods of comparative analysis.

We will use $F = (F_1, F_2, \ldots, F_k)$ to denote a set of hydrological maps; S $(s_1, s_2, \ldots, s_N)$ is used to denote a set of elements of the coding grid; $T = (t_1, t_2, \ldots, t_\ell)$ is a set of isotherm nominals, where $s \in \{ij\}$, $t \in \{f\}$; $i = 1, \ldots, n$; $j = 1, \ldots, m$; $f = 1, \ldots, \ell$; $N = n \times m$, m is the number of rows in the coding grid, ℓ is the number of isotherm nominals.

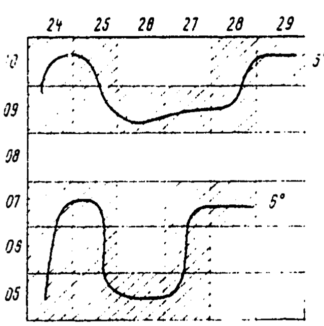

For each map F_i it is possible to discriminate the subset $S^i \subset S$ and $T^i \subset T$; then the ratio $\Sigma^i \leqslant T^i \times S^i$ is the formal registry of the map; $(t, s) \in \Sigma^i$ means that the isotherm of the nominal t passes through an element of the coding grid s, $t \in T^i$, $s \in S^i$.

The figure shows a fragment of a hydrological map. The grid S = (2405, 2505, ..., 2810, 2910) and the isotherms T = (5, 6) are stipulated. Then $\sum = \{(5;$ 2409, 2410,...,2810, 2910); (6; 2405, 2406,..., 2707, 2807)$\}$.

The list of elements of the coding grid through which the isotherm of the nominal t passes is written as $\sum < t > = \{s;\ (t, s) \in \sum\}$; then the map is represented by the combination of the list of isotherms

$$\Sigma < T^i > = \bigcup_{t \in T^i} \Sigma < t >.$$

The coding grid for each map has its own structure (following from the preceding ratio) $S = (S_0^i, S_1^i, S_2^i, \ldots, S_l^i)$, where S_f^i is the region occupied by the f-th isotherm of the i-th map and S_0^i is an empty region, $f = 1, \ldots, l$.

For each subset S_f^i we compute the parameters $\underline{g}^i$, $\overline{g}_f^i$, $\underline{V}_f^i$, $\overline{V}_f^i$, determining the horizontal and vertical boundary points of the isotherms respectively. The rectangle with the coordinates of the lower left corner $(\underline{g}_f^i, \underline{V}_f^i)$ and with the coordinates of the upper right corner $(\overline{g}_f^i, \overline{V}_f^i)$ will be called the region of definition of the f-th isotherm; the notation is W_f^i.

The region situated between the isotherm S_f^i and the row with the number $\overline{g}_j^i$ (column $\underline{V}_f^i$) will be called the frontal zone of the isotherm $(Z_f^{fr}(i))$, and the region between S_j^i and the row $\underline{g}_f^i$ (column $\overline{V}_f^i$) will be called the rear zone of the isotherm $(Z_f^r(i))$.

In this case the region of determination of the f-th isotherm is $W_f^i = Z_f^{fr}(i) \cup S_f^i \cup Z_f^r(i)$.

We introduce the parameter

$$\gamma = \frac{\overline{V}_f^i - \underline{V}_f^i}{\overline{g}_f^i - \underline{g}_f^i},$$

which characterizes the isotherm in the following way: $\gamma > 1$ is an isotherm elongated along the horizontal; $\gamma < 1$ is an isotherm elongated along the vertical; $\gamma \approx 1$ the isotherm has a region of definition which is close to square.

By using the concepts cited above it is possible to carry out a preliminary analysis of individual isotherms from the description of the map stored on the external carriers of the computer.

In the figure for the 5° isotherm we have: $\underline{V}_5^1 = 24$; $\underline{g}_5^1 = 0.9$; $\overline{V}_5^1 = 29$; $\overline{g}_5^1 = 10$; $W_5^1 =$ (2409, 2410,...,2910, 2909), the coordinates (0924, 1029) $Z_5^{fr}(1) =$ (2610, 2710); $Z_5^r =$ (2909); $\gamma = 29 - 24/10 - 09 = 5$, the isotherm is elongated along the horizontal.

In those cases when the difference in the nominals of the individual isotherms is not important for an analysis of the maps, common regions of definition can be constructed for them.

For the set of isotherms $\{S_i\}$ the common region can be computed in the following way:

$$g^i_{*l} = (\min_f \underline{g}^i_f); \quad g^{*i}_l = (\max_f \overline{g}^i_f);$$

$$V^i_{*l} = (\min_f \underline{V}^i_f); \quad V^{*i}_l = (\max_f \overline{V}^i_f),$$

where (g^i_{*l}, V^i_{*l}) are the coordinates of the lower left corner; (g^{*i}_l, V^{*i}_l) -- the coordinates of the upper right corner of the common region of definition M^i.

The comparative analysis procedure has three principal aspects:
-- comparison of the isotherms of one nominal from several hydrological maps;
-- comparison of hydrological maps with respect to a group of isotherms;
-- comparison of groups of hydrological maps with respect to one or more isotherms.

As the basis for the procedure it is possible to describe two measures of isotherm comparison: one is related to discrimination of identical elements in the description of isotherms and the other is related to computation of the distance between isotherms. Both measures are used as an explanation of the concepts of similarity, the difference of the compared objects.

Definition 1. Two isotherms will be considered β-indistinguishable if the intersection of their regions of definition contains not less than β-elements:

$$|W_1 \cap W_2| \geqslant \beta.$$

Definition 2. Two isotherms will be considered β-close if the distance between them is not greater than β:

$$R(S_1, S_2) \leqslant \beta.$$

The distance between isotherms is determined by the number of coding grid elements situated between them.

The general comparative analysis scheme is identical for both measures and differs in the nature of the computations:

a) Comparison of the isotherms of one nominal from several hydrological maps.

Assume that the set of isotherms $\{S^i_f\}$ is stipulated, where f determines the nominal and i is the number of the map, $i = 1, \ldots, k$.

In order to discriminate identical elements in the description of isotherms we will consider all possible intersections of the elements S_f^i. We obtain the set of numbers $\{\beta_j\}$ determining the number of elements entering into the intersections. In dependence on the purpose of the comparison of the isotherms it is possible to obtain the following results:
-- ordering of the isotherms of relative similarity (β-indistinguishability) with any pre-stipulated isotherm;
-- breakdown of the maps into groups with respect to the compared isotherm with stipulation of some indistinguishability threshold β;
-- breakdown of the maps with respect to the compared isotherm with max β-indistinguishability within the group.

The second measure is used in determining how much higher (lower) the isotherms pass relative to one another or what the distance between them is; in this case it is necessary to discriminate some sectors in the S_f^i set where these evaluations are possible.

Using the resulting set of threshold numbers $\{\beta_j\}$ it remains possible to obtain results similar to those enumerated above.

b) Comparison of the hydrological maps with respect to the group of isotherms.

A set of hydrological maps $F = (F_1, F_2, \ldots, F_k)$ is stipulated; each map is described by a set of isotherms; $\{S_f^i\}$, $i = 1, \ldots, k$; $f = 1, \ldots, \ell$.

Definition 3. Two maps F_1 and F_2 will be called α-indistinguishable if they are β-indistinguishable not less than according to the α-isotherms.

By varying the α and β thresholds, it is possible to obtain the following results:
-- ordering of the maps with respect to prestipulated degree of similarity (difference);
-- breakdown of maps into groups with respect to stipulated thresholds;
-- breakdown of maps by groups with respect to groups on the basis of max criteria of α - and β-indistinguishability.

Both comparison measures are used.

c) Comparisons of groups of hydrological maps on the basis of one or more isotherms.

Assume that in the F set there is a priori stipulation of a breakdown into groups (equivalence ratio) $E \leqslant F \times F$, $F = (\Phi_1, \Phi_2, \ldots, \Phi_g$, with

$$\Phi_i \cap \Phi_j = \varnothing;\ \Phi_i \neq \varnothing;\ \bigcup \Phi_i = F,$$

where $i, j = 1, \ldots, g$; $i \neq j$; g is the number of groups.

The comparison of the groups of maps consists of two stages. In the first we construct a description of groups as sets of maps in the terms of common regions of isotherms, as a combination of their regions of definition. In the second stage there is a direct comparison of groups of maps with respect to discriminated regions. The following possibilities are ensured:

-- construction of a description of map groups in terms of regions of definition of isotherms with satisfaction of the condition of α- indistinguishability;
-- discrimination of the most informative regions of isotherms for the analyzed groups retaining the properties of α-indistinguishability;
-- use of the resulting descriptions in prognostic problems of commercial oceanography.

On the basis of the proposed representation we created an archives of 10-day hydrological maps of the northwestern part of the surface of the Pacific Ocean. For the processing of this archives we used a complex of programs with a YeS computer system with extensive use of YeS-7064 terminals and A5433 terminals (graphic displays) for organizing a dialogue regime and output of individual fragments of operation of the programs and a YeS-7054 terminal (curve plotter) for obtaining copies of the results.

The complex included programs for checking, correcting, preliminary and comparative analyses of elements in the archives. A number of programs have been filed in the State Archives of Algorithms and Programs.

The method for representation of hydrological maps described in the article was used for solution of problems in long-range and routine prediction of the approach of Cololabis in the fishing region.

The experience of work during 1976-1978 indicated the effectiveness of this method for the representation of hydrological maps for the needs of commercial oceanography and the possibility of its use in problems of predicting the temperature regimes of the ocean.

UDC 551.464(262.54)

INFLUENCE OF NONLINEAR EFFECTS OF CHANGES IN STREAMFLOW ON THE SALINITY OF THE SEA OF AZOV

Moscow METEOROLOGIYA I GIDROLOGIYA in Russian No 6, Jun 80 pp 78-83

[Article by Candidates of Geographical Sciences N. P. Goptarev and I. A. Shlygin, State Oceanographic Institute, submitted for publication 12 October 1979]

[Text]

Abstract: By means of solution of a differential equation for the salt balance of the sea for a nonsteady state the authors make computations of the salinity of a water body and the time it is stabilized with different inflows of fresh water. The nonlinearity of the dependence of the rate of change of salinity on streamflow has the result that in the case of short time intervals in order to reduce salinity it is necessary to have a greater volume of runoff than the volume of the total water withdrawal responsible for its increase.

Modern changes in the hydrological, hydrochemical and hydrobiological regimes of the Sea of Azov have occurred primarily under the influence of anthropogenic effects on the river runoff in the basin -- regulation and unreturned withdrawal of fresh water. Further development of the economy assumes a decrease in inflow to the sea to 18-20 km^3 by the year 2000 [5]. The increase in water consumption will continue beyond the limits of the current century and according to the statements of water users can attain 35-36 km^3/year [3].

In order to compensate for the effects of the increase in water use and in order to reduce the strain on the water balance the need has arisen for bringing in runoff from other basins. However, the implementation of projects for such transfer requires a very long time. Until then the hydrological regime of the sea, and especially its salinity, will continue to experience negative changes. In this connection, and also taking into account the known economic and scientific difficulties in bringing in new runoff in great volumes, a study was made of the many effects of modification of changes in river runoff on salinity. The fundamental problem was formulated in the following way: how to change sea salinity when withdrawing definite volumes of fresh water and what quantity of additional inflow must be supplied during specific times in order to restore the initial salinity? A solution of this problem is completely akin to the problems of control of the sea regime.

The mean salinities of waters of the Sea of Azov $\bar{S}$ necessary for the computations were determined by solution of a simplified salt balance equation for the entire sea

$$\frac{d\bar{S}}{dt} = \frac{1}{B}\,(S_р\,V_р + S_ч\,V_ч - S_А\,V_А), \tag{1}$$

[Here and in the text and formulas which follow the three principal notations are the subscripts: р = r = river; А = A = Sea of Azov; ч = BS = Black Sea] where V_r, V_{BS}, V_A are the volumes of river runoff, water inflow from the Black Sea and the outflow of Sea of Azov water through Kerch Strait respectively; S_r, S_{BS}, S_A are the salinities of the corresponding waters; B is the volume of the sea.

The parameters necessary for solution of equation (1) are expressed by the following dependences:

$$V_А = 0.66\,V_р + 24.35; \tag{2}$$
$$V_ч = -0.34\,V_р + 45.85; \tag{3}$$
$$S_А = 0.98\,\bar{S} + 0.69; \tag{4}$$
$$S_ч = 0.16\,\bar{S} + 14.97. \tag{5}$$

Expressions (2) and (5) were taken from [1]; equation (4) was taken from [4]; the dependence for V_{BS} was derived from the equation for a steady water balance of the sea with the substitution of the mean long-term precipitation and evaporation values and expressions for Sea of Azov flow in the form (2).

The joint solution of equations (1)-(5) with B = 324.3 km^3 gives an expression for the change in salinity:

$$\frac{d\bar{S}}{dt} = 2.0703 - 0.0158\,V_р - \bar{S}\,(0.0510 + 0.0022\,V_р). \tag{6}$$

By solving equation (6) for a mean runoff for the series of observations from 1923 through 1976 (V_r = 36.7 km^3) on the assumption that $d\bar{S}/dt = 0$ we obtain the actual mean salinity for this period of 11.3°/oo. This fact is evidence of absence of systematic errors in evaluating the parameters of equations (1)-(5).

The solution of linear equation (6) has the form

$$S = e^{-\int_0^t p\,dt}\left(C + \int_0^t q e^{\int_0^t p\,dt}\,dt\right). \quad (7)$$

where $p = 0.0510 + 0.0022\ V_r$; $q = 2.0703 - 0.0158\ V_r$.

If the changes in river runoff V_r occur in a jump, during the computation periods the p and q parameters will be constant, which considerably simplifies expression (7):

$$S = \frac{q}{p} + Ce^{-pt}. \quad (8)$$

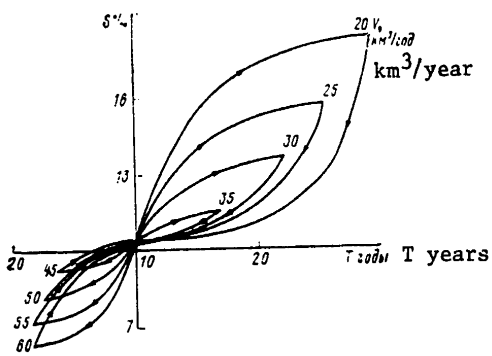

Fig. 1. Limiting salinity values and times required for their stabilization with different river runoff values and with an initial sea salinity 10.5°/oo

The integration constant C is determined for each computation period i from the condition $S|_{t_i = 0} = S|_{t_i = 1}$. In the indicated condition i are the computation periods with a constant river runoff, t are the years in these periods. With $t \to \infty$ $\bar{S} \to S_\infty$ (const), that is, the salinity tends to some limiting value, in this case with a constant river runoff. Thus, each value of constant river runoff corresponds to a definite steady salinity value. In order to lessen the volumes of the computations we will denote by T the time of stabilization of a salinity differing from the limiting value (S_∞) by 0.1°/oo. The computations revealed that the period of setting-in of salinity from any initial value to its limiting value with a modified river runoff is to all intents and purposes equal to the period of setting-in of the initial salinity with restoration of the former stationary regime. Figure 1 shows the time for stabilization of the salinity T with different river runoffs and an initial salinity 10.5°/oo (being stationary with a runoff of about 40 km³/year).

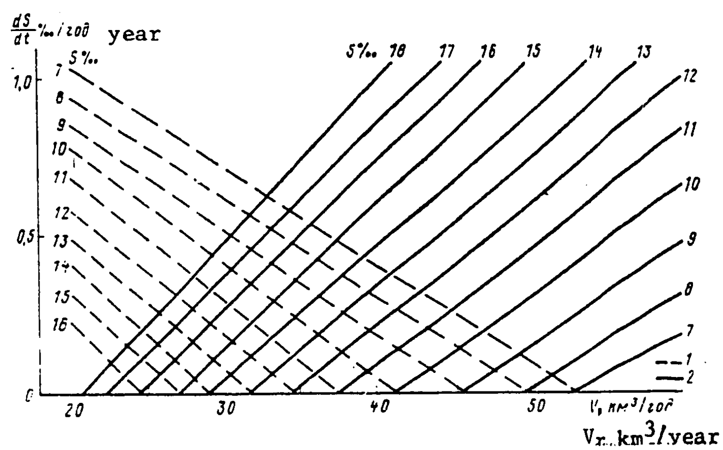

Fig. 2. Rate of change in sea salinity in dependence on its salinity and fresh inflow. 1) stage of increase in salinity, 2) stage of decrease in salinity.

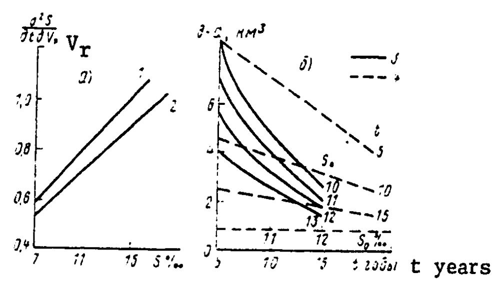

Fig. 3. Dependence of relative rate of change in salinity (per km^3) on mean sea salinity (a) (1 -- stage of increase in salinity, 2 -- stage of decrease in salinity) and value b - a on computation period with different S_0 (3) and on initial salinity (4) (b).

For practical purposes this means that with a sufficiently long time interval (several decades) the withdrawal of part of the fresh water results in a corresponding increase in salinity (to the limiting value). It is possible to restore the former stationary salinity during this same prolonged time interval by supplying a corresponding initial water volume. In this case as well withdrawals of fresh water relative to an initial constant inflow must be compensated by an adequate quantity of fresh water supplied from the outside, that is, the total volume of the transfer is equal to the total withdrawals during the time of increase in salinity T.

However, with a shortening of the computation time interval the picture substantially changes. Already in an examination of the process of change in salinity to values differing from S_∞ by $0.2^o/oo$ the following regularity is observed: an increase in salinity occurs more rapidly than its decrease.

Figure 2 illustrates the dependence of the rate of change (increase and decrease) in sea salinity on its salinity and fresh inflow. The slope of the family of straight lines characterizing the increase in salinity is greater than the slope of the straight lines representing the process of its decrease. A generalization of these results has been presented in Fig. 3a, showing the dependence of the rate of change in salinity per cubic kilometer on mean sea salinity. In the stage of an increase in salinity the value $\partial S^2/\partial t \partial V_p$ [p = river] in all cases is greater than in the stage of its decrease for one and the same salinity values; with an increase in salinity this difference increases.

Accordingly, in real 5- - 10-year time intervals a decrease in sea salinity, after its increase as a result of withdrawals of river water, with restoration of the former inflow occurs over a longer time interval than the increase. Therefore, the integral volume of water transfer for the optimization of salinity is considerably greater than the total volume of the withdrawals responsible for the salinity increase.

Now we will examine this phenomenon in general form. We will assume that the process of change in salinity is as follows: beginning at some moment when the salinity in the sea is S_0 the river runoff is reduced by the value a. During the time t salinity is increased to S_{t1}, after which river runoff increases by the value b and during this same time interval t the salinity decreases to the initial value S_0.

In the stage of an increase in salinity equation (8) has the form

$$S_{t_1} = \frac{q_1}{p_1} + C_1 e^{-p_1 t}, \tag{9}$$

where

$$p_1 = 0{,}0510 + 0{,}0022(V_p - a),$$
$$q_1 = 2{,}0703 - 0{,}0158(V_p - a),$$
$$C_1 = S_0 - \frac{q_1}{p_1}.$$

In the stage of a decrease in salinity

$$S_0 = \frac{q_2}{p_2} + C_2 e^{-p_2 t}. \tag{10}$$

Here

$$p_2 = 0{,}0510 + 0{,}0022(V_p - a + b) = p_1 + 0{,}0022\, b,$$

$$q_2 = 2{,}0703 - 0{,}0158\,(V_p - a + b) = q_1 - 0{,}0158\, b,$$

$$C_2 = S_{t_1} - \frac{q_2}{p_2}.$$

With the assumed conditions the computation expression (10) is transformed to the form

$$\frac{S_0 p_2 - q_2}{S_{t_1} p_2 - q_2} = e^{-p_2 t}.$$

Substituting the values S_{t1}, p_2, q_2, we obtain

$$\frac{(S_0 p_1 - q_1) + (0{,}0022\ S_0 + 0{,}0158)\ b}{(S_0 p_1 - q_1)\ e^{-p_1 t} + \left\{ \frac{0{,}0022}{p_1} [q_1 + (S_0 p_1 - q_1)\ e^{-p_1 t}] + 0{,}0158 \right\} b} = \tag{11}$$

$$= e^{-p_1 t - 0{,}0022\ b}.$$

It is convenient to solve the transcendental equation (11) graphically. The table gives the a and b values for two cases of decrease in river runoff to 20 and 25 km^3. The computations show that the b values decrease almost linearly with an increase in t, but in all cases $b > a$.

Values of the Parameters a and b With Decrease in River Runoff to 20-25 km^3

	t лет years	S_0 ‰ 10	11	12	13	10	11	12	13
		V_r $V_p - a = 20$ км³				$V_p - a = 25$ км³			
a км³	—	21,2	18,7	14,5	11,5	16.2	13.7	9,5	6,5
b км³	5	32,5	27,4	22,9	16,6	24.5	20.4	14.9	10.4
	10	27,2	22,9	20,0	15,4	20.7	17.5	12,6	8,9
	15	24,5	20,5	17,3	13,9	18,6	15,7	11,2	7,9

It therefore follows that in order to restore salinity to the initial values during the same time during which it had increased it is necessary to have a greater quantity of fresh water than that which was withdrawn and which was responsible for the increase in salinity.

With an increase in the initial salinity the excess of the additional inflow over the volume of the withdrawals (difference b - a) decreases (Fig. 3b). The difference b - a also decreases with an increase in the computation period. This occurs due to the nonlinearity of the function $S = f(t)$ (Fig. 1). With an increase in time the rate of increase in salinity decreases and therefore less additional flow is required in order to reach the initial salinity. We will determine the limit of decrease of the difference b - a. With $t \to \infty$ from expression (10)

$$b_{t \to \infty} = \frac{q_1 - S_0 p_1}{0{,}0022\ S_0 + 0{,}0158}.$$

From equation (9)

$$V_p - a = \frac{2{,}0703 - 0{,}051\ S_{t_1}}{0{,}0022\ S_{t_1} + 0{,}0158}$$

or taking into account the dependences for p_1, q_1 and S_{t1}

$$a = \frac{q_1 - S_0 p_1}{0{,}0022\ S_0 + 0{,}0158}.$$

Thus $b \equiv a$, and this confirms the conclusion drawn above that with infinitely prolonged development of the process the restoration of the initial stationary salinity occurs by restoration of the initial river runoff.

With $t < \infty$ $b > a$, that is, the nonlinear effects of the dependence of changes in salinity on streamflow have the result that during real short time intervals it is possible to restore salinity only by having additional inflow exceeding the volume of the withdrawals. In actual practice this means that the restoration of salinity of the Sea of Azov requires a greater volume of water than the total water withdrawals. And the more rapidly the reduction in salinity of Sea of Azov waters is desired, the greater is the inflow which must be organized from other basins.

The computed data are confirmed by retrospective observational data. For example, under quasistationary conditions during the period from 1948 through 1966 an increase in salinity from 10.8 to 12.3°/oo occurred in 7 years (between 1949 and 1955) as a result of a total decrease in runoff by 43.7 km^3. A decrease in salinity to the initial value already occurred in 11 years (1955-1966) and required a total increase in runoff by 62.3 km^3.

Accordingly, the question arises about the need for accelerating the development of plans for transfer of runoff from other basins and also determination of the comparative effectiveness of other measures for reducing sea salinity, in particular, regulation of water exchange through Kerch Strait.

BIBLIOGRAPHY

1. Al'tman, E. N., "Computation of Salinity in the Sea of Azov," TRUDY GOIN (Transactions of the State Oceanographic Institute), No 125, 1975.

2. Lineykin, P. S., "Method for Computing the Distribution of Salinity in a Shallow-Water Sea (Sea of Azov)," TRUDY GOIN, No 20, 1955.

3. Osmer, N. A., "Need for Regulating Water Exchange Between the Black Sea and the Sea of Azov," IZV. SEVERO-KAVKAZSKOGO NAUCHNOGO TSENTRA VYSSHEY SHKOLY (News of the Northern Caucasus Scientific Center of the Higher School), No 1, 1973.

4. "Present-Day and Long-Range Water and Salt Balance of the Southern Seas of the USSR," TRUDY GOIN, No 108, 1972.

5. Shiklomanov, I. A., "Dynamics of Anthropogenic Changes in Annual Runoff of Rivers in the USSR," TRUDY GGI (Transactions of the State Hydrological Institute), No 239, 1977.

6. Shlygin, I. A., "Salinity of the Gulf of Taganrog With a Change in its Water Exchange With the Sea of Azov," METEOROLOGIYA I GIDROLOGIYA (Meteorology and Hydrology), No 4, 1978.

UDC 556.535.6

CORRELATION BETWEEN THE HEIGHT OF SAND RIDGES AND THE PARAMETERS OF RIVER FLOW AND CHANNEL

Moscow METEOROLOGIYA I GIDROLOGIYA in Russian No 6, Jun 80 pp 84-92

[Article by Candidate of Technical Sciences B. F. Snishchenko, State Hydrological Institute, submitted for publication 13 August 1979]

[Text]

Abstract: Extensive data are used in an analysis of the correlation between the height of ridges, depth and velocity of flow, grain size and discharge of bottom sediments. It was found that there is a nonlinear nature of the dependence of ridge height on depth and an explanation of this fact is given on the basis of the hydraulic resistances of river channels. It is proposed that the derivation of formulas for the height of ridges be based on the laws of change in channel resistance and the discharge of sediments with allowance for the magnitude of the flow.

Height is an extremely important geometrical characteristic of ridges, occupying a leading place among the elements of macroroughness in solving the problem of hydraulic resistances and also in computing solid discharge and river bottom deformations. Among the three varieties of channel microforms (ripples, ridges, antidunes) we will examine only ridges, having predominant occurrence in natural channels. The range of analyzed characteristics of microforms and flow in flumes, rivers and channels is rather great (Table 1). The body of data, including, in addition to the materials from the State Hydrological Institute, most of the published information [8], amounts to about 600 measurements.

Table 1 gives the flow and channel characteristics usually measured in the experiments: depth h, velocity V and diameter of the bottom particles d. As is well known, information on other important characteristics, such as flow slope and width and solid runoff is, unfortunately, still rarely encountered. Accordingly, the three mentioned parameters serve as a basis for writing different dimensionless combinations entering into the computation formulas for the height of ridges.

At the same time, an analysis of data from different experiments indicates a contradictory nature of the simplest parametric relationships between the mentioned flow characteristics and the parameters of ridges. This leads to substantially different results when using the expressions for the height of ridges. Accordingly, in this study emphasis is on establishing an unambiguity of the sought-for functional relationships applicable to the height of ridges. The massive character of the material used gives basis for such an analysis.

If the experimental points are represented on the graph $h_r = f(d)$, the absence of a correlation between the size of the sediments and the height of the ridges becomes appreciable. Their positioning is evidence only of an insignificant tendency of a decrease in h_r with an increase in d. The correlation coefficient between h_r and d was equal to 0.42.

The weak dependence of the size of the ridges formed by fine-grained material on the variation of its grain size is noted by K. V. Grishanin, who attributes this circumstance to the capacity of the flow for autoregulation of macroroughness of its bottom [1].

The steepness of the ridges (height related to length) also does not reveal any correlation to particle size. This fact is extremely noteworthy. It is evidence that the diameter of the fine particles exerts no influence on resistance to the flow through size of the ridges and is related to energy losses only as an element of granular roughness.

Observations in laboratories and rivers indicate that the height of the ridges is directly dependent on mean flow velocity. On the graph $h_r = f(V)$ (it is not shown in this study) this correlation appears weak, but is confirmed. The correlation coefficient is 0.37.

Finally, we will proceed to an analysis of the correlation $h_r = f(h)$. The height of the ridges increases linearly with depth of the flow -- such is the generally accepted opinion of this dependence, which leads to the law h_r/h = const. V. F. Pushkarev [5] asserts the validity of this law on the basis of the results of his experiments. A simple comparison of the heights of ridges and the magnitude of the flows forces us to doubt the nondependence of the relative height of the ridges on the scale of the flow. Whereas in laboratories it is possible to observe ridges constituting 1/3-1/2 of the flow depth, in the Volga, Irtysh, Ob' and other large rivers the height of the ridges rarely exceeds 1/5 of the depth.

We will represent all the experimental points on the same graph $h_r = f(h)$ (Fig. 1). The graph shows that the line averaging the points cannot be approximated by a straight line in the entire range of depths: with an increase in the value $h > 100$ cm the relative height of the ridges h_r/h decreases. The essentially nonlinear dependence between h_r and h can be represented approximately in the form of two linear correlations:

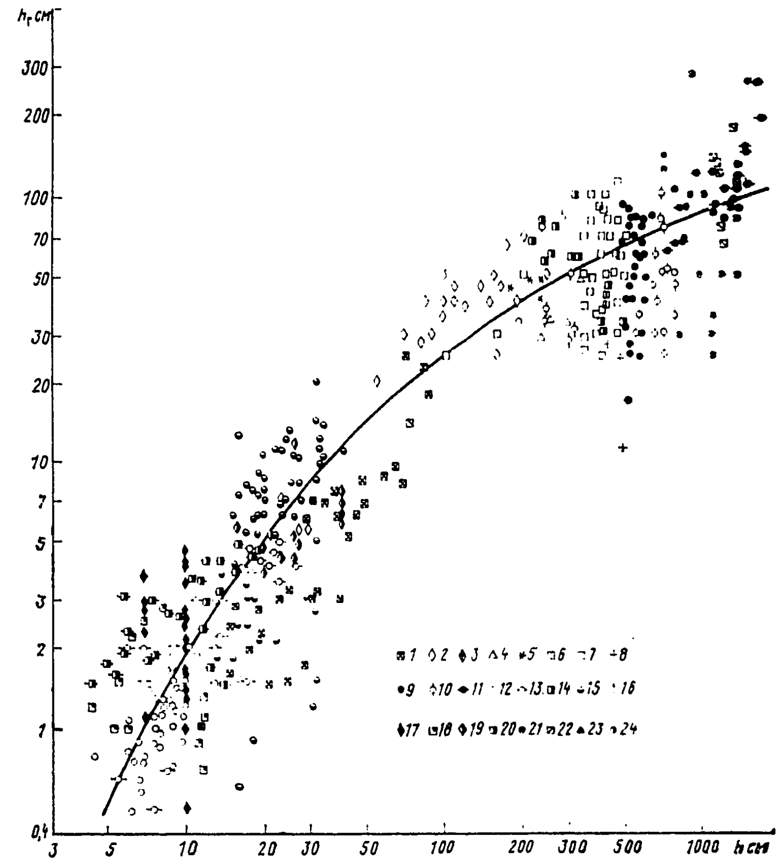

Fig. 1. Dependence of height of ridges h_r on depth of flow h according to laboratory and field data. Field data: 1) Hiya River and canals of Japan (Sinohara and Tsubaki); 2) Polomet' River (Korchokha); Polomet' River; 4) Sev. Dvina River; 5) Oka River; 6) Don River; 7) Karakumskiy Canal; 8) Volga River; 9) Volga River; 10) Vychegda River; 11) Danube River; 12) Luga River (Snishchenko, State Hydrological Institute); 20) Selenga River (State Hydrological Institute); 21) Volga River (State Hydrological Institute, Gidroproyekt); 22) Irtysh River (State Hydrological Institute); 23) Dnepr River (Kulemina); 24) Don River (Karaushev). Laboratory data: 12) Pushkarev; 13) Kopaliani; 14) Znamenskaya; 15) Gay, Saymons and Richardson; 17) Goncharov, Lapshin; 18) model of Irtysh River (State Hydrological Institute); 19) Zheleznyakov, Debol'skiy.

$$h_r = 0.25 \text{ h cm with } h < 100 \text{ cm}; \quad (1)$$
$$h_r = 20 + 0.1 \text{ h cm with } h > 100 \text{ cm}. \quad (2)$$

It follows from (1) and (2) that under laboratory conditions and in rivers with shallow depths ridges are characterized by a relative height greater than in deep flows, that is, in a general case $h_r/h \neq$ const.

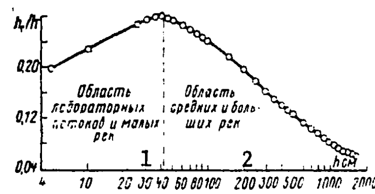

Fig. 2. Nature of change in relative height of ridges with depth of flow in laboratory flows and natural rivers. The points correspond to the averaging curve in Fig. 1.

KEY:

1. Region of laboratory flows and small rivers
2. Region of medium and large rivers

The relatively small scatter of experimental points, taking into account the presence of only one argument in the formulas (the standard deviation was 44%), makes it possible to recommend dependences (1) and (2) for approximate computations. The reasons for the scatter of the measurement data for the ridges were analyzed earlier in [8, 9].

Taking into account the great importance of the established fact of the relative height of ridges on flow magnitude, we will examine this phenomenon from the point of view of hydraulic resistance of the channel because the h_r/h value is a characteristic of its macroroughness. As the object of the analysis we will use the graph $h_r/h = f(h)$ (Fig. 2), constructed from the coordinates of the curve in Fig. 1.

The left side of the graph, reflecting the increase in h_r/h with an increase in h, is related primarily to laboratory flows. Their characteristic feature is a bed roughness which is increased in comparison with rivers due to the granular and ridge components, which are evaluated by the corresponding hydraulic friction coefficients λ_d and λ_v.

Known relationships exist between λ_d and λ_r and the parameters of the granular and ridge roughness

$$\lambda_d = f(d/h) \text{ and } \lambda_r = f(h_r/h,\ h_r/\ell_r).$$

With small fillings of the flume the resistance of the particles and the resistance of the ridges introduce a close contribution to the general resistance. With an increase in depth there is a redistribution of the roles between the resistance of the granular roughness and the resistance of the ridges -- the role of the first inevitably decreases; the flow compensates this intensification of macroroughness as a result of an increase in the parameter h_r/h.

Table 1

Extremal Values of Characteristics of Microforms, Flow, Channel

Экстремумы 1	h см	V см/с 2	d мм	$\sqrt{Fr}$	h_r/h 3	h_r/d	h_r/l_r 4	l_r/h
5 Лабораторные лотки и модели русл								
7 Минимум	4,3	18	0,18	0,14	0,06	1.5	0,003	1,1
8 Максимум	40	290	6,50	3,40	0,51	986	0,250	13,6
6 Естественные реки и каналы								
7 Минимум	10	43	0,064	0,08	0,02	8,1	0,004	1,3
8 Максимум	1710	177	4,5	0,53	0,60	64000	0,177	15,3

KEY:

1. Extrema
2. cm/sec
3. Γ = r
4. Γ = r
5. Laboratory flumes and models of channels
6. Natural rivers and canals
7. Minimum
8. Maximum

Granular and ridge roughness are only some of the sources of resistance to flow in flumes. I. F. Karasev [3] indicated that with $\chi/R < 30$ (χ is the wetted perimeter, R is the hydraulic radius) a significant role in the increase observed in the resistance to flow is exerted by the braking influence of the walls, which can be evaluated using the coefficient λ_w. It is obvious that for such flumes the sum of λ_d, λ_r and λ_w will give the general hydraulic friction coefficient λ. According to Grishanin, for prismatic channels $\lambda \sim I \cdot B/h$ [1]. Applicable to flumes, we write

$$\lambda = \lambda_d + \lambda_r + \lambda_c \sim I \cdot \chi/R. \quad (3)$$

In experiments in flumes of a constant width lesser I and χ/R corresponded to greater fillings of the flumes (as a result of a more rapid increase in R). In this case λ_r and λ_w increase. Since $\lambda_w = f(\chi/R)$, then with h = const there will be a change in the relationship between λ_w and λ_r in troughs of different width, and accordingly, also the parameter h_r/h. The indicated circumstance explains one of the reasons for the scatter of experimental values h_r obtained using apparatus of different width.

The correlation between the coefficients λ_r and λ_w is evidence of the need for taking flume width into account when writing expressions for the height of the ridges. The first experience in such attempts already is available in studies which have been reviewed by N. S. Znamenskaya in [2].

Table 2

Characteristics of Flows of Different Magnitudes

Характери-стики 1	2 Порядок (размер) потока i							
	I	II	III	IV	V	VI	VII	VIII
h м	0,045	0,068	0,098	0,147	0,216	0,319	0,472	0,701
B/h	5.78	10,20	16,29	23,81	32,47	41.67	51,28	59,88
$I \cdot 10^{-3}$	134	49,2	20,0	8,9	4,2	2,1	1,14	0,63
ΔI_i %		63,28	59,37	55,50	52,81	43,81	47,22	44.74
$\Delta(B/h)_i$ %		76,47	59,71	46,16	36,37	28,33	23,06	16,77
α	1,76	1,60	1,46	1,36	1,28	1.23	1,17	1,14
β	0,37	0,41	0.44	0,47	0,51	0,53	0,55	0,57
$\alpha\beta$	0,65	0,66	0,64	0,64	0,65	0,65	0,64	0,65
3 $h_Г$ м	0,0045	0,0094	0,018	0,033	0,058	0,09	0,117	0,184
$h_Г/h$	0,100	0,138	0,184	0,224	0,268	0,282	0,248	0,262
$I \cdot B/h$	0,774	0,502	0,325	0,212	0,136	0,090	0,058	0,038

Характери-стики 1	2 Порядок (размер) потока i						
	IX	X	XI	XII	XIII	XIV	XV
h м	1,022	1,505	2,220	3,198	4,676	6.777	10,0
B/h	68,49	75,76	81.97	88,50	92,59	97.09	100.0
$I \cdot 10^{-3}$	0.36	0,215	0,129	0,079	0,049	0,031	0,020
ΔI_i %	42,86	40,28	41,39	38,76	37,34	37.37	35,48
$\Delta(B/h)_i$ %	14,38	10,61	8,20	7,97	4,62	4,86	3,00
α	1,11	1,08	1,08	1,05	1,05	1,03	
β	0,60	0,60	0,61	0,63	0,63	0,65	
$\alpha\beta$	0,66	0,65	0,66	0,66	0,66	0,67	
3 $h_Г$ м	0,25	0,33	0,42	0.51	0,62	0,74	0,86
$h_Г/h$	0,245	0,219	0,189	0,159	0,132	0.109	0,086
$I \cdot B/h$	0.025	0.016	0,011	0,007	0,005	0.003	0,002

KEY:

1. Characteristics
2. Magnitude
3. Г = r

The transition to natural flows with great depths and a low granular roughness value occurs on the graph through the maximum at a depth of 40 cm, which cannot be assigned a universal value. It is obvious that with another set of experimental data it can be displaced in the direction of both lesser and greater h values.

Now we will investigate the right branch of the curve. The author has demonstrated that in natural channels with a ridged bottom, consisting of fine sediments, the total hydraulic friction coefficient is close to the friction coefficient for the ridges [7].

As is well known, with an increase in the size of the rivers (and depths) the slope of the flow decreases, whereas the relative width B/h increases. According to R. Horton [10], the slope of the rivers decreases with an increase in their magnitude i in a geometric progression.

Rzhanitsyn [6] quantitatively demonstrated that with a decrease in slope the B/h value increases with an increase in flow magnitude (Table 2).

We carried out an analysis of the relative change in I and B/h with transition from one river magnitude to the next (see the ΔI_i and $\Delta(B/h)$ values in Table 2).

The results of the calculations lead to an important conclusion: with an increase in the magnitude of the rivers the slope decreases more rapidly than the relative width increases. A conclusion valid for flows greater than the third magnitude, in accordance with formula (3), means that a more rapid dropoff of the slope in comparison with the increase in B/h corresponds to a decrease in the coefficient λ (or an increase in the Chezy coefficient C). Observations on rivers show that in actuality with the transition from small to intermediate and from intermediate to large rivers λ decreases (or C increases).

According to V. S. Knoroz [4], the total coefficient of ridge resistance is

$$\lambda_r = f\,(h_r/h,\ h_r/l_r,\ \lambda_d),$$

[r = r(idge)]

this dependence is direct. It follows from this that lesser λ_r values must correspond to lesser h_r/h and h_r/l_r values. As already noted, the steepness is not dependent on river size.

Accordingly, with an increase in the magnitude of the rivers, an increase in their slope and and increase in river depth there is a decrease in resistance as a result of a decrease in bottom roughness. This decrease should be substantial because an increase in resistance due to an increase in B/h must compensate the flow. In actuality, in accordance with Fig. 2, with an increase in depth from 0.4 to 20.0 m the h_r/h parameter decreases by a factor of 5.

The established pattern of a decrease in resistance with an increase in river size also follows from a comparative analysis of the resistances of flows of "adjacent" magnitudes. In a case when $\lambda_{i+1}/\lambda_i < 1$, resistance should decrease with an increase in the magnitude of the flow.

We will represent (3) in the form

$$\lambda_{i+1}/\lambda_i \approx (I_{i+1}/I_i)\frac{(B/h)_{i+1}}{(B/h)_i} = \alpha\beta.$$

We will make computations using Rzhanitsyn's data, and we will summarize the results in Table 2. It follows from this that

$$\alpha\beta \approx 0{,}65 = \text{const}.$$

Thus, with transition from the preceding flow magnitude to the next the flow resistance coefficient decreases in accordance with the expression $\lambda_{i+1} \approx 0.65\,\lambda_i$.

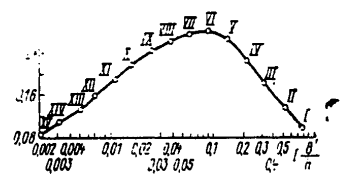

Fig. 3. Nature of change in resistance in flows of different magnitudes (sizes).

Using Rzhanitsyn's data, we constructed (Fig. 3) the correlation $h_r/h = f(I\ B/h)$. The sizes of the ridges were read from the curve (Fig. 1). The results of the computations are given in Table 2.

The constructed curve, like the curve in Fig. 2, has a maximum and two branches. The left branch takes in natural flows with depths greater than 0.3-0.4 m, whereas the right branch takes in both laboratory and small natural flows with depths 0.045-0.32 m.

Following along the left branch in the direction of an increase in the size of the flows, we see that the parameters of the curve decrease; this confirms the conclusion that there is a decrease in resistance with an increase in the magnitude of the river. In small and laboratory flows with an increase in their magnitude the parameter h_r/h, as on the graph $h_r/h = f(h)$, increases, whereas the total resistance decreases (term I B/h). Vice versa, with a decrease in depth there is a decrease in h_r/h and an increase in total resistance.

Thus, an analysis of the graph in Fig. 3 indicates a general law of decrease in resistance with an increase in flow magnitude. At the same time it indicates a different contribution of the resistance components under laboratory and natural conditions.

Nevertheless, it seems obvious that a knowledge only of the energy aspect of the process is a necessary but inadequate condition for the derivation of universal computation formulas. Indeed, the ridges, expressing the structural form of the transport of sediment, should form their dimensions by the flow also in dependence on the volume of solid runoff, thereby satisfying the principle of autoregulability of the flow - channel system.

A study by the author of the pattern of the spatial distribution of ridges on the bottom of natural river channels (Medveditsa, Polomet', Don, Danube, Ob' Rivers) led to a number of results confirming the conclusion drawn. They can be summarized briefly as follows:

-- the dimensions of the ridges are nonuniform in the width of the channel and over the area of the river bottom;
-- the sizes of the ridges by no means always unambiguously correspond to the local characteristics of the flow (h, V, d);
-- the solid discharge is also nonuniformly distributed over the width of the channel;
-- the dimensions of the ridges are in a regular relationship with the volume of the solid discharge; the greatest length and height of the ridges correspond to the maximum of the smooth curve of discharge of bottom sediments.

We note, for example, that in meandering and secondary channels the maximum discharges of bottom sediments are associated with the zone of the beach or side channel slope, on which the largest ridges are situated, whereas they are expressed insignificantly in the zone of maximum depths along the concave shore of the meander.

Table 3

Computation of Height of Ridges for Dnepr River

h, м	V, м/с 1	d, мм	$q_т \cdot 10^{-5}$, м²/с 2	3 Высота гряд		
				$h_г$ набл., м 4	$h_г$ рассч., м 5	отклонение, % 6
7,9	0,89	0,48	0,83	0,7	0,82	17,2
6,9	1,04	0,49	2,40	1,0	1,03	3,0
5,7	0,94	0,50	2,00	1,0	0,96	4,0
5,9	0,64	0,36	0,22	0,6	0,52	13,3

KEY:

1. m/sec
2. $q_{sol} \cdot 10^{-5}$
3. Height of ridges
4. h_r, obs
5. h_r, comp
6. deviation

In order to confirm the relationship between solid runoff and the height of the ridges we will make comparative computations using observational data for the Dnepr River, obtained by an expedition of the division in 1977 under the direction of B. A. Ivanov.

The observation sector was situated in the lower pool of the Kremenchugskaya Hydroelectric Power Station. The channel was close to prismatic. The dimensions of the ridges did not change as a result of daily regulation. The discharge q_{sol} of solid sediments was determined by the volumetric method -- by periodic measurements in a transverse trench intersecting the entire river channel.

The computed value of height of the ridges was determined using the formula

$$h_{\Gamma} = \frac{q_{T} (gh)^{3/2}}{0{,}011\ V^{4}}. \quad (4)$$

[Γ = r; T = sol]

which we obtained from the dependence derived by B. F. Snishchenko and Z. D. Kopaliani for the velocity of ridge movement [8]. The initial data and the results of the computations are listed in Table 3. They indicate a good correspondence between the observed and computed values.

Formula (4) can be recommended as a computation formula. The difficulty in its use is in the determination of the solid runoff, which, incidentally, remains one of the principal problems in channel process theory. It obviously must be solved taking into account the mechanism of spatial distribution of a flow of sediments in a river channel.

Greater attention must be devoted to the study of movement of sediments in rivers in the network of channel stations of the State Committee on Hydrometeorology and at institutes of other departments.

The following conclusion can be drawn from the analysis of the relationship between the height of ridges and flow and channel parameters presented in this article: the derivation of computation formulas for determining the height of ridges should rest on the laws of resistance to flow in a channel with a ridged bottom and transport of sediments. Work in this direction is now being done at the State Hydrological Institute.

BIBLIOGRAPHY

1. Grishanin, K. V., DINAMIKA RUSLOVYKH POTOKOV (Dynamics of Channel Flows), Leningrad, Gidrometeoizdat, 1969.

2. Znamenskaya, N. S., DONNYYE NANOSY I RUSLOVYYE PROTSESSY (Bottom Sediments and Channel Processes), Leningrad, Gidrometeoizdat, 1976.

3. Karasev, I. F., RUSLOVYYE PROTSESSY PRI PEREBROSKE STOKA (Channel Processes in the Transfer of Runoff), Leningrad, Gidrometeoizdat, 1975.

4. Knoroz, V. S., "Influence of Macroroughness of a Channel on its Hydraulic Resistance," IZV. VNIIG im. B. E. Vedeneyev (News of the All-Union Scientific Research Institute of Hydroengineering imeni B. Ye. Vedeneyev), Vol 62, 1959.

5. Pushkarev, V. F., "Motion of Entrained Sediments," TRUDY GGI (Transactions of the State Hydrological Institute), No 8(62), 1948.

6. Rzhanitsyn, N. A., MORFOLOGICHESKIYE I GIDROLOGICHESKIYE ZAKONOMERNOSTI STROYENIYA RECHNOY SETI (Morphological and Hydrological Laws of Structure of the River Network), Leningrad, Gidrometeoizdat, 1960.

7. Snishchenko, B. F., "Flow Velocity Regime in a Navigable River Channel," TRUDY LIVT (Transactions of the Leningrad Institute of Water Transport Engineers), No 61, 1964.

8. Snishchenko, B. F., Kopaliani, Z. D., "Rate of Movement of Ridges in Rivers and Under Laboratory Conditions," TRUDY GGI (Transactions of the State Hydrological Institute), No 252, 1978.

9. Snishchenko, B. F., "Computation of the Length of Sand Ridges in Open Flows," METEOROLOGIYA I GIDROLOGIYA (Meteorology and Hydrology), No 2, 1980.

10. Khorton, R. Ye., EROZIONNOYE RAZVITIYE REK I VODOSBORNYKH BASSEYNOV (Erosional Development of Rivers and Water Collection Basins), Moscow, IL, 1948.

UDC 556.565

NUMERICAL EVALUATION OF CHANGE IN THE THERMAL REGIME OF A PEAT DEPOSIT AS A RESULT OF ITS DRAINAGE

Moscow METEOROLOGIYA I GIDROLOGIYA in Russian No 6, Jun 80 pp 92-100

[Article by N. M. Khimin and Candidate of Technical Sciences I. L. Kalyuzhnyy, State Hydrological Institute, submitted for publication 30 November 1979]

[Text]

Abstract: This article gives a mathematical model of the thermal regime of the active layer of a peat deposit, making it possible, with the use of some hydro- and thermophysical characteristics of a natural and drained peat bog, as well as the meteorological parameters of the atmospheric surface layer, to carry out a numerical evaluation of the change in the thermal regime. A numerical evaluation of these changes is made and the role of individual factors is clarified as a result of this mathematical modeling.

Natural swamp areas, after removal of the moisture excess, constitute the most valuable lands suitable for agricultural use. In the continental regions of the middle and northern taiga subzones with a short growing season, low mean daily temperature in the winter months and a stable snow cover their use for agriculture is difficult and at times impossible.

For example, in the Komi ASSR the drainage of swamp areas leads to the formation of permanently frozen horizons of the deposit at a depth of 60-70 cm [7]. It is noted in a study by I. N. Skrynnikova [11] that in old worked peat bogs the appearance of a frozen layer, which exists to the middle of the summer, causes a considerable change in the hydrological regime of the soil. There are lenses of top water above the frozen layer. The permeability of the frozen horizons of the peaty soils is extremely insignificant and with the infiltration of melt water into the frozen soil the conditions arise which are examined in [6]. The appearance of top water over the permanently frozen layer, in combination with the low temperatures of the drained peat bog, exert a negative influence on the heating of the peaty soils during the growing season for agricultural crops. Thus, the close interrelationship between the temperature and water regimes in drained peat bogs must be taken into account in developing a method making it possible to evaluate the anticipated changes in the thermal regime of the peat deposit as a result of its drainage and subsequent agricultural exploitation of these lands.

A solution of this problem is possible by the mathematical modeling of the process of heat transfer in the active layer of the peat bog in the course of a number of annual cycles and the subsequent comparison of its temperature regimes before and after drainage.

Description of Model

Heat transfer in the active layer of the soil is a complex physical process which is very closely related to moisture transfer and the phase transformations of moisture. At the present time there is not a single workable model which describes all the processes exerting an influence on the thermal regime of the active soil layer to a full degree. Along the path to constructing such a model are difficulties of a hydrometeorological and mathematical nature.

In the model proposed below we have made the following fundamental assumptions simplifying the description of the process of interest to us, to wit:

1) neglecting of the influence of drainage of a swamp area on the thermal regime of the surface atmospheric layer;

2) neglecting the processes of moisture transfer, having little energy effect. These evidently include the migration of moisture to the freezing front and the infiltration of rain. However, the process of percolation of melt water into a frozen peat bog cannot be neglected because due to the setting free of latent heat during the freezing of melt water the energy effect of this process is extremely significant.

We will use H to denote the thickness of the active layer of the peat deposit, h(t) is the depth of the snow cover, where t is time (h(t) - 0 corresponds to the absence of snow on the soil surface). We will introduce the coordinate axis z, directed vertically upward, with its origin at the lower boundary of the active layer. In a general case the segment (0, H + h(t)) is broken down into several zones (for example, snow, frozen and thawed zones) with movable boundaries between them. The most effective method for computing heat transfer in the layer (0, H + h) is the smoothed coefficients method, or, as it is otherwise called, the "through calculation" method [3, 13, 14].

The idea of smoothing of the coefficients is as follows. At the boundaries of contact of the different zones the coefficients of the thermal conductivity equation experience a discontinuity. Accordingly, for the entire integration segment it is impossible at once to write a single equation which describes the heat transfer process. If these coefficients are smoothed in the neighborhood of the boundaries in such a way that they become sufficiently smooth functions of the z coordinate, then heat transfer can be described by a single equation with natural boundary conditions and a homogeneous difference scheme is used for its solution.

In order to smooth the dependence of the thermal conductivity coefficient $\lambda(z)$ and the heat capacity coefficient $c(z)$ in the neighborhood of the contact between the thawed and frozen zones, in this neighborhood it is sufficient to smooth the dependence $w(z)$, where w is the volumetric moisture content of the liquid phase. Assume that $(\delta T, 0)$ is the temperature range in which there is an intensive process of crystallization of unfreezing moisture, w^* is the moisture content on the curve of nonfreezing water at the point $T = \delta T$, where $T = T(z)$ is the soil temperature, $w^* = w(\delta T)$. Then the smoothing of the dependence $w(T)$ using formula (1) ensures an adequate smoothness of the dependences $\lambda(z)$ and $c(z)$ in the neighborhood of the contact between thawed and frozen zones.

$$w(T) = \begin{cases} W, \text{ with } T \geqslant 0 \\ W-(W-w^*)T/\delta T(2-T/\delta T), \quad \text{with } \delta T < T < 0 \\ w^*, \text{ with } T < \delta T. \end{cases} \tag{1}$$

Here W is volumetric moisture content, $W-(W-w^*)\frac{T}{\delta T}\left(2-\frac{T}{\delta T}\right)$,

$$W = w + \rho_{ice}/\rho_{water}\ vic,$$

where vic is volumetric ice content, ρ_{ice} and ρ_{water} are the densities of ice and water.

The dependence of the thermal conductivity coefficient on temperature and moisture content in the frozen zone is determined using the Ivanov formula [5]

$$\lambda(W, T) = \lambda_M(W) - [\lambda_M(W) - \lambda_T(W)]\frac{w(T)}{W}. \tag{2}$$

where "M" and "T" apply to the corresponding values in frozen and thawed zones.

We will determine, as this was assumed, the effective volumetric heat capacity of the soil c by the ratio

$$c = \rho_c c_c + \rho_B c_B w + \rho_Л c_Л Л + \rho_Л L\frac{\partial W}{\partial T}. \tag{3}$$

[Here and in the text which follows: B = water; Л = ice]

The subscript "c" characterizes the soil skeleton, L is the latent heat of water crystallization.

Due to the smoothing of (1) the dependences $\lambda(z)$ and $c(z)$ are continuous functions in the entire thickness of the peat deposit regardless of the number of contacting thawed and frozen zones. We note that the temperature regime of the peat bog is extremely sensitive to the shape of the curve for nonfreezing water. A natural peat deposit in the first approximation is homogeneous and it can be characterized by a single curve for nonfreezing water; a drained peat bog has a clearly expressed density stratification. The experiments show that the values of the volumetric moisture content in the liquid phase at negative temperatures in the upper horizons of a drained peat bog exceed by a factor of 1.5-2.5 the content of nonfreezing water in horizons situated below the drainage level at these same temperatures. Accordingly, the w^* parameter in formula (1) in our model is assumed to be dependent on the coordinate z in the drainage layer $w^*(z)$; it increases linearly in the segment $[H - z_0]$, where z_0 is the depth at which the drainage system is laid.

We will carry out smoothing of the λ coefficient at the snow-soil boundary, that is, in the neighborhood of the point z = H, using the formula

$$\tilde{\lambda}(z) = \begin{cases} \lambda(z), \text{ when } z < H \\ \lambda(H) + [\lambda_c - \lambda(H)] \frac{z-H}{\Delta z}\left(2 - \frac{z-H}{\Delta z}\right), \text{ when } H < z < H + \Delta z \\ \lambda_c, \text{ when } z > H + \Delta z. \end{cases} \tag{4}$$

$[\lambda_c = \lambda_{snow}]$ Here Δz is the smoothing interval, λ_{snow} is the thermal conductivity of the snow. The function $\tilde{\lambda}(z)$ is differentiable in the entire thickness of the snow. The function $\tilde{c}(z)$ -- the smoothed heat capacity -- is determined in a similarly way.

Taking (1)-(4) into account, we can now write a single thermal conductivity equation at once for the entire segment [0, H + h(t)] with natural boundary conditions at its ends:

$$c\frac{\partial T}{\partial t} = \frac{\partial}{\partial z}\left(\tilde{\lambda}\frac{\partial T}{\partial z}\right) + \delta(-T)\,\delta(H-z)\,\rho_B L\,\frac{\partial W}{\partial t}, \tag{5}$$

$$\delta(x) = \begin{cases} 0, & x \leq 0 \\ 1, & x > 0, \end{cases}$$

$$\frac{\partial T(0,\, t)}{\partial z} = 0,\quad T[H + h(t)] = T_1(t),\quad T(z,\, 0) = T_2(z). \tag{6}$$

The last term in equation (5) is the heat influx into an elementary soil volume as a result of the crystallization of melt water entering into the frozen soil during the spring snow melting, minus the heat expended on the part of the freezing bound water which is beginning to thaw. We neglected the heat flux of the percolating melt water, because, as indicated in [8], the magnitude of this flux is small in comparison with the flux of latent heat.

We have simplified the process of absorption of melt water into the frozen soil to the greatest extent possible because we are interested only in the thermal effect as a result of crystallization of infiltrating water.

After excluding the dynamics of absorption from consideration, we will assume that during the autumn-winter period, up to the time of onset of snow melting, the moisture content profile in the drained peat bog is in equilibrium. Below the level where the drainage system is laid the moisture content of the deposit can be considered equal to the maximum moisture capacity W_m.

We will denote the moisture content at the soil surface by means of W_0. This value can be determined experimentally. The equilibrium moisture content profile is parameterized using equation (7).

$$W(z) = \begin{cases} W_m, & 0 \leq z \leq H - z_0 \\ W_m - (W_m - W_0)\left(\frac{z - z_0}{H - z_0}\right)^2, & H - z_0 < z \leq H. \end{cases} \tag{7}$$

The curve corresponding to this equation is in satisfactory agreement with the experimental curve.

Assume that during the time Δt from the moment of onset of snow melting the moisture reserves in the snow have decreased by Δh. It is assumed here that until the aeration zone is completely filled with water all the melt water is expended in replenishing the moisture supplies of this layer; otherwise surface runoff occurs. The parameterization of the moisture content profile for the upper layer in the form given below corresponds to the assumption

$$W(z) = \begin{cases} W_m - \left(W_m - W_0 - \frac{3\Delta h}{H - z_0}\right)\left(\frac{z - z_0}{H - z_0}\right)^2, \text{ if} \\ \qquad\qquad W_m - W_0 \geq 3\Delta h\,(H - z_0). \\ W_m, \text{ if } \quad W_m - W_0 < 3\Delta h\,(H - z_0). \end{cases} \tag{8}$$

In our model the discharge of water into a drainage network begins immediately after disappearance of the snow. In the parameterization of discharge we take into account the experimentally established fact that the moisture content in the drained sector decreases exponentially with time to its equilibrium value W_{equil} in accordance with the dependence

$$W(t) = W_{equil} + (W_{onset} - W_{equil})e^{-\alpha t}, \tag{9}$$

where W_{onset} is the moisture content corresponding to the moment of onset of discharge. The parameter α is determined by the characteristic time of the discharge, which for the zone of interest to us is approximately 20 days. It is obvious that if there is ice in the drained layer the discharge will occur more slowly. This can be taken into account by making the parameter α variable in time, dependent on the phase state of the soil. Assume that $\overline{ice}$ is the mean ice content for the drained layer; $\overline{ice} = \overline{ice}(t)$. We will determine the dependence $\alpha(t)$ using the expression

$$\alpha(t) = \alpha_0\left(1 - \frac{\overline{A}(t)}{W_m}\right). \tag{10}$$

After the substitution of (10) into (9) we obtain a formula describing the discharge of melt water.

We will complete description of the model by determining the boundary conditions (6). It is known that the influence of the initial condition on solution of the parabolic equation decreases exponentially with time. Accordingly, any plausible function can be taken as $T_2(z)$ in (6). We assumed $T_2(z) = T_0$ = const and confirmed that the influence of such an initial condition on the solution is completely annihilated after three-four years -- the solution enters a periodic regime. This occurs for both drained and undrained swamp areas.

It is known [2] that there is a rather close correlation between the temperature of the surface of the swamp area and the air temperature at a standard height, which is expressed by the regression equation

$$T_{surface} = 1.1\ T_{air} - 0.5. \tag{11}$$

An exception is the period of snow melting when positive air temperatures correspond to a temperature of the snow surface equal to zero. Thus, as the function $T_1(t)$ it is possible to take the following

$$T_1(t) = \begin{cases} 0, \text{ if } T_{surf} \times h(t) > 0 \\ T_{surf}, \text{ if } T_{surf} \times h(t) \leqslant 0, \end{cases}$$

where T_{surf} is determined using equation (11).

Numerical Application of Model

Solution of a problem of the Stefan type by the smoothed coefficients method is reduced to the true solution when the smoothing interval tends to zero [9]. However, a numerical solution gives good results when the smoothing interval covers not less than 4-6 points of intersection of the difference grid [3]. In order to make the smoothing interval sufficiently narrow, placing a sufficient number of points of intersection of the difference grid within it, and at the same time keeping the total number of points of intersection quite small, it is necessary to use a nonuniform grid having a region of increased density of points of intersection in the neighborhood of the point of discontinuity of the coefficients of the thermal conductivity equation. In our problem the smoothing is carried out in the neighborhood of the point z = H at the boundaries of contact between the thawed and frozen zones. Under ordinary conditions a frozen zone is formed in the upper part of a peat deposit, that is, with z values close to H. Therefore, we selected the following construction of a spatial grid:

$$\left.\begin{array}{l} z_0 = 0;\ z_1 = \Delta z_1 = H(r-1)/(r^N - 1) \\ \Delta z_i = \Delta z_{i-1} \times r;\ z_i = z_{i-1} + \Delta z_i;\ i = 2, 3, \ldots, N \\ \Delta z_{N+1} = h(t)(q-1)(q^L - 1) + H \\ \Delta z_i = \Delta z_{i-1} \times q;\ z_i = z_{i-1} + \Delta z_i;\ i = N+2,\ N+3, \ldots, N+L \\ z_N = H;\ z_{N+L} = h(t) + H \end{array}\right\} \quad (12)$$

With $r < 1$ and $q > 1$ the grid (12) has an increased density of points of intersection in the neighborhood $z = H$, that is, at the soil surface. By changing the r and q values it is possible to regulate the maximum and minimum values of the interval in the z coordinate.

The grid (12) is time-movable. For scaling the grid solution to new points of intersection with transition to the next time layer it is necessary to carry out the interpolation as in [1]; we did this using the cubic spline method [10].

In applying the model we also use a nonuniform time grid. The most rapid transformation of the temperature profile is characteristic of the snow melting period, when a great quantity of heat is released as a result of crystallization of melt water. The use of a long time interval during this period can result in blunders. During the entire snow melting period the time interval in our case was 2 hours; otherwise the time was 1 day.

As information for determining the function $T_1(t)$ we used materials from direct observations of air temperature published in [12]. Scaling to points of the time grid was accomplished by interpolation by the cubic spline method. Similarly we determined the temporal variability of the depth of the snow cover and snow density.

Equation (5) was approximated in the grid (12) by a system of algebraic equations using a purely implicit, nonlinear model

$$c_i^{m+1} \frac{T_i^{m+1} - T_i^m}{t^{m+1} - T^m} = \frac{1}{\Delta z_i}\left(a_{i+1} \frac{T_{i+1}^{m+1} - T_i^{m+1}}{\Delta z_{i+1}^{m+1}} - a_i \frac{T_i^{m+1} - T_{i-1}^{m+1}}{\Delta z_i^{m+1}}\right) +$$

$$+ \delta(-T_i^{m+1})\,\delta(H - z_i)\,\rho_0 L \frac{W_i^{m+1} - W_i^m}{t^{m+1} - t^m}, \quad 1 \leqslant i \leqslant N + L - 1; \quad (13)$$

$$c_i^{m+1} = \tilde{c}\,(W_i^{m+1},\ T_i^{m+1});\ \Delta \bar{z}_i = (\Delta z_i^{m+1} + \Delta z_i^{m+1})\,2;$$

$$a_i = \frac{1}{2}\,[\tilde{\lambda}\,(W_i^{m+1},\ T_i^{m+1}) + \lambda\,(W_{i-1}^{m+1},\ T_{i-1}^{m+1})].$$

The boundary conditions have the form

$$T_0^m = T_1^m;\ T_{N+L}^m = T_1(t^m);\ T_i^0 = T_0,\ 0 \leq i \leq N \tag{14}$$

We used 1 September as the beginning of time reckoning (at this time a snow cover is absent). The initial temperature distribution in the snow thickness immediately after falling of the snow was stipulated by a linear function

$$T_i^{m_1+1} = T_N^{m_1-1} + [T_1(t^{m_1}) - T_N^{m_1-1}]\frac{z_i^{m_1} - H}{h^{m_1}},\ N+1 \leq iN+L, \tag{15}$$

where t^{m1} is the moment of onset of a snow cover, h^{m1} is the initial thickness of the snow cover, assumed to be equal to the mean 10-day thickness of the snow cover during the first 10 days after the onset of its existence.

System (13)-(15) was solved by the traditional iterations method in combination with fitting.

Results of Computations

On the basis of the mathematical model cited above we carried out computations of the temporal variability of the temperature regime of drained peat bogs for 15 places in the northern part of the Nonchernozem zone in the RSFSR. It was assumed that the depth of the drainage system z_0 is 1 m; the seasonal variation of ground temperature is completely absent at a depth of 6 m; the characteristics of the meteorological regime of the atmospheric surface layer correspond to the observed mean 10-day values [12] and the thermophysical properties are identical for all the peat bogs in this zone.

It was established as a result of mathematical modeling that under the conditions prevailing in the northern part of the Nonchernozem zone of the RSFSR the drainage of swamp areas leads to a substantial decrease in the temperature of the upper layer of the peat deposit. The table gives the mean temperatures of the upper meter layer of the peat deposit at the end of each month before and after drainage. An analysis of the table shows that the mean monthly temperature of the active layer during the growing season is 1-2°C lower in the drained swamp areas. A temperature decrease is observed during the entire year.

An increase in the depth of snow in drained swamp areas at the same air temperatures as before drainage leads to a decrease in the temperature difference of the active layer in the peat bog before and after drainage. Thus, the mean monthly temperature of the meter layer of the deposit in January, February and March, computed using observational data for the Verkhniy Shugor meteorological station, is positive, whereas during these same months the similar temperatures computed for Nar'yan-Mar station are negative. This is a result of the fact that the snow depth in the region

Results of Mathematical Modeling of Peat Deposit Temperature, °C

	Метеостанция 1	Состояние болотного массива 2	Глубина промерзания, см 3	IX	X	XI	XII	I	II	III	IV	V	VI	VII	VIII	Наибольшая высота снежного покрова, см 4	Среднегодовая температура воздуха, °C 5
6	Жижгин Остров	е 21	29	3,5	2,9	2,5	2,1	1,7	1,2	1,2	1,2	2,1	3,2	3,8	4,2	10	0,6
		о 22	36	2,6	2,2	1,7	1,1	0,7	0,3	0,6	1,0	1,4	2,2	2,6	2,9		
7	Пинега	е	6	4,2	3,6	3,3	3,1	2,9	2,7	2,6	1,6	3,7	4,7	5,1	5,7	41	−0,2
		о	24	3,0	2,5	2,1	1,8	1,5	1,3	1,4	1,7	2,4	3,1	3,4	3,9		
8	Варандей	е	73	1,1	0,8	0,5	0,1	−0,3	−0,7	−0,9	−0,9	−0,7	0,3	0,7	1,4	37	−5,6
		о	82	0,6	0,1	−0,4	−1,2	−1,6	−2,2	−1,8	−1,4	−0,7	−0,1	0,2	0,9		
9	Верхний Шугор	е	0	3,3	3,2	3,1	3,0	2,9	2,8	2,7	2,6	2,5	4,0	4,7	5,1	131	−4,0
		о	13	2,6	2,5	2,3	2,2	2,0	1,9	1,8	1,9	1,9	3,0	3,4	3,7		
10	Ходовариха	е	65	1,2	0,9	0,5	0,1	−0,2	−0,5	−0,6	−0,6	−0,4	0,4	1,1	1,4	44	−4,6
		о	67	0,8	0,5	−0,2	−0,6	−1,0	−1,2	−1,2	−0,8	−0,2	0,3	0,7	1,0		
11	Моржовец, остров	е	1	3,5	3,3	3,0	2,8	2,6	2,5	2,4	2,3	2,8	3,2	3,8	4,3	57	−0,8
		о	20	2,7	2,2	2,0	1,7	1,5	1,4	1,4	1,5	1,7	2,2	2,7	3,0		
12	Якша	е	0	4,8	4,4	4,2	4,0	3,8	3,7	3,6	3,4	4,5	5,5	6,0	6,3	86	−1,0
		о	15	3,3	2,8	2,5	2,3	2,1	1,9	1,9	2,0	2,8	3,5	3,8	4,2		
13	Усть-Шугор	е	0	4,0	3,8	3,6	3,4	3,3	3,2	3,1	2,9	3,8	4,9	5,4	5,7	94	−2,5
		о	16	2,9	2,6	2,3	2,1	1,9	1,8	1,7	1,9	2,5	3,3	3,6	4,1		
14	Ижма	е	10	3,7	3,1	2,9	2,6	2,4	2,3	2,2	2,2	3,2	4,1	4,5	5,0	55	−2,0
		о	26	2,7	2,2	1,9	1,5	1,3	1,1	1,1	1,4	2,0	2,9	3,1	3,7		
15	Петрунь	е	38	2,3	2,0	1,7	1,4	1,0	0,7	0,6	0,6	1,2	2,2	2,9	3,2	36	−4,4
		о	57	1,3	0,8	0,3	−0,2	−0,8	−0,9	−0,8	−0,3	0,5	1,1	1,5	1,7		
16	Нарьян-Мар	е	28	2,7	2,4	2,2	1,9	1,6	1,3	1,2	1,1	1,7	2,5	3,2	3,4	38	−3,5
		о	48	1,5	1,2	0,8	0,3	−0,1	−0,3	−0,3	0,1	0,9	1,5	1,7	2,1		
17	Индига	е	49	1,9	1,5	1,2	0,9	0,5	0,2	0,0	0,0	0,7	1,4	1,9	2,2	28	−2,8
		о	59	1,3	0,8	0,4	−0,1	−0,7	−1,0	−0,9	−0,4	0,1	0,8	1,2	1,6		
18	Троицко-Печорское	е	0	4,5	4,1	3,9	3,7	3,5	3,4	3,2	3,5	4,5	5,5	5,9	6,4	68	−1,2
		о	16	2,9	2,7	2,4	2,2	2,0	1,8	1,8	2,3	2,9	3,6	3,9	4,5		
19	Койнас	е	0	4,4	3,7	3,5	3,3	3,1	3,0	2,9	2,8	3,6	4,7	5,4	6,0	66	−1,1
		о	19	3,0	2,6	2,2	1,9	1,7	1,6	1,6	1,8	2,6	3,1	3,5	3,9		
20	Мутный Материк	е	19	3,0	2,8	2,5	2,3	2,0	1,8	1,7	1,7	2,4	3,5	3,9	4,6	43	−2,8
		о	43	1,7	1,4	1,0	0,5	0,1	0,0	0,1	0,6	1,4	2,2	2,4	2,8		

KEY TO TABLE:

1. Meteorological station
2. State of swamp area
3. Depth of freezing, cm
4. Maximum depth of snow cover, cm
5. Mean annual air temperature, °C
6. Zhizhgin Ostrov
7. Pinega
8. Varandey
9. Verkhniy Shugor
10. Khodovarikha
11. Morzhovets, ostrov
12. Yaksha
13. Ust'-Shugor
14. Izhma
15. Petrun'
16. Nar'yan-Mar
17. Indiga
18. Troitsko-Pechorskoye
19. Koynas
20. Mutnyy Materik
21. Natural swamp area
22. Drained swamp area

---

of the first station is 131 cm, whereas at the second it is 38 cm. The mean annual air temperatures are -4.0 and -3.5°C respectively.

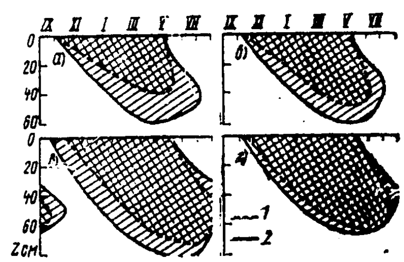

Fig. 1. Dynamics of change in thickness of frozen zone of peat bog before (1) and after (2) drainage for stations Petrun' (a), Indiga (b), Varandey (c) and Khodovarikha (d).

The computations indicate that with drainage there is also an increase in the depth of freezing, thickness and lifetime of the frozen layer of the deposit. In individual cases a frozen layer was not observed in the swampy area in a natural state; after drainage the freezing attains 20 cm.

The figure shows the dynamics of development of the frozen zone in the course of freezing and thawing of a peat deposit for four computation points. The figure shows that at Petrun' station the freezing depth increased by 20 cm and the lifetime of the frozen layer increased by two months.

As a result of the latter circumstance the existence of a frozen layer can be observed during the entire year. The thickness of the frozen layer with a depth of laying of the drainage system of 1 m can be increased in dependence on external conditions by 30 or more percent. With an increase in the depth of laying of the drainage system the thickness of the frozen layer increases. The latter circumstance has the following result: with full working and settling of the upper layer of the peat deposit the drainage system can cease to function both as a result of clogging of the drains by an ice layer and due to formation of an impermeable layer above the depth of laying of the drains. Accordingly, an important circumstance is the formulation of effective measures for preventing the malfunctioning of a drainage system in the course of its operation. The formulated measures can be based on principles of an increase in the heat capacity of the peat deposit at the beginning of the freezing period or a decrease in heat losses in the "peat deposit - surface layer" system. The effectiveness of these measures can be evaluated by mathematical modeling of the temperature regime of the drained peat bog using the proposed or improved model.

BIBLIOGRAPHY

1. Alalykin, G. B., Godunov, S. K., Kireyeva, I. L., Pliner, L. A., RESHENIYE ODNOMERNYKH ZADACH GAZOVOY DINAMIKI V PODVIZHNYKH SETKAKH (Solution of One-Dimensional Problems in Gas Dynamics in Moving Grids), Moscow, Nauka, 1970.

2. Bavina, L. G., "Refinement of Computation Parameters of Evaporation from Swamps Using Observational Data from Swamp Stations," TRUDY GGI (Transactions of the State Hydrological Institute), No 145, 1967.

3. BOLOTA ZAPADNOY SIBIRI, IKH STROYENIYE I GIDROLOGICHESKIY REZHIM (The Swamps of Western Siberia, Their Structure and Hydrological Regime), Leningrad, Gidrometeoizdat, 1976.

4. Budak, B. M., Solov'yeva, Ye. N., Uspenskiy, A. B., "Difference Method With Smoothing of Coefficients for Solution of the Stefan Problem," ZHURNAL VYCHISLITEL'NOY MATEMATIKI I MATEMATICHESKOY FIZIKI (Journal of Computation Mathematics and Mathematical Physics), Vol 5, No 5, 1965.

5. Ivanov, N. S., TEPLO- I MASSOPERENOS V MERZLYKH GORNYKH PORODAKH (Heat and Mass Transfer in Frozen Ground), Moscow, Nauka, 1969.

6. Kalyuzhnyy, I. L., Morozova, N. S., Pavlova, K. K., Romanov, V. V., "Thermophysical Method for Computing Losses of Melt Water in Infiltration into Frozen Soil," METEOROLOGIYA I GIDROLOGIYA (Meteorology and Hydrology), No 1, 1972.

7. Kochetkova, V. L., "Characteristics of the Thermal Regime of Peaty Soils of the Intinskiy Industrial Region," TRUDY KOMI FILIALA AN SSSR (Transactions of the Komi Affiliate USSR Academy of Sciences), Syktyvkar, No 11, 1961.

8. Motovilov, Yu. G., "Numerical Modeling of the Process of Water Infiltration into Frozen Soils," METEOROLOGIYA I GIDROLOGIYA, No 9, 1977.

9. Oleynik, O. A., "One Method for Solving the General Stefan Problem," DOKLADY AN SSSR (Reports of the USSR Academy of Sciences), Vol 135, No 5, 1960.

10. Samarskiy, A. A., Moiseyenko, B. D., "Economic Scheme for Through Reckoning for the Multidimensional Stefan Problem," ZHURNAL VYCHISLITEL'NOY MATEMATIKI I MATEMATICHESKOY FIZIKI, Vol 5, No 5, 1965.

11. Skrynnikova, I. N., "Water and Temperature Regime of Seasonally Frozen Peaty Old Worked Soils of River Valleys in the Middle Taiga of the Komi ASSR," MEZHDUNARODNYY SIMPOZIUM PO GIDROLOGII ZABOLOCHENNYKH TERRITORIY (International Symposium on Hydrology of Swampy Territories), Minsk, Nauka i Tekhnika, Vol 1, 1973.

12. SPRAVOCHNIK PO KLIMATU SSSR (Handbook on USSR Climate), No 1, Part II, Leningrad, Gidrometeoizdat, 1965.

13. Stechkin, S. B., Subbotin, Yu. N., SPLAYNY V VYCHISLITEL'NOY MATEMATIKE (Splines in Computational Mathematics), Moscow, Nauka, 1976.

14. Khimin, N. M., "Mathematical Model of Freezing of Finely Dispersed Soils," MATEMATICHESKIYE I STATISTICHESKIYE MODELI V GIDROLOGICHESKIKH ISSLEDOVANIYAKH (Mathematical and Statistical Models in Hydrological Investigations), Leningrad, Gidrometeoizdat, 1974.

UDC 551.509.33

PREDICTION OF THE AIR TEMPERATURE ANOMALY VARIATION OVER THE COURSE OF A MONTH BY FIVE-DAY PERIODS

Moscow METEOROLOGIYA I GIDROLOGIYA in Russian No 6, Jun 80 pp 101-104

[Article by R. I. Burakova, USSR Hydrometeorological Scientific Research Center, submitted for publication 17 October 1979]

[Text]

Abstract: The temporal variation of the air temperature anomaly by five-day periods in the course of a month is represented analytically using orthogonal Chebyshev polynomials. The prediction of the temporal variation of air temperature by five-day periods over the course of a month is reduced to computation of the values of the Chebyshev expansion coefficients and restoration of these fields using these coefficients.

It is customary to use some prognostic indications in the routine practice of predicting weather changes over the course of a month. However, these indications do not always have a reliable success.

There are methods for predicting changes in surface pressure and geopotential of the 500-mb isobaric surface with time by a statistical approach using an analytical representation of evolution of a meteorological field by means of natural orthogonal components or by means of Chebyshev polynomials [1, 2, 4].

In this study our objective is to develop a statistical method for predicting changes in air temperature over the course of a month from five-day period to five-day period. In developing the method we used the following hypothesis: the change in the temperature anomaly from five-day period to five-day period over the course of the several preceding months determines the temperature fluctuation from five-day period to five-day period over the course of the month for which the forecast is prepared.

In order to evaluate the nature of variations in the temperature anomaly from five-day period to five-day period we used the procedure of analytical representation of the time sequence of meteorological fields by Chebyshev polynomials [2].

The totality of the mean five-day temperature anomalies, determined at 36 points (European USSR and Western Siberia), can be written in the form of matrices of the following type:

$$\| \Delta T_{ij} \| \quad (i = 1, 2, \ldots, 6,$$
$$j = 1, 2, \ldots, 6).$$

Six such matrices give the characteristics of the temporal variation of the temperature anomaly over the course of a month by five-day periods. In order to obtain the expansions we used polynomials to the fifth degree inclusive.

The change in the mean five-day temperature anomaly in the course of one particular month is represented analytically as follows:

$$\Delta T(x, y, t) = \\ = \sum A_{ksr} \varphi_k(x) \psi_s(y) \chi_r(t), \tag{1}$$

where x, y are the coordinates of the point, t is time (1, 2, 3, 4, 5, 6); φ, ψ, χ are Chebyshev polynomials; k, s, r are the numbers of the polynomials.

The coefficients A_{ksr} are computed using the formula

$$A_{ksr} = \frac{\sum_x \sum_y \sum_t \Delta T(x, y, t) \varphi_k \psi_s \chi_r}{\sum_x \varphi_k^2 \sum_y \psi_s^2 \sum_t \chi_r^2}. \tag{2}$$

If the A_{ksr} coefficients are normalized:

$$\bar{\varphi}_k = \frac{\varphi_k}{\sqrt{\sum_x \varphi_k^2}}, \quad \bar{\psi}_s = \frac{\psi_s}{\sqrt{\sum_y \psi_s^2}}, \\ \bar{\chi}_r = \frac{\chi_r}{\sqrt{\sum_t \chi_r^2}}, \tag{3}$$

then formula (2) can be written more simply:

$$\bar{A}_{ksr} = \sum_x \sum_y \sum_t \Delta T(x, y, t) \bar{\varphi}_k \bar{\psi}_s \bar{\chi}_r. \tag{4}$$

Table 1

Ratio of Number of Significant Correlation Coefficients to Total Number of Coefficients, %

Весенние месяцы 1	2 Месяцы года											
	I	II	III	IV	V	VI	VII	VIII	IX	X	XI	XII
3 Март	41	41	18	22	15	6	26	26	9	12	32	47
4 Апрель	22	9	26	9	9	18	18	9	6	22	9	29
5 Май	15	15	42	6	9	9	20	9	9	18	18	6

KEY:
1. Spring months
2. Months of year
3. March
4. April
5. May

Table 2

Коэффициенты разложения 1	A_{000}	A_{010}	A_{020}	A_{001}	A_{002}	A_{100}	A_{101}	A_{201}	A_{022}
act σ_{Φ}/σ_n 2	3,05	1.74	1.82	3,54	3,40	1.82	3,86	3,67	5,82

KEY:
1. Expansion coefficients
2. Φ = act

Coefficients of this type were computed for the field of air temperature anomaly in the course of a month by five-day periods for all months for the 25-year period 1950-1974.

A precise representation of evolution of the temperature anomaly field, averaged for five days in the course of a month (ρ = 1.0; Q = 0.0), gives 216 expansion coefficients. An evaluation of their role indicated that the use of 34 expansion coefficients ($k + s + r \leqslant 4$) gives an adequate accuracy in approximation of evolution of the ΔT field in the course of a month by five-day periods ($\rho \geqslant 0.80$; $Q \leqslant 0.50$).

We proceeded in the following way for predicting the A_{ksr} coefficients. First of all we determined the influence of the coefficients with a definite number (ksr) on the future value of the coefficients with the same number (ksr). For this we computed the paired correlation coefficients between the corresponding expansion coefficients for March and each preceding month of the year. Similar computations were made for April and

Table 3

Evaluation of Prediction

Оценка Evaluation	Март March						Апрель April						Май May					
	Пентада Five-day period																	
	1	2	3	4	5	6	1	2	3	4	5	6	1	2	3	4	5	6
$\rho_{ср}$	0,26	0,24	0,22	0,36	0,36	0,28	0,42	0,31	0,28	0,23	0,25	0,20	0,22	0,29	0,28	0,34	0,26	0,26
Q mean	0,98	1,00	0,95	0,85	0,88	0,94	0,76	0,73	0,78	0,79	0,81	0,87	1,09	1,22	0,98	0,89	0,97	1,11
P%	90	80	75	90	85	85	85	90	80	85	80	75	90	100	95	95	85	75
r	0,41	0,38	0,45	0,56	0,56	0,44	0,66	0,49	0,44	0,36	0,39	0,31	0,35	0,45	0,44	0,53	0,41	0,41

Table 4

Evaluations of Prediction of Sharp Changes in Five-Day Air Temperature Anomaly

Оценка Evaluation	Март March		Апрель April		Май May	
	Пентада Five-day period					
	Предыдущая Preceding	Последующая Following	Предыдущая	Последующая	Предыдущая	Последующая
$\rho_{ср}$	0,29	0,17	0,29	0,22	0,34	0,30
Q mean	1,298	1,404	0,955	0,985	1,153	1,268
P%	73	73	82	68	90	90
r	0,45	0,27	0,45	0,35	0,53	0,47

Table 5

Evaluations of Predictions

Year Год	Пентада Five-day period											
	1		2		3		4		5		6	
	ρ	Q	ρ	Q	ρ	Q	ρ	Q	ρ	Q	ρ	Q
1972	0,22	0,38	−0,56	1,76	−0,44	1,24	0,11	0,58	0,39	0,68	0,67	0,63
1973	−0,17	0,85	−0,06	0,80	0,06	0,84	0,11	0,57	0,33	1,06	0,39	0,98
1974	0,22	0,96	0,28	0,73	0,17	0,90	0,17	1,18	0,06	1,01	−0,11	0,63

May. We selected the significant correlation coefficients from the 216 correlation coefficients (r) characterizing the correlation between the evolution of the mean five-day air temperature anomalies for the two months. For this we used the confidence interval for r, equal to

$$\operatorname{th}\left(z - 1.96\sqrt{\frac{1}{n-3}}\right) < r < \operatorname{th}\left(z + 1.96\sqrt{\frac{1}{n-3}}\right), \tag{5}$$

where

$$z = \frac{1}{2}\ln\left(\frac{1+\hat{r}}{1-\hat{r}}\right).$$

In order to evaluate the correlation of evolution of the fields of mean five-day air temperature anomalies between the two months we ascertained the number of significant correlation coefficients from the 34 coefficients relating to these A_{ksr} with $k + s + r < 4$. Table 1 gives the number of significant correlation coefficients, expressed in percent, characterizing the correlation of the evolution of the mean five-day anomalies between the two months.

The following conclusions can be drawn from the data presented in the table. The closest correlation of the evolution of the mean five-day temperature anomaly in March is noted with the evolution of the field in December, January and February (the number of significant correlation coefficients is 40% of all the considered correlation coefficients characterizing the correlation of evolution of the fields of mean five-day air temperature anomalies). Thus, for prediction of the ΔT variation in March it is desirable to use information for two groups of months: first -- December, January, February; second -- October, November, December. For a prediction for April it is desirable to use three groups: first -- December, January, March; second -- October, December, January; third -- November, December, January and for May, also three groups: first -- July, November, March; second -- December, October, March; third -- December, January, February.

The method for predicting the A_{ksr} value is as follows: each of the 216 expansion coefficients for the month for which the forecast is given is represented in the form of a linear combination of the corresponding expansion coefficients of the most informative months obtained by the above-mentioned method. The prognostic equation has the following form:

$$\hat{A}_{ksr} = \Sigma C^{(i)}_{ksr} A^{(i)}_{ksr}. \tag{6}$$

We introduce the notations:

$$x_1 = A^{(1)}_{ksr}, \quad x_2 = A^{(2)}_{ksr}, \quad x_3 = A^{(3)}_{ksr};$$

then

$$\hat{A}_{ksr} = \sum_{l=1}^{3} C_l x_l. \tag{7}$$

In this case we solve 216 systems of normal equations whose principal matrices will be matrices in the form

$$B_l = \left\| \begin{matrix} b_{11} & b_{12} & b_{13} \\ b_{21} & b_{22} & b_{23} \\ b_{31} & b_{32} & b_{33} \end{matrix} \right\|. \tag{8}$$

The elements of this matrix are determined in the following way:

$$b_{ij} = \Sigma x_i x_j, \tag{9}$$

where summation is for all the months entering into the series.

In order to obtain less smoothed values [3] of the mean five-day temperature anomaly we used the ratio σ_{act}/σ_n, where σ_{act} is the standard deviation of each expansion coefficient, obtained on the basis of actual data, and σ_n is the standard deviation of the expansion coefficients, obtained as a result of computations using formula (6). The values of the σ_{act}/σ_n ratios for some A_{ksr} coefficients (March) are given in Table 2.

Using dependent material for each of the groups of most informative months we evaluated all of the cases entering into the series.

The most successful evaluations are obtained if the A_{ksr} coefficients for the preceding October, November and December are used as predictors in a forecast for March; in a prediction for April -- December, January and March; in a prediction for May -- July, November and March. We note that the computations of all the expansion coefficients by the method noted above leads to a more successful result than when making computations using a limited number of A_{ksr} coefficients. Table 3 gives evaluations of predictions using ρ and Q, as well as the probabilities of realization of positive ρ values (P%) and the correlation coefficients r.

In order to discriminate cases of a marked change in the mean five-day temperature anomaly from one five-day period to the next we computed, using actual data, the values of the similarity parameter for each two successive five-year periods, and also a value equal to the ratio of the number of stations at which the differences in the ΔT_1 values of two successive five-day periods exceeded σ_1, to the total number of stations $\overline{B}$. The determination of the corresponding probability distribution functions of the ρ and $\overline{B}$ values made it possible to discriminate equiprobable classes of the ρ and $\overline{B}$ values characterizing nonsignificant, normal and marked changes in the field of mean five-day temperature anomalies from one five-day period to the next. Table 4 gives evaluations of the method for predicting marked changes in the field of mean five-day temperature anomalies from one five-day period to the next.

The forecasting method was also checked for cases not entering into the series used in statistical processing. As an example of the results of this checking Table 5 gives evaluations of a forecast for March.

The results indicate the desirability of use of the preceding temperature change with time for the purposes of long-range weather forecasting.

BIBLIOGRAPHY

1. Bagrov, N. A., Zverev, N. I., "Method for Predicting the H_{500} Geopotential Field for Intermediate Times," TRUDY TsIP (Transactions of the Central Institute of Forecasts), No 108, 1961.

2. Zverev, N. I., Purganskaya, I. P., "Practical Procedures for Expanding the Fields of Meteorological Elements Using Chebyshev Polynomials," TRUDY TsIP (Transactions of the Central Institute of Forecasts), No 123, 1963.

3. Karpeyev, G. A., "Relative Error as a Measure of the Success in Forecasting Meteorological Fields," TRUDY GIDROMETTSENTRA SSSR (Transactions of the USSR Hydrometeorological Center), No 44, 1969.

4. Yudin, M. I., Repinskaya, R. P., "Prediction of the Intramonthly Variation of Pressure by a Physical-Statistical Method," METEOROLOGIYA I GIDROLOGIYA (Meteorology and Hydrology), 1974.

UDC 551.551

INFLUENCE OF OROGRAPHY ON THE SURFACE WIND

Moscow METEOROLOGIYA I GIDROLOGIYA in Russian No 6, Jun 80 pp 104-105

[Article by S. M. Kozik, Central Asiatic Regional Scientific Research Institute, submitted for publication 10 April 1979]

[Text]

Abstract: On the basis of data from three observation points in Turkmenia the author briefly describes a method for the climatic processing of the surface wind vector, making it possible to obtain stable characteristics of the effect exerted on the wind by a mountain range not determined in ordinary climatic processing.

Usually in the climatic processing of the wind its velocity and direction are considered separately. Below, using a small example, we outline one of the possible procedures for climatic processing of the wind vector. We examined data for three meteorological stations in Turkmenia: Ashkhabad (Keshi) during the period 1923-1935, Kaakhka and Yerbent during the period 1936-1965. All three meteorological stations are situated on a plain to the north of the Kopet-Dag mountain range, running almost linearly from WNW to ESE in the azimuth 120°. Their distances from the axis of the range are: for Ashkhabad -- about 30 km, the same for Kaakhka, and about 150 km for Yerbent. The mountain peaks attain 2-3 km. The few passes have elevations of 1.5-2 km. Schematically it is possible to represent the range as a wall with a length of 600 km and a height of 2 km. We used data on the wind at a height of about 10 m above the ground, obtained using a Wild vane at 1300 hours local mean solar time, represented in vector form.

The wind vector is represented by a segment whose length is proportional to the wind velocity. The end of the vector is matched with the observation point. The statistical study of the wind vectors at a particular point involves an investigation of the distribution of the initial points of the vectors. The mean vector has as its beginning the "center of gravity" of the set of these points. The scatter of points relative to their center of gravity is characterized by the dispersion. It is assumed that in the free atmosphere in the complete absence of orographic and other obstacles the dispersion of points in all horizontal directions is identical.

Mean Long-Term Characteristics of Surface Wind

Время года 1	Средняя скорость ветра, м/с 2	Направление среднего вектора ветра, град 3	Направление рассеяния точек начал векторов, град 4	Отношение осей эллипсов равновероятной плотности точек 5	Средняя дисперсия точек 6
7 Ашхабад (Кеши)					
10 Зима	2,3	41	120	0.43	2,9
11 Весна	2,9	27	115	0.41	4,1
12 Лето	2,8	−5	114	0,41	3,4
13 Осень	2,5	48	116	0.38	2,7
14 Год			116	0,41	
8 Каахка					
Зима	2.8	41	115	0,48	4,3
Весна	3,6	17	116	0,47	6,6
Лето	3,8	−12	116	0.51	6,1
Осень	3,3	33	112	0.47	5,1
Год			115	0,48	
9 Ербент					
Зима	4,3	67	106	0,57	10,3
Весна	4,9	35	108	0,58	13,9
Лето	4.2	−4	104	0.70	9.7
Осень	4,2	59	109	0,63	9,4
Год			107	0,62	

KEY:

1. Season
2. Mean wind velocity, m/sec
3. Direction of mean wind vector, degrees
4. Direction of scattering of points of beginning of vectors, degrees
5. Ratio of axes of ellipses of equiprobable density of points
6. Mean dispersion of points
7. Ashkhabad (Keshi)
8. Kaakhka
9. Yerbent
10. Winter
11. Spring
12. Summer
13. Autumn
14. Year

Note. The direction in degrees indicates the azimuth reckoned from north (+ eastward, - westward).

The presence of obstacles leads to a dependence of dispersion on direction.

For all practical purposes the scatter of points adheres closely to a normal correlation (that is, a significance of deviations of the third-order central moments from zero can be discovered only when there is extensive and reliable observational data). Accordingly, the dispersion is usually adequately characterized by its mean value, the azimuth of maximum scattering and the ratio of the axes of the ellipses of equiprobable density of arrangement of points.

The table shows that although the mean wind velocity and the direction of its mean vector differ in different seasons of the year it is important that the azimuth of the greatest scattering of points and the ratio of the axes of the scattering ellipses are extremely stable climatic characteristics at each of the three points and do not reveal any appreciable annual variation. The ellipse of scattering of the points is drawn out approximately parallel to the mountain range and with increasing distance from it the elongation of the ellipse is reduced. The mean dispersion of points is close to half the square of wind velocity.

It is desirable to make a geographic study of these characteristics in the surface layer, in particular, near mountain ranges with a different orientation, and also a similar investigation of the wind in the higher layers of the atmosphere.

UDC 556.16(100)

CHANGE IN RIVER RUNOFF FOR LARGE REGIONS OF THE EARTH

Moscow METEOROLOGIYA I GIDROLOGIYA in Russian No 6, Jun 80 pp 106-107

[Article by Candidate of Technical Sciences P. P. Denisov, submitted for publication 22 February 1979]

[Text]

Abstract: As a result of processing of series of runoff observations for major regions and for the continents as a whole for the period from 1918 through 1966 it was possible to detect trends in the course of river runoff for different territories of the earth. A positive trend in the course of river runoff was noted for the rivers of the following basins: Arctic, Pacific (except for South America) and Indian Oceans. A negative trend is observed on the rivers of the Atlantic Ocean basin and in the regions of internal runoff of the continents.

Computations of the world water balance carried out by Soviet researchers [3] made it possible to evaluate the variation of river runoff by years for large regions during the period from 1918 through 1966. These materials make it possible to analyze the existing trends in the course of river runoff which must be taken into account in drawing up long-range plans for water management construction.

The trend and the intensity of changes in the course of river runoff (increase or decrease in its quantity) can be evaluated by a method proposed in [1]. As a characterization of the change in the quantity of river runoff this method recommends writing of regression equations in the form

$$Q=\overline{Q}+q(t-\overline{t}),$$

where $\overline{Q}$ is the mean water discharge during the computation period; $\overline{t}$ is the middle year in the considered calendar series; q is the mean annual increment in water discharge (trend value).

Table 1

Trend in Variation of River Runoff in Period 1918-1966 for Ocean Basins

Basin	Continent	$\overline{Q}$	q
Arctic Ocean	North America	1450	4.53
	Asia	2326	1.34
	Europe	667	0
Pacific Ocean	North America	2450	5.80
	Asia	4170	1.31
	Australia	113	0.53
	South America (including Chilean Archipelago)	1350	-3.13
Indian Ocean	Africa	485	3.21
	Asia	3660	2.60
	Australia	178	0.56
Atlantic Ocean	North America	2730	-3.688
	South America (with Tierra del Fuego and regions of internal runoff)	10420	-1.68
	Africa	3700	-3.47
	Europe	1744	-1.45
	Asia	199	-0.39
Regions of internal runoff	Asia	438	-0.68
	Europe	317	-0.44
	Australia	8.85	-0.006

Using the least squares method, the trend value can be determined using the formula

$$q=\frac{\sum_{i=1}^{N}(Q_i-\overline{Q})(t_i-\overline{t})}{\sum_{i=1}^{N}(t_i-\overline{t})^2},$$

where N is the number of terms in the considered series.

As a convenience in computations in the analysis we used series with an odd number of terms in the series, specifically a 49-year series from 1918 through 1966 (middle year -- 1942). Accordingly, the regression equations for all the investigated basins will have the form

$$Q=\overline{Q}+q(t-1942).$$

As a result of processing of series of observations of river runoff cited in [3] we obtained the parameters of the regression equation (see Table 1, where runoff Q is expressed in km^3/year and the trend q in the course of river runoff is expressed in km^3/year per year).

Table 2

Trend in Course of River Runoff in Period 1918-1966 by Continents

Continent	$\bar{Q}$	q
North America	6630	6.65
Asia	10810	3.50
Australia	300	1.08
Africa	4190	-0
Europe	2730	-1.92
South America	11760	-4.83

An analysis of the results of computations of the trend in the course of river runoff by large regions of the earth indicates that during the period 1918-1966 (see Table 1) there was an increase in the runoff on rivers of the basins of the Arctic, Pacific and Indian Oceans, whereas the runoff of rivers of the Atlantic Ocean basin and the regions of internal runoff of all the continents decreased.

An exception was the European rivers of the Arctic Ocean basin for which the trend in the course of their total river runoff is not traced and the South American rivers of the Pacific Ocean basin, which during the considered period are characterized by a negative trend in the course of total river runoff.

Since the South American rivers of the Atlantic Ocean basin also have a tendency to a decrease in volume carried, during the considered period the total volumes carried by the rivers of the entire South American continent decreased. Although in individual regions of South America, especially on the Pacific coast, this can cause alarm, for the entire continent this reduction in volume is of no great importance due to the great total river runoff of this continent (see Table 2).

The situation is worse with European rivers, in the course of whose river runoff there is also a negative trend, and the volume of total river runoff is far less than for the rivers of the South American continent.

This decrease in water volume is particularly strongly observable in regions of internal runoff (Table 1), which usually have a far lesser total runoff than the outer regions of the continents.

During the considered period there is virtually no trend in the total runoff of African rivers, although, as indicated in Table 1, for individual regions in Africa there is a significant trend in the course of river runoff. This is attributable to the fact that the negative trend observed in the course of river runoff in one region is almost completely compensated by a positive trend observed in the course of river runoff in another region.

The example of Africa graphically shows that the general direction in the course of river runoff in any major region does not mean that in individual basins in the territory of this region there may not be a course of runoff with an opposite general direction of the trend. Such a situation is possible due to the specific conditions of relief and climate of any basin.

However, these computations of the trend in the course of river runoff show that extensive territories of the earth are characterized by a trend of the same sign. This must be remembered when evaluating the accuracy of the results since it indicates the nonrandomness of the collected data on the nature of the trends in the course of river runoff over the earth.

The correctness of the conclusions presented in Table 1 is also indicated by the circumstance that investigations made earlier on the basis of other data [2] for determining the change in water volume of rivers in the Caspian Sea basin indicated a result close to that which was obtained in Table 1 for the region of internal runoff in Europe.

However, it must be remembered that the determined trend values in the course of river runoff are averages for the considered period and that the possibility of a change in trend with time is not precluded.

BIBLIOGRAPHY

1. Denisov, P. P., "Method for Evaluating Trends in the Course of River Runoff," METEOROLOGIYA I GIDROLOGIYA (Meteorology and Hydrology), No 4, 1975.

2. Denisov, P. P., "Change in the Water Volume in Rivers," TRUDY IV VSESOYUZNOGO GIDROLOGICHESKOGO S"YEZDA (Transactions of the Fourth All-Union Hydrological Congress), Vol 2, Leningrad, Gidrometeoizdat, 1976.

3. MIROVOY VODNYY BALANS I VODNYYE RESURSY ZEMLI (World Water Balance and the Earth's Water Resources), Leningrad, Gidrometeoizdat, 1974.

APPROVED FOR RELEASE: 2007/02/08: CIA-RDP82-00850R000300030024-9

UDC 551.(952+510.4)

OZONOMETRIC APPARATUS FOR CREATING SAMPLE OZONE-AIR MIXTURES

Moscow METEOROLOGIYA I GIDROLOGIYA in Russian No 6, Jun 80 pp 108-111

[Article by V. A. Kononkov and Candidate of Physical and Mathematical Sciences S. P. Perov, Central Aerological Observatory, submitted for publication 26 November 1979]

[Text]

Abstract: The article describes a laboratory apparatus and method for preparing test ozone-air mixtures. The measurement of the concentration of ozone in test mixtures (at pressures 100-760 mm Hg) is accomplished using a special two-ray optical analyzer for ozone based on the absorption of UV radiation in the Hartley band at a wavelength 253.65 nm. The threshold response of the UV analyzer for optical density is $D_{thr} = 4 \cdot 10^{-4}$. The standard deviation in measurement of the ozone concentration in the range 0.5-300 ppm at atmospheric pressure does not exceed $\pm 5\%$.

One of the important components in the gas composition of the atmosphere is ozone. In the global system for observations of the state of the ozonosphere for the purpose of investigating its climatology and timely detection of possible anthropogenic influences a major role is played by satellite methods. However, this does not lessen the timeliness of innovation and development of contact methods for measuring ozone by means of meteorological rockets. These methods ensure good vertical resolution and a satisfactory absolute accuracy of the measured parameter. Moreover, rocket methods and instruments must be regarded as reference tools which can be used in developing methods for remote observations and in establishing a scale of the absolute concentrations.

At the Central Aerological Observatory specialists have developed a chemiluminescent method and applied it to work with the M-100B rocket. It ensures obtaining a continuous ozone profile with the descent of the nosecone with the analyzer by parachute from the peak of the trajectory (75 km) to the earth's surface [5]. The method has a whole series of advantages

-- high response and low inertia (high speed), a wide range of the measured concentrations and a high specific reaction to ozone in comparison with other gases. However, like most contact methods it is a relative instrument and requires the use of a sample means of calibration.

Until recently Soviet industry has not produced instruments for analyzing microconcentrations of ozone in the air or apparatus ensuring the preparation of test ozone-air mixtures. The electrochemical methods and instruments which have come into wide use in laboratory investigations [1] (such as the "Atmosfera-II") were ill-suited for solving the above-mentioned problem for a number of reasons: as a result of destruction of ozone during its measurement in a fluid cell, due to the influence of impurities in the stoichiometry of the reaction between ozone and a reagent (usually KI), due to limitations on the pressure of the investigated air.

The apparatus examined in this article was created for the purpose of developing and investigating the vertical distribution of the ozone concentration in the stratomesosphere by the chemiluminescent measurement method. The basis for its effect is the classical spectrophotometric method for measuring ozone. A merit of this method when it is used under the conditions of a special laboratory apparatus is a sufficiently high response (with measurement of ozone on the basis of its absorption of near-UV radiation in the Hartley band [4, 6]), selectivity to ozone, absence of an effect on the measured ozone-air mixture when using ordinary (usually low-power) UV radiation lamps.

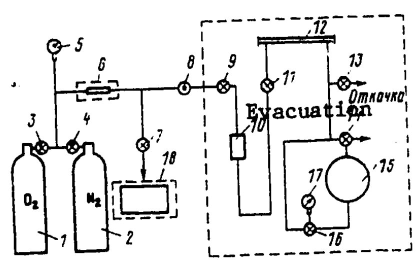

Fig. 1. Diagram of system for feeding and mixing of gases. 1, 2) cylinders with gas: 3, 4, 7, 9, 11, 13, 14, 16 -- valves; 5, 17 -- pressure gages; 6 -- gas-drying unit; 8 -- inflow; 10 -- ozonator; 12 -- optical cell; 13 -- receiving cylinder; 18 -- device for measuring moisture content of gases.

The initial variant of the laboratory ozonometric apparatus described below was described earlier in [3]. Here it should be noted that during recent years the idea of use of spectral-optical methods in the solution of a number of metrological problems in gas analysis measurements has been acquiring special timeliness and is gaining an increasing number of supporters [2].

The ozonometric apparatus proper consists of a system for the admission and mixing of gases and an ozone analyzer. The operation of the system for the admission and mixing of gases is based on the following principle.

The ozonometric apparatus proper consists of a system for the admission and mixing of gases and an ozone analyzer. The functioning of the system for the admission and mixing of gases is based on the following principle (Fig. 1): in a pre-evacuated (to a pressure of about 10^{-4} mm Hg) receiving tank 15 oxygen and nitrogen are admitted from the tanks 1, 2 through the valves 3, 4, 9, 11, the inflow element 8 and the optical vacuum cell 12. The ozonator 10 is switched on while the oxygen is being admitted; it operates on the known principle of a barrier discharge. By means of a change in the variable voltage fed to the electrodes of the discharge tube it is possible to vary the ozone concentration in the ozone-air mixture. The design of the discharge tube precludes the possibility of contact between oxygen and ozone and the metal. The admission of oxygen and nitrogen continues to such partial pressures that the composition of the mixture is similar to atmospheric air ($\approx 21\%$ O_2 and $\approx 79\%$ N_2). The pressure in the receiving tank is measured with a barometer of the VK-316 type. Oxygen of a high purity (TU 6-21-8-73) and nitrogen of an exceptional purity (GOST 9293-74). In order to check the water vapor content in the admitted gases provision is made for the possibility of connecting a coulometric device for measuring the moisture content of gases of the "Baykal-3" type (through the valve 7). The measurements indicated that the moisture content of the used gases of high purity is $1.0\text{-}1.5 \cdot 10^{-3}\%$ by volume, which approximately corresponds to the water vapor content in the stratosphere-mesosphere. In case of necessity the working gases can be additionally dried by means of passing them through a special dessicator 6 (in Fig. 1 surrounded with a dashed line).

The gases stored in the receiving tank are mixed by diffusion (mixing time about 20 minutes) and thus form an ozone-air mixture with some constant relative ozone concentration. The receiving tank consists of two interconnected spherical containers made of molybdenum glass and with a total volume of 25 liters. All other parts of the vacuum apparatus are also fabricated of molybdenum glass. Some quantity of prepared ozone-air mixture is then sampled from the receiving tank for measuring the ozone concentration by means of an optical analyzer.

Now we will examine the operating principle for the UV ozone analyzer (Fig. 2). A ray from the source 1, formed by the diaphragms 2, 4, falls on the ray separator 3; one part is reflected and is incident on the photodetector of the reference channel 11, whereas the other part passes through the vacuum optical cell 5, the monochromator 7, and is incident on the photodetector of the measurement channel 8.

The photodetector signals are then amplified by independent d-c amplifiers 9 and 12. The output voltages of the d-c amplifiers are subtracted at the input of the analog recorder 13, which thus registers the difference of the signals in the reference and measurement channels $\Delta I = I_0 - I$, where I_0 is the reference channel photodetector signal, I is the measurement channel photodetector signal. When there is no ozone in the cell (the cell is evacuated to a forevacuum) the difference in the signals is $\Delta I =$

0. Then the investigated ozone-air mixture is fed into the cell and the unbalance signal at the output of the recorder 13 is measured.

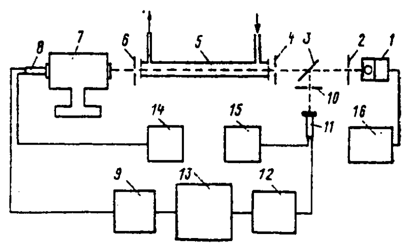

Fig. 2. Block diagram of UV spectrophotometer - ozone analyzer. 1) radiation source; 2, 4, 6 -- diaphragms (cannot be regulated); 3 -- ray divider; 5 -- optical vacuum cell; 7 -- monochromator; 8, 11 -- ray detectors of measurement and reference channels; 9, 12 -- d-c amplifiers; 10 -- diaphragm (can be regulated); 13 -- analog recorder; 14, 15, 16 -- power source units.

Computations of the ozone concentration are made on the basis of the Bouguer-Lambert-Behr law. The working formula has the form

$$\gamma = 2.08 \times 10^{3} \times \frac{T}{p} \times D, \qquad (1)$$

where γ is the relative ozone concentration (mixture ratio), ppm; T is the absolute temperature of the ozone-air mixture; p is the pressure of the ozone-air mixture in the optical cell, mm Hg; $D = \lg\ I_0/I_0 - \Delta I$.

The legitimacy of use of this formula applicable to this measurement scheme was demonstrated in a special experiment in which we employed a set of light filters with a known (for a wavelength of 253.65 nm) optical density. The light filters were alternately put in front of the input (and output) windows of the evacuated cell, after which in each case the measurement channel photodetector signal was measured.

As the radiation source 1 use is made of an instrument of the PPBL-3 type with a mercury spherical electrodeless VSB-2 lamp. The measurements then are made in the resonance line of mercury with $\lambda = 253.65$ nm, where the optical absorption coefficient of ozone attains a maximum value and is equal to 133.9 cm^{-1} [4]. The photodetectors 8, 11 are photomultipliers of the FEU-124 type, whose photocathodes have virtually no response to visible light. A special experiment indicated that with an appropriate choice of the regime of current supply to the lamp 98-99% of the total photomultiplier signal measuring the lamp radiation in the entire spectral region (approximately from 200 to 600 nm) is accounted for by emission in the mercury resonance line. This circumstance, in the solution of some problems, in principle makes it possible to simplify the analyzer circuit, eliminating the DMR-4 monochromator from it.

The d-c voltage for supplying current to the photomultipliers (about 700 V) is fed from one and the same high-voltage unit of the BNVZ-05 type (two identical blocks have been arbitrarily shown in Fig. 2), supplemented by a special parallel output device. This makes it possible to eliminate virtually completely the measurement errors caused by an instability of the output voltage of the high-voltage unit (instability of the output d-c voltage of the BNVZ-05 unit does not exceed ±0.3% of the established value).

The output currents of the photomultiplier are amplified and measured using IMT-0.5 instruments, whose main measurement error does not exceed ±1.5%. Analog registry is with a KSP-2-017 automatic potentiometer.

The stability of the signal I_0 of the reference channel is monitored using an Shch-1413 digital voltmeter.

The optical vacuum cell (5) is a tube of molybdenum glass with a length of 1 m and a diameter of 45 mm, supplied at the ends with quartz windows.

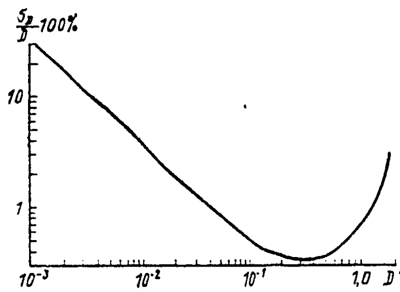

Fig. 3. Graph of the dependence of the standard relative measurement error $\sigma D/D$ as a function of D.

The following expressions are used in evaluating the maximum relative error in measuring the γ parameter:

$$\frac{\delta\gamma}{\gamma} = \sqrt{\left(\frac{\delta T}{T}\right)^2 + \left(\frac{\delta p}{p}\right)^2 + \left(\frac{\delta D}{D}\right)^2}. \quad (2)$$

$$\frac{\delta D}{D} = \frac{0,4343}{(I_0 - \Delta I)\ D} \times$$

$$\times \sqrt{\left[\frac{\Delta I}{I_0}\ \delta (I_0)\right]^2 + [\delta (\Delta I)]^2}. \quad (3)$$

Temperature is measured with a mercury thermometer with a graduation 0.2° C; the error in measuring pressure in the cell is ±1 mm Hg and therefore the contribution of these values to the total error (2) is small (not more than 0.15%).

The relative error in measuring optical density is computed using formula (3), in which we must substitute the values of the mean square errors in measuring the reference channel signal $\sigma(I_0)$ and the zero signal of the circuit $\sigma(\Delta I)$. Special measurements indicated that the values of these mean square errors are $\sigma(I_0) \approx \sigma(\Delta I) \approx 1.5 \times 10^{-13}$A. Assuming that these errors determine the threshold response of the analyzer, we obtain D_{thr} = 0.0004. Figure 3 gives the results of computations using formula (3) in the form of a curve of the relative measurement errors $\sigma D/D$ as a function of D.

It is easy to compute that with a pressure in the optical cell of 760 mm Hg and a temperature of +20°C the standard error in measuring the relative ozone concentration in the range 3-100 ppm does not exceed ±1%. We also note here that the normalized error in existing experimental models of electrochemical ozone analyzers of the "Atmosfera-II" type is ±20%.

When measuring high ozone concentrations (optical density $D > 1$) in order to decrease the error it is far more convenient to use a single-ray scheme for cutting-in the described analyzer; there is successive measurement with the photodetector 8 (Fig. 2) of the intensities of the two light fluxes I_0 and I corresponding to cases of an evacuated cell and a cell filled with an ozone-air mixture.

The time required for making measurements with this instrument does not exceed several seconds and is determined primarily by the inertia of the automatic recorder used.

Special experiments for evaluating the rate of ozone destruction indicated that in a cell at atmospheric pressure the rate of destruction does not exceed 1.5%/hour, and in the receiving tank -- 0.1%/hour. This difference is evidently attributable to the geometrical dimensions of these containers. Such a small rate of ozone destruction makes it possible to conclude that the principle of storage and brief retention of ozone-air mixtures in containers of a suitable inert material (glass, quartz, teflon, etc.) can be extremely productive in ozonometric work.

We note in conclusion that the ozonometric apparatus described in this article can be used in developing any contact methods for on-board measurements of the ozone content in the stratomesosphere and also for creating an optical thickness of ozone in the modeling of conditions for the absorption of solar radiation in the atmosphere and adjusting optical instruments for measuring ozone (surface and on-board spectrometers, filter instruments). It is characterized by simplicity of design and construction. It is assembled completely of Soviet-produced components with the use of standard, metrologically certified units and instruments.

In the opinion of the authors, the principle for constructing this apparatus is the best for creating a sample higher-accuracy ozonometric apparatus in which laboratory and on-board ozonometers must be checked and calibrated. The determination of the spectral ozone absorption constants must be done in a special investigation with the use of independent physical or physicochemical methods for the absolute measurement of the ozone concentration.

The authors consider it their pleasant duty to express appreciation to A. A. Krotov and A. I. Zolkin for direct participation in creation of the instrument and also D. M. Lisitsyn, a specialist at the Institute of Chemical Physics, for valuable practical advice and interest in this work.

BIBLIOGRAPHY

1. Al'perin, V. Z., Sayfi, R. N., "Electrochemical Gas Analyzers for Determining Toxic Substances in Air," ZHURNAL VSESOYUZNOGO KHIMICHESKOGO OBSHCHESTVA IM. D. I. MENDELEYEVA (Journal of the All-Union Chemical Society im. D. I. Mendeleyev), Vol XV, No 5, 1970.

2. Gorelik, D. O., Konopel'ko, L. A., Tenenbaum, B. G., "Principles for Constructing Sample and Initial Means for the Monitoring of Atmospheric Contamination," IZMERITEL'NAYA TEKHNIKA (Measurement Apparatus), No 12, 1977.

3. Kon'kov, V. I., Perov, S. P., Udonova, L. A., "Laboratory Apparatus and Method for Investigating Chemiluminescent Ozone Sensors at Low Pressures," TRUDY TsAO (Transactions of the Central Aerological Observatory), No 127, 1977.

4. Hearn, A. G., "The Absorption of Ozone in the Ultraviolet and Visible Regions of the Spectrum," PROC. PHYS. SOC., Vol 78, Pt 5(i), 1961.

5. Konkov, V. I., Perov, S. P., "Some Preliminary Results of Chemiluminescent Measurements of Atmospheric Ozone by Meteorological Rockets M-100B," PROC. JOINT SYMP. ATMOS. OZONE, Dresden, Vol 2, 1977.

6. Vigroux, E., "Coefficients d'absorption de l'ozone dans la bande de Hartley," SYMPOSIUM SUR L'OZONE ATMOSPHERIQUE, 1968, 2-7 Septembre, Monaco, CNRS, 1969.

UDC 551.508.822(091.2)(47+57)

FIFTIETH ANNIVERSARY OF RADIOSONDE OBSERVATIONS IN THE USSR

Moscow METEOROLOGIYA I GIDROLOGIYA in Russian No 6, Jun 80 pp 112-117

[Article by Candidate of Technical Sciences G. P. Trifonov, Central Aerological Observatory, submitted for publication 28 November 1979]

[Text]

Abstract: The article gives a brief history of atmospheric radiosonde observations in the USSR, the status and some prospects of such work.

The date 30 January 1980 marked the fiftieth anniversary of the launching of the world's first radiosonde at Pavlovsk by Professor P. A. Molchanov of the Pavlovsk Aerological Observatory.

The invention of the radiosonde, an instrument for measuring atmospheric parameters and their transmission by radio, opened a new stage in the development of investigations of the free atmosphere and made possible the creation of a world network for making radiosonde observations of the atmosphere and on the basis of its data the preparation of hydrodynamic weather forecasts. The day of the first launching of the radiosonde also marked the birth of a new field of technology -- radiotelemetry, whose brilliant achievements are widely used in modern life.

Instrumental observations of the state of the free atmosphere were initiated at the end of the last century. They were carried out using automatic instruments -- meteorographs carried aloft by kites, pilot balloons and balloons.

In the 1920's the pilot balloon method came into extensive use throughout the world for investigating the atmosphere. These carried a meteorograph aloft and became particularly popular after the introduction of the rubber envelope proposed by Assman to replace a fabric envelope. A shortcoming of this method was that after falling many meteorographs were not found, especially in inaccessible wooded and swar y terrain, and very poor results were obtained from the launchings.

In 1923 Professor P. A. Molchanov of the Pavlovsk Aerological Observatory near Leningrad proposed and began development of an instrument which was to be carried aloft by balloons and which transmitted measurement data by radio.

In 1927 the author presented a report at an international conference in Leipzig on the operating principles of such an instrument. This work was considerably advanced after 1929 when the government allocated funds for developing the design of instruments and the first radiosondes were developed under the direction of P. A. Molchanov in collaboration with the Nizhegorodskaya Radio Laboratory. P. A. Molchanov launched the world's first radiosonde at Pavlovsk on 30 January 1930. It reached an altitude of 9 km. Eleven successful launchings of radiosondes were made during 1930.

Work on creation of a radiosonde was also carried out in France and Germany. A French instrument, called the "barothermoradio," was launched on 8 May 1930 and reached an altitude of 14 km. On 15 May of that same year Duchert achieved the first launching of a radiosonde at Lindenberg. Beginning with that time the atmospheric radiosonde method came into wide use throughout the world, laying the beginning for systematic measurements of the parameters of the free atmosphere and thereby creating a basis for the development of hydrodynamic weather forecasting, supporting aviation flights and servicing of different branches of the national economy.

Invention of the radiosonde afforded new possibilities for studying the stratosphere. Its use for the first time made it possible to obtain information on the stratosphere in arctic and ocean areas. The development of aviation aroused considerable interest in investigations of the stratosphere in the 1930's. Stratospheric balloons and rockets began to be developed for flights into the stratosphere. Under the program for stratospheric investigations in the USSR, in which P. A. Molchanov was an active participant, flights of stratospheric balloons were made: the "SSSR-1" on 30 September 1933 and the "Osoaviakhim" on 30 January 1934, attaining altitudes of 19 and 22 km respectively.

An All-Union Conference on Study of the Stratosphere was held in Leningrad in 1934. It was under the chairmanship of S. I. Vavilov, President of the USSR Academy of Sciences, who played a major role in the further development of stratospheric research.

On the proposal of P. A. Molchanov automatic methods for making measurements in the stratosphere were used in automatic stratospheric balloons. The first automatic stratospheric balloon for investigating cosmic rays with an S. N. Vernov instrument was launched on 1 April 1935 at Pavlovsk; later the method of automatic stratospheric balloons came into wide use in investigations of the stratosphere.

The vigorous development of a network of stations for making atmospheric radiosonde observations throughout the world began in 1935. For example, in 1940 there were 40 stations in the USSR, in 1950 -- 106, in 1960 -- 157, and at the present time there are about 200.

During the 50 years of its development radiosonde observations of the atmosphere have undergone a series of qualitative stages which have been characterized by an increase in the altitude of sounding, an increase in measurement accuracy, an increase in the degree of automation of measurements and the processing of data. The improvement in equipment and methods for making radiosonde observations of the atmosphere was always closely associated with the development of radioelectronics and reflected advances in this field. The first experiments in the use of radar for the tracking of balloons with passive reflectors, carried out in the USSR in 1943 at the Central Aerological Observatory by G. I. Golyshev and V. V. Kostarev, afforded the possibility for determining wind velocity and direction to the maximum possible altitudes of balloon ascent and laid the basis for modern radiotheodolite and radar measurements of the wind (until then measurements of radiosonde coordinates were made using optical theodolites and were limited by the cloud cover altitude). This made it possible to combine measurement of meteorological elements and the wind in one radiotechnical system for sounding the atmosphere. The design of the Molchanov radiosonde, including its modified variant, the RZ-049, was used in the network for almost 30 years.

The "A-22-Malakhit" radiosonde system (1957) was the first system which combined measurements of temperature, pressure, humidity and wind and at the same time increased the accuracy of their measurement. The creation of the complex system for sounding of the atmosphere, the "RKZ-Meteor" (B. G. Rozhdestvenskiy, M. V. Krechmer, 1958), based on the principle of use of a response signal for measuring range, and in which for the first time there was automation of the process of measuring and registering the coordinates of the radiosonde and telemetric information, marked a qualitative jump in the increase in accuracy of measurements of wind velocity and direction and the use of an electric temperature sensor (thermoresistor) ensured an increase in the accuracy of temperature measurements at great altitudes.

Finally, the development of electronic computers made it possible to bring about a new qualitative stage in the development of sounding systems by means of automation of the tedious processing of data. The "Atmosfera" centralized field system for the processing of data received from the "A-22-Malakhit" sounding system [5, 29] made it possible to accumulate the first experience in this direction and the development of the "OKA-3" complex [33-36] for the centralized processing of data from the "RKZ-Meteorit" sounding system for the first time made it possible to introduce automatic processing into the routine practice of sounding at a whole series of aerological stations.

Since the 1950's the investigation of the atmosphere using radiosondes has begun to acquire a global character in connection with the organization of observations first in the Arctic and in Antarctica, and then over the world ocean. The first aerological observations on drifting ice were made in 1951 by P. F. Zaychikov and V. K. Babarykin. A major contribution to the organization of systematic aerological observations in the Arctic and in Antarctica was made by A. Ye. Shchekin, S. S. Gaygerov, V. I. Shlyakhov, G. A. Kokin, A. M. Borovikov and others.

The broadening of atmospheric sounding on scientific research ships during the last decade made it possible to carry out a whole series of international complex scientific experiments, such as GATE, "Monsoon," "Typhoon," IGE, which make possible a better understanding of the nature of large-scale processes in the tropical zone, to a considerable degree exerting an influence on global circulation of the atmosphere, and the mechanism of interaction between the atmosphere and ocean, which in the long run should serve the purposes of improving long-range weather forecasting.

The development of the network of aerological measurements would be impossible without scientific investigations in the field of the processes of measurement, processing and interaction between the sensors and the environment. Investigations of the influence of solar radiation on a temperature sensor (S. M. Shmeter, P. F. Zaychikov, V. D. Reshetov) made it possible to develop the theoretical principles of radiation corrections [9, 30, 31, 41], which for the first time began to be introduced into temperature readings after 1957, and investigations of an adsorption-deformation humidity sensor [31] made it possible to determine its errors and the limits of applicability.

The development of the scientific and methodological principles for measuring and processing of data in systems for sounding of the atmosphere (O. V. Marfenko, P. F. Zaychikov) ensured a unity of measurements and uniformity of data from the aerological network and investigations of the optimum density of distribution of aerological stations and the choice of sounding times on the basis of variability of atmospheric parameters (V. D. Reshetov) created [32] the organizational basis for activity of the network.

The last decade has been marked by a further improvement in the sounding system, with the result that the "RKZ-5-Meteorit-2" system was created and introduced at most of the stations in the aerological network (G. I. Golyshev, B. G. Rozhdestvenskiy, Ya. Kh. Chernobrod, V. I. Shlyakhov, G. P. Trifonov, A. F. Kuzenkov). This system is characterized by a great range of reliable reception of radiosonde signals, a high accuracy in measuring the wind both in the surface layer and at great altitudes [18, 39]. In this system wind sounding was ensured by means of an A-28 transmitter-responder and corner reflectors. An important achievement of this decade is the introduced automatic processing of radiosonde data at a whole series of stations in the aerological network by means of the "OKA-3" complex. This period was also marked by automation of the collection and accumulation of climatic data, the extensive introduction of atmospheric sounding on scientific research ships, the development of a small radiosonde with integrated microcircuits, new special radiosondes and sensors for measuring temperature and humidity.

The automation of processing of data from the "RKZ-5"-"Meteorit-2" sounding system was successfully developed on the basis of centralized processing, which ensures the best economic effectiveness both as a result of the rational use of computers at the center and at sounding points and as a result of the great flexibility of the system, determined by the flexibility and broad possibilities of universal computers at computation centers.

The "OKA-3" complex for the centralized automatic processing of data from the "RKZ-5"-"Meteorit-2" sounding system was developed on the basis of this principle in 1971 [33, 34, 36]. It consists of a device for the automatic registry of data from the "Meteorit" radar on teletype and "OKA-70" mathematical support, intended for use at territorial centers with "Minsk-22" and "Minsk-32" electronic computers.

In 1973 the "OKA-3" complex was for the first time introduced into routine operation at the aerological stations Minsk, Brest, Gomel' in Belorussia [35] and then began to be introduced in the entire aerological network, including on weather ships. The basis for constructing the system for the automatic processing of sounding data was work on mathematical formalization and algorithmization of the processing process [34].

The problems involved in ensuring the safety of aircraft flights and a further economy and reliability of the sounding system required the development of a small radiosonde. The development of integrated circuits created the basis for developing a massive, light and economical radiosonde. On the basis of development of a SHF semiconductor generator [2] and LF radiosonde units based on semiconductors [22] it was possible to create models of small radiosondes weighing up to 300 g and these were tested. In order to increase the reliability of the telemetric channel and channels for tracking the radiosonde coordinates work was developed on the use of frequency manipulation of the radiosonde superheterodyne generator [14, 15], which makes it possible to increase the mean power of the radiosonde transmitter with limitations on the supply voltages. An increase in the integration level and a simplification of the process of radiosonde calibration by the use of stable sensors with calibration characteristics which can be described by a functional family with several parameters will make it possible to create not only a small, but also an economical radiosonde.

The objectives of increasing the accuracy and economy imposed new requirements on the radiosonde sensors: an increase in stability of the characteristics, the possibility of their description by a functional family with a small number of parameters for lessening the cost of the calibration process, a decrease in the radiation correction for the temperature sensor and broadening of the range of operation of the humidity sensor into the region of negative temperatures.

The development of sensors for the radiosonde was impossible without corresponding chambers for reproducing the stipulated temperature, humidity, pressure, air flow velocity and solar radiation values which would make it possible to accomplish checking and purposeful improvement of sensor characteristics. For these purposes during recent years specialists have developed a thermopressure solar chamber [1] in which it is possible to create stipulated pressure, air flow velocity and solar radiation values and a universal humidity generator [38] in which the method of two temperatures and two pressures is embodied. In this method the forming of the stipulated humidity is accomplished by increasing the temperature or reducing the pressure of the saturated air. Theoretical computations and experimental investigations indicated that this chamber makes it possible to set relative humidity values from 1 to 95% with a simultaneous change in temperature from +30 to -50° and a pressure from 1100 to 10 mb with an error of 1% in the region of positive temperatures and 3% in the case of negative temperatures. Using this apparatus it was possible to investigate aluminum oxide humidity sensors [19] whose operating principle is based on the adsorption of water vapor by a porous layer of aluminum oxide and the accompanying change in the complex resistance of the sensor, and also the operation of a film sensor at negative temperatures.

A new thermistor was developed for measuring temperature. It has an increased stability of the characteristics, a possibility for their description by a functional family with three parameters and a radiation error reduced by half. As a result of investigations of different coverings in the production of standard-produced radiosondes there is now painting of thermistors which makes possible a 10-15% reduction in the radiation error when measuring temperature.

Scientific and methodological studies made during the last decade have made it possible to solve fundamental problems in the method for making measurements with the "RKZ-5"-"Meteorit-2" atmospheric sounding system; this involves the metrological support of operation of the system under land and shipboard conditions. It has been possible to find refraction corrections when computing altitude from radar data on the basis of a more rigorous allowance for the theory of refraction of radio waves in the atmosphere [4] and it has been possible to carry out an evaluation of the accuracy of data from radiosonde observations using extensive statistical data [21]. The necessary methodological aids for operation of the "RKZ-5"-"Meteorit-2" system have been written and are in practical use [26, 27]. A many-sided investigation of the variability of meteorological elements in the atmosphere was generalized in the monograph [32], published in 1973. The results of this investigation were also used extensively in the reference - norm-setting aid published by the Main Administration of the Hydrometeorological Service on the makeup, accuracy and spatial resolution of hydrometeorological information for the national economy and forecasts [28].

At the present time the aerological network of the USSR State Committee on Hydrometeorology is for the most part supplied with the "RKZ-Meteorit" system. The mean annual maximum altitude of ascent during the last two decades has increased by a factor of 2.5 and is 28 km. About 20 aerological stations routinely carry out automatic processing using the "OKA-3" complex, which considerably reduced the expenditures of work (the carrying out of sounding with automatic processing is accomplished at a number of stations by a staff of 12-14 persons instead of 18-20 required when manual processing is used), and has increased the quality and ease in obtaining aerological telegrams in 30-50 minutes.

During the last decade work has been done on the automation of collection and accumulation of climatic aerological data. A network of regional and territorial centers has been created for ensuring the collection and accumulation of climatic data. The automation of collection, conversion and transmission of aerological information created premises for transformation of the aerological network into a unified automated system of aerological stations and computation centers which perform the function of collection, processing, accumulation and dissemination of aerological data.

The radiosonde method has also been successfully developed for measuring a whole series of nonstandard atmospheric parameters -- long-wave radiation, ozone, fluxes of corpuscular radiation.

The ARZ-1 radiosonde was developed in 1961 (G. N. Kostyanoy, V. I. Shlyakhov) and a network for actinometric sounding consisting of 10 stations was organized. Actinometric sounding was also carried out in all international experiments on weather ships. Materials from the actinometric sounding network were used in computing different statistical characteristics of the field of long-wave radiation. A manual on the field of long-wave radiation in the free atmosphere was published [6]. A model of a standard actinometric atmosphere was proposed [3, 7]. On the basis of measurements of the profiles of fluxes of long-wave radiation it was possible to obtain the integral absorption and radiation coefficients, which are used for determining the rates of radiation cooling and heating at different altitudes in the atmosphere [12]. At the same time, work was done on development of a method and instruments for measuring long-wave radiation during the daytime.

Investigations of the distribution of radiation fluxes in the atmosphere are closely associated with investigations of the distribution of some components of the gas composition of the atmosphere which are insignificant in concentration but very important, such as ozone and carbon dioxide, exerting a considerable influence on the radiation regime of the atmosphere and in the last analysis -- on planetary climate. The timeliness of study of the distribution of the gas composition of the atmosphere is due to the influence exerted on it by the ever-accelerating process of development of industrial production and electric power and man's economic activity.

The problem of ozone monitoring of the atmosphere and the creation of a mass ozonosonde for these purposes has acquired special timeliness in connection with the development of stratospheric aviation and the effect of man's economic activity on the ozone layer of the atmosphere. The different directions in the development of such an ozonosonde has led to the designing of an ozonosonde of the electrochemical type whose operating principle is based on determination of the quantity of iodine released in the electrolyte solution (potassium iodide) under the influence of ozone. The originality of the design of the developed models of ozonosondes in comparison with foreign ozonosondes of the electrochemical type is that interaction between the electrolyte and air ozone occurs on the surface of a rotating drum submerged in the electrolyte and the volume of air whose ozone reacted with the electrolyte is determined by the area of the electrolyte and the rate of probe ascent. On the basis of the change in the electric current flowing through the electrolyte it is possible to compute the quantity of reacting ozone.

The need for investigations of solar-terrestrial relationships and background corpuscular streams in the atmosphere made it necessary to develop a radiosonde for corpuscular radiation. The radiosonde contains a telescopic system of self-quenched radiation counters [17] and measures the integral flux of charged particles and also their angular distribution. Measurements of corpuscular streams with these instruments were organized in the Arctic, and also on one of the ships in the POLEX experiment. An important result of experimental observations was the establishing of a close relationship between air density in the stratosphere and the corpuscular stream gradient.

The prospects for further development of the method for making radiosonde observations in the atmosphere are related to an increase in the economy, reliability and accuracy of sounding systems. The development of integrated circuitry is the basis for creating a massive, inexpensive radiosonde intended for measuring standard and special atmospheric parameters. The improvement of hydrogen extraction is of definite importance for increasing the economy of the sounding system and developing high-speed and high-altitude envelopes not requiring preparation before launching. The process of integration of sounding into a unified automated system for the collection, transmission, processing and accumulation of aerological information noted in the past decade requires a systemic approach to the planning of this system for the purpose of its optimization. The prospects for constructing an optimum system are dependent to a considerable degree on the development of means for the transmission of data, including with the possible use of satellite systems for the transmission of data and the extensive use of micro- and miniprocessors for processing.

The broadening of shipboard sounding for the solution of problems in creating a model of general circulation of the atmosphere and long-range weather forecasting involves the construction of a compact, reliable and easy to use shipboard sounding system which does not require stabilized platforms for its extensive use on ships of different classes. Possible ways for constructing such a system can provide for the use of both navigational and radar methods with electronic stabilization of the antenna.

The results of development of radiosonde observations of the atmosphere over a 50-year period and the modern forecasting service based on it, the contribution of recent years of radiosonde observations to the international program for the investigation of global atmospheric processes, in which the USSR plays as active part, makes it possible to hope that the radiosonde method can make an important contribution in solving the problems of general circulation of the atmosphere and long-range weather forecasting, climatic monitoring and preservation of the environment.

*****

BIBLIOGRAPHY

1. Afanas'yeva, N. S., Zaychikov, B. P., Fridzon, M. B., "Simulation of Solar Radiation Using a DKSSh-1000 Lamp," TRUDY TsAO (Transactions of the Central Aerological Observatory), No 111, 1972.

2. Gaynanov, Kh. N., Ivanov, V. E., Kazantsev, Yu. F., Pomytkin, V. P., Kharitonov, F. V., Plotnikov, Ye. M., "Hybrid-Film SHF Autooscillator With an 'Uncased' Transistor," TRUDY VUZOV ROSSIYSKOY FEDERATSII (Transactions of Colleges of the Russian Federation), Sverdlovsk, Ural'skiy Politekhnicheskiy Institut, 1976.

3. Ginzburg, A. S., Kostyanoy, G. N., Mullamaa, Yu. A., PREDVARITEL'-NAYA RADIATSIONNAYA MODEL' OBLACHNOY ATMOSFERY (TEPLOVOYE IZLUCH-ENIYE I KUCHEVYYE OBLAKA) (Preliminary Radiation Model of a Cloudy Atmosphere (Thermal Radiation and Cumulus Clouds)), Preprint, IFA AN SSSR, 1977.

4. Golubev, A. N., Marfenko, O. V., Prilepin, M. T., "Corrections for the Refraction of Radio Waves in Radar Aerological Observations," TRUDY TsAO (Transactions of the Central Aerological Observatory), No 118, 1976.

5. Yefimov, P. L., "Centralized Field Computation-Telemetric System 'At-mosfera' for Processing Sounding Results," METEOROLOGIYA I GIDROLOG-IYA (Meteorology and Hydrology), No 4, 1965.

6. Zaytseva, N. A., Kostyanoy, G. N., POLE DLINNOVOLNOVOY RADIATSII V SVOBODNOY ATMOSFERE (SPRAVOCHNYYE DANNYYE) (Field of Long-Wave Radiation in the Free Atmosphere (Reference Data)), Moscow, Gidrometeo-izdat, 1974.

7. Zaytseva, N. A., Kostyanoy, G. N., Shlyakhov, V. I., "Model of a Standard Radiation Atmosphere (Long-Wave Radiation)), METEOROLOGIYA I GIDROLOGIYA, No 12, 1973.

8. Zaytseva, N. A., Krasnova, T. M., "Variability of the Fields of Long-Wave Radiation in GATE Polygons," TRUDY MEZHVEDOMSTVENNOY EKSPEDITSII "TROPEKS-74" (Transactions of the Interdepartmental Expedition "TROPEX-74"), Leningrad, Vol I, 1976.

9. Zaychikov, P. F., "Method for Determining Radiation Corrections to Temperature Readings With A-22-III, RKZ-1 and RZ-049 Radiosondes Us-ing Data on the Temperature Differences 'Day Minus Night'," TRUDY TsAO, No 43, 1962.

10. Zaychikov, P. F., "Method of Triple Checking and its Use for Invest-igating the Accuracy of Radiosondes," TRUDY TsAO, No 16, 1956.

11. Kostarev, V. V., Golyshev, G. I., IZMERENIYE VETRA NAD OBLAKAMI METODOM ODNOPUNKTNOY PELENGATSII: INFORMATSIONNYY SBORNIK GUGMS (Wind Measurement Over Clouds by the Single-Station Direction-Finding Method: Collection of Informative Articles Main Administration of the Hydrometeorological Service), 1945.

12. Kravchenko, I. M., Shlyakhov, V. I., "Parameters Determining the Vertical Structure of the Field of Long-Wave Radiation in the Atmosphere," METEOROLOGIYA I GIDROLOGIYA, No 12, 1975.

13. Krechmer, M. V., "Errors in Determining Wind Direction and Velocity Due to Inaccurate Measurement of Coordinates," TRUDY TsAO, No 74, 1966.

14. Kuzenkov, A. F., Yegorov, A. N., Vakhtomov, Kh. N., "Frequency Radiosonde for the 'Meteorit-2' Radar," TRUDY TsAO, No 117, 1976.

15. Kuzenkov, A. F., Yermakov, V. I., "Aerological Radiosonde," AUTHOR'S CERTIFICATE USSR No 319913, 1971.

16. Kuzenkov, A. F., Lozinskiy, A. M., Orayevskaya, S. P., "Instructional Experiment in the Field of Balloon Geodesy," NAUCHNYYE INFORMATSII ASTROSOVETA AN SSSR (Scientific Information of the USSR Astronomical Council), No 35, 1977.

17. Kuzenkov, A. F., Ryzhikova, T. T., "Device for Measuring and Registering Radioactive Radiation in the Atmosphere," USSR AUTHOR'S CERIFICATE, No 158119, 1965.

18. Kuzenkov, A. F., Trifonov, G. P., "Instrument Complex for Radiosonde Measurements in the Atmosphere," TRUDY TsAO. AEROLOGIYA-1970 (Transactions of the Central Aerological Observatory. Aerology-1970), No 100, 1971.

19. Malikov, B. A., Sholokhova, N. L., Prokorov, P. S., Fridzon, M. B., "Humidity Sensor Based on an Aluminum Oxide Film," MATERIALY 2-y VSESOYUZNOY KONFERENTSII PO PRIMENENIYU AEROZOLEY V NARODNOM KHOZYAYSTVE (Materials of the Second All-Union Conference on the Use of Aerosols in the National Economy), Odessa, 1972.

20. Marfenko, O. V., "Random Errors in Measuring Meteorological Elements in the Free Atmosphere With A-22-III and RKZ-1A Radiosondes," TRUDY TsAO, No 43, 1962.

21. Marfenko, O. V., "Evaluation of the Accuracy of Results of Radiosonde Measurements in the Aerological Network of the Soviet Union," METEOROLOGIYA I GIDROLOGIYA, No 3, 1969.

22. Matviyenko, V. A., Gaynanov, Kh. N., "Generator," USSR AUTHOR'S CERTIFICATE No 471658, 1975.

23. Molchanov, P. A., "Radiosonde With Transmission of Humidity Signals," VESTNIK YeGMS (Herald of the United Hydrometeorological Service), No 3, 1935.

24. Molchanov, P. A., AEROLOGIYA (Aerology), Leningrad, Gidrometeoizdat, 1939.

25. NASTAVLENIYE GIDROMETEOROLOGICHESKIM STANTSIYAM I POSTAM (Instructions for Hydrometeorological Stations and Posts), Leningrad, Gidrometeoizdat, No 4, Part III, 1954.

26. NASTAVLENIYE GIDROMETEOROLOGICHESKIM STANTSIYAM I POSTAM, VYP. 4, CH. IIIa: TEMPERATURNO-VETROVOYE ZONDIROVANIYE ATMOSFERY SISTEMOY (Instructions for Hydrometeorological Stations and Posts, No 4, Part IIIa: Temperature-Wind Sounding of the Atmosphere by the 'Meteorit-RKZ' System), 1973.

27. NASTAVLENIYE GIDROMETEOROLOGICHESKIM STANTSIYAM I POSTAM, VYP. 4, CH. IIIb: TEMPERATURNO-VETROVOYE ZONDIROVANIYE ATMOSFERY SISTEMOY "METEORIT-RKZ" NA SUDOVYKH STANTSIYAKH (Instructions for Hydrometeorological Stations and Posts, No 4, Part IIIb: Temperature-Wind Sounding of the Atmosphere by the "Meteorit-RKZ" System on Shipboard Stations), 1974.

28. O SOSTAVE, TOCHNOSTI I PROSTRANSTVENNO-VREMENNOM RASRESHENII INFORMATSII, NEOBKHODIMOY DLYA GIDROMETEOROLOGICHESKOGO OBESPECHENIYA NARODNOGO KHOZYAYSTVA I SLUZHBY GIDROMETEOROLOGICHESKIKH PROGNOZOV (Makeup, Accuracy and Spatial Resolution of the Information Necessary for Hydrometeorological Support of the National Economy and the Hydrometeorological Forecasting Service), edited by M. A. Petrosyants, Leningrad, Gidrometeoizdat, 1975.

29. Prashko, D. V., Trifonov, G. P., "Experience in Preparing a Program for Processing the Results of Temperature-Wind Sounding on a Digital Computer," TRUDY TsAO, No 74, 1966.

30. Reshetov, V. D., "On the Radiation Heating of a Comb Radiosonde and its Influence on Atmospheric Sounding," TRUDY TsAO, No 24, 1958.

31. Reshetov, V. D., "Development of Methods and Instruments for Aerological Observations at the Central Aerological Observatory," TRUDY TsAO, No 26, 1959.

32. Reshetov, V. L., IZMENCHIVOST' METEOROLOGICHESKIKH ELEMENTOV V ATMOSFERE (Variability of Meteorological Elements in the Atmosphere), Leningrad, Gidrometeoizdat, 1973.

33. Trifonov, G. P., "Device for the Readout of Data from the 'Meteor' Meteorological Radar Onto a Teletype," TRUDY TsAO, No 115, 1972.

34. Trifonov, G. P., ALGORITM I PROGRAMMA DLYA TSENTRALIZOVANNOY AVTOMATICHESKOY OBRABOTKI DANNYKH RADIOZONDIROVANIYA ATMOSFERY (Algorithm and Program for Centralized Automatic Processing of Data from Atmospheric Radiosonde Observations), Moscow, Gidrometeoizdat, 1973.

35. Trifonov, G. P., Plotnikov, G. A., Gol'tsova, K. I., "Belorussian Experiment for the Centralized Automatic Processing of Atmospheric Sounding Data," METEOROLOGIYA I GIDROLOGIYA, No 10, 1974.

36. Trifonov, G. P., Pshonkin, Ye. S., Plotnikov, G. A., "Complex for the Automatic Processing of Data from Radiosonde Observations of the Atmosphere," METEOROLOGIYA I GIDROLOGIYA, No 1, 1972.

37. Fridzon, M. B., Il'yasov, S. G., Krasnikov, V. V., Shlyakhov, V. I., "Methods for Measuring the Spectral Thermoradiation Characteristics of Light-Scattering Materials," TRUDY TsAO, No 114, 1973.

38. Fridzon, M. B., Sholokhova, N. L., Malikov, B. A., Koptelov, Yu. K., Talanov, V. D., Prokhorov, A. S., "Humidity Generator Employing the Two Temperatures Method," TRUDY TsAO, No 111, 1972.

39. Shlyakhov, V. I., "Status and Prospects of Development of Temperature-Wind and Special Sounding," TRUDY TsAO, No 90, 1969.

40. Shlyakhov, V. I., Kurakin, V. I., Fridzon, M. B., "New Instruments for Measuring Radiation Fluxes in the Atmosphere," METEOROLOGIYA I GIDROLOGIYA, No 8, 1970.

41. Shmeter, S. M., "Random Errors in Measuring Air Temperature and Pressure in the Free Atmosphere Using Comb Radiosondes," TRUDY TsAO, No 13, 1954.

REVIEW OF MONOGRAPH "ODNORODNOST' METEOROLOGICHESKIKH RYADOV VO VREMENI I V PROSTRANSTVE V SVYAZI S IZMENENIYEM KLIMATA" (HOMOGENEITY OF METEOROLOGICAL SERIES IN TIME AND SPACE IN RELATION TO CLIMATIC CHANGE), BY YE. S. RUBINSHTEYN, LENINGRAD, GIDROMETEOIZDAT, 1979, 80 PAGES

Moscow METEOROLOGIYA I GIDROLOGIYA in Russian No 6, Jun 80 p 118

[Review by Professor A. Kh. Khrgian]

[Text] The problems of climatology differ from some other problems in the modern science of the atmosphere in that work on their solution essentially rests on observational data and investigations made decades and even centuries ago. Numerous new investigations are making a major contribution to the interpretation of climatological material, to the modeling of climate and to an understanding of some of its regularities, but add but little to the fundamental material of long-term observations. However, both the phenomenological and highly improved statistical investigations now available rest on long series of observations, collected over a long period of years, whose degree of homogeneity and comparability we must be able to evaluate.

The book of Ye. S. Rubinshteyn, a veteran of Soviet climatology, who has given more than 60 years of his work to this science, is devoted precisely to this relationship between past and present-day climatology.

In adhering to recent tradition, the author in this book first of all defines some physical model validating the spatial relationship of climatological data. Maps of isocorrelates, such as in Figures 3 and 6, describe the structure of long waves in the atmosphere of the temperate and subpolar zones of the northern hemisphere. These maps characterize, in particular, the intensification of meridional atmospheric processes in summer in comparison with winter. Then Tables 2-3 in the book characterize the general warming of climate (primarily in the high latitudes) occurring in the 18th-20th centuries, a physical phenomenon determining a number of statistical properties of climatological series of observations.

These and many other ideas in physical climatology enable the author to develop clearly statistical methods for the combining of "fragmented" series, reduction to long-term periods and search for correlations, cycles and secular trends. The author devotes particular attention to the acute practical problem, even having international significance, of a rational choice of the principal climatological period. On pages 70-71 in the book we find an important conclusion -- that the requirement of unity of the main observation period (for example, the proposal that 1931-1960 be selected as such) for large territories is unrealistic and is not scientifically sound, since within such large regions the spatial and temporal correlations are weak.

The book contains a section on climatological mapping, in particular, on the interpolation of data at the points of intersection of a cartographic grid (p 79) -- a procedure used widely in climatological and other models. Without entering into polemics concerning the methods for such interpolation, the author tells in detail about the many local factors (in particular, concerning relief) impairing the linearity of the distribution (in particular, such elements as precipitation) and requiring a more detailed approach to the interpolation method. These comments are especially important because in modern models of circulation of the atmosphere (such as in the Kasahara-Washington model) serious experiments are already being made to take into account the earth's relief. The conclusion sometimes drawn in this case (for example, in the studies of the mentioned authors) concerning a small influence of relief is possibly associated with the smoothing of relief in such a linear interpolation.

Young climatologists and a wide range of scientific workers involved in what are now extremely timely climatological investigations will undoubtedly appreciate the book of Ye. S. Rubinshteyn, clearly defining a number of important concepts in climatological practice and theory.

BOOK REVIEW: "GIDROMETEOROLOGICHESKIY REZHIM OZER I VODOKHRANILISHCH. BRATSKOYE VODOKHRANILISHCHE" (HYDROMETEOROLOGICAL REGIME OF LAKES AND RESERVOIRS. BRATSK RESERVOIR), LENINGRAD, GIDROMETEOIZDAT, 1978, 165 PAGES

Moscow METEOROLOGIYA I GIDROLOGIYA in Russian No 6, Jun 80 pp 118-119

[Review by Candidate of Geographical Sciences M. Sh. Furman]

[Text] The Irkutskoye, Bratskoye and Ust'-Ilimskoye Reservoirs were formed as a result of hydroengineering construction on the Angara River. The hydrological regime of the Angara experienced appreciable changes under the influence of the cascade of reservoirs.

All these changes in the regime of the Angara during the period of formation and stabilization of the largest, the Bratskoye Reservoir, were investigated by subdivisions of the Irkutsk Administration of the Hydrometeorological Service.

The Bratskoye Reservoir is an artificial water body which in its area (5,470 km^2) is second only to the Kubyshevskoye Reservoir, but in volume is three times greater (170 km^3) and has no equal in the Soviet Union. The reservoir shoreline is 6,000 km.

Since the time of its formation (1961) there has been a many-sided study of the hydrometeorological regime of the water body. This investigation has been made by the Bratsk Zonal Hydrometeorological Observatory, by a network of lake and meteorological stations and posts situated in the zone of the reservoir water area.

This monograph summarizes observations of the hydrometeorological regime of the reservoir during the period of filling (1961-1967) and normal operation through 1975. The generalization of data and the preparation of the scientific-practical manual were accomplished by the personnel of the Bratsk Zonal Hydrometeorological Observatory under the direction of the State Hydrological Institute.

The basis for the computation schemes and formulations presented in the monograph is the observational data collected by the network of stations and posts of the Irkutsk Administration of the Hydrometeorological Service, including data from unique observations on a floating meteorological station.

In addition, use was made of materials from special expeditionary investigations carried out on the reservoir by the Bratskaya Zonal Hydrometeorological Observatory, Institute of the Earth's Crust Siberian Department USSR Academy of Sciences, planning institutes and a number of other organizations.

The reference consists of 10 chapters. It gives a brief description of physiographic conditions and the meteorological regime in the zone of the Bratskoye Reservoir. The chapter entitled "Levels Regime" examines the annual variation of level and its relative and short-period variations. The thermal regime is examined in relation to temperature of the water surface layer and the water mass, heat reserves and heat balance of the reservoir. It describes the ice regime during the period of freezing and opening-up of the water body, ice cover and ice conditions in the lower pool of the Bratskaya Hydroelectric Power Station. The water balance of the reservoir and its principal components are considered. Data are given on wind waves and currents in different parts of the water body.

Much attention is devoted to the formation of banks and its prediction. An interrelationship is shown between the dynamics of banks and the principal factors exerting any influence on their development. Scientists at the Institute of the Earth's Crust Siberian Department USSR Academy of Sciences participated in preparing the section "Reservoir Shores."

The last chapter gives the hydrochemical characteristics of Bratskoye Reservoir. It discusses the factors determining the composition of the water and regime, mineralization and composition of the main ions, inflow and runoff of dissolved substances, etc.

The tables, graphs, diagrams and appendices included in the handbook reveal the characteristics of the hydrometeorological regime of the abyssal water body under the conditions prevailing in eastern Siberia.

The work done and the results obtained were the basis for studying the hydrometeorological regime of the Ust'-Ilimskoye Reservoir.

Due to the short series of observations and the inadequate investigations the individual regime elements (currents, wind waves) have not yet been adequately investigated. A shortcoming of the handbook is the lack of a section on "Water Use," in which it would be possible to obtain an idea concerning the influence exerted on the water resources of a reservoir by economic activity.

This is the first handbook on reservoirs in the eastern part of our country. The handbook is a useful scientific investigation which is of practical interest for all who are concerned with the many-sided rational use and conservation of the water, biological and recreational resources of Bratskoye Reservoir, and also for prediction and ecological-economic evaluation of the interaction between a water body and the environment in Siberia.

SIXTIETH BIRTHDAY OF KIRILL YAKOVLEVICH KONDRAT'YEV

Moscow METEOROLOGIYA I GIDROLOGIYA in Russian No 6, Jun 80 pp 120-121

[Article by a group of comrades]

[Text] Professor Kirill Yakovlevich Kondrat'yev marked his 60th birthday on 14 June 1980. He is a leading Soviet scientist, a Corresponding Member USSR Academy of Sciences, a member of the CPSU since 1943, a veteran of the Great Fatherland War, a recipient of the WMO Prize and the author of the second memorial monograph of the WMO (RADIATSIONNYYE PROTSESSY V ATMOSFERE (Radiation Processes in the Atmosphere), Geneva, 1972).

After graduating from Leningrad University in 1946, K. Ya. Kondrat'yev progressed from assistant to rector of the university. Heading the Department of Atmospheric Physics for 20 years at Leningrad State University, Kirill Yakovlevich created a major team which for the first time carried out important investigations of the earth from space and also a series of studies on problems in atmospheric physics.

Over the course of many years K. Ya. Kondrat'yev headed the Radiation Research Section at the Main Geophysical Observatory where during the last 15 years he has carried out work on the radiation energetics of the atmosphere and remote methods for sensing environmental parameters, widely known in our country and abroad, and also on problems related to the development of the physical principles of climate. One of the important international stages in these studies was the Soviet-American expedition "Bering" (1973). The monograph by K. Ya. Kondrat'yev entitled METEOROLOGICHESKIYE SPUTNIKI (Meteorological Satellites) (1963), as well as monographs written in collaboration with other specialists PRAKTICHESKOYE ISPOL'ZOVANIYE DANNYKH METEOROLOGICHESKIKH SPUTNIKOV (Practical Use of Meteorological Satellite Data), 1966, and POLE IZLUCHENIYA ZEMLI KAK PLANETY (Radiation Field of the Earth as a Planet), 1967), established the priority of our country in the development of many important directions in space research and generalization of the results.

In monographs which were published in the years which followed (TERMICHESKOYE ZONDIROVANIYE ATMOSFERY SO SPUTNIKOV (Thermal Sounding of the Atmosphere from Satellites), 1970; METEOROLOGICHESKOYE ZONDIROVANIYE ATMOSFERY IZ KOSMOSA (Meteorological Sounding of the Atmosphere from Space), 1978), which he wrote in collaboration with Yu. M. Timofeyev, there was description of a new stage in the development of satellite meteorology, associated with solution of inverse problems with numerical modeling of the absorption of IR radiation in the atmosphere, the interpretation of measurement data obtained using satellites.

The monograph METEOROLOGICHESKOYE ZONDIROVANIYE PODSTILAYUSHCHEY POVERKHNOSTI IZ KOSMOSA (Meteorological Sounding of the Underlying Surface) (1979), of which K. Ya. Kondrat'yev was a co-author, summarized investigations associated with the development of remote methods for determining the parameters of the underlying surface and ascertaining temperature and moisture content of the ground at different depths.

Many of the writings of K. Ya. Kondrat'yev have been translated into foreign languages and are widely known abroad. His book ATMOSPHERIC RADIATION, published by the Academic Press in the United States in 1969, is of great importance; it gives an extensive treatment of the problems of actinometry and atmospheric optics.

In Great Britain the Pergamon Press is preparing to publish an enlarged and supplemented edition of the monograph PLANETARY METEOROLOGY by K. Ya. Kondrat'yev (1977).

The results of the many years of investigations by K. Ya. Kondrat'yev have been published in 36 monographs and in more than 500 articles.

Kirill Yakovlevich is the initiator and organizer of much work in implementing the Complex Energy Experiment (CENEX), which was part of the GARP program.

The succesful implementation of the CENEX program, completed by participation in the GATE radiation subprogram and in Soviet-American cooperation on environmental problems, made it possible to begin work under the program of the Global Aerosol-Radiation Experiment (GAREX). These studies became part of the national program of GARP (1978-1979) and constitute the basis for Soviet-American cooperation on the problem "Aerosol and Climate" in the coming five-year period.

During the course of the last two decades K. Ya. Kondrat'yev has done much work in the WMO. He was a member of the WMO Consultative Committee and is presently a co-reporter on radiation in the Commission on Atmospheric Sciences.

Kirill Yakovlevich has done active work in the International Astronautics Federation on strengthening the priority of the USSR in such important fields as the use of manned spaceships for scientific research, etc.

In 1969 he was elected an active member of the International Astronautics Academy and was designated co-chairman of the International Committee on Applied Satellites, which was created on his initiative.

For twenty-five years Kirill Yakovlevich has been chairman of the Soviet Commission on Radiation of the International Geophysical Committee. He is a member of Working Group II (now transformed into Commission A) of COSPAR.

K. Ya. Kondrat'yev is doing much work as a member of the editorial board of many Soviet and international journals.

Kirill Yakovlevich has many students and he has established an entire scientific school of specialists in the field of investigation of radiation processes and satellite actinometry.

A leading public figure, K. Ya. Kondrat'yev was elected a delegate to the 23d Congress CPSU, a member of the Leningrad City and Vasileostrovskiy Rayon Soviet of People's Deputies. Over the course of 20 years Kirill Yakovlevich has been carrying out much work as Deputy Chairman and Chairman of the Leningrad Division of the society "USSR-Great Britain."

The Soviet government has expressed high appreciation for the scientific and public services of K. Ya. Kondrat'yev, awarding him the Order of Lenin and two orders of the Red Banner of Labor.

The scientific activity of Kirill Yakovlevich has received wide international recognition: he was elected an Honorary Member of the British Royal Meteorological Society, an Honorary Member of the United States Academy of Arts and Sciences, a member of the "Leopoldina" Academy of Natural Sciences, an Honorary Doctor of Budapest and Lille Universities. He was awarded the Simons Medal of the British Royal Meteorological Society.

In congratulating Kirill Yakovlevich on his 60th birthday, which he meets at the height of his creative powers, we would like to wish him good health and successes and the same productive activity as before for the well-being of our Soviet science.

SIXTIETH BIRTHDAY OF NIKOLAY IL'ICH ZVEREV

Moscow METEOROLOGIYA I GIDROLOGIYA in Russian No 6, Jun 80 pp 121-122

[Article by a group of comrades]

[Text] The professional meteorologist Nikolay Il'ich Zverev, Doctor of Physical and Mathematical Sciences, on 8 April marked his 60th birthday and more than 37 years of scientific research activity.

Nikolay Il'ich graduated in 1941 from the Physics-Mathematics Faculty of the Pedagogic Institute and in 1943 from the Higher Military Hydrometeorological Institute in the "meteorology" field of specialization.

Nikolay Il'ich successfully defended his Candidate's dissertation in 1953. He selected one of the most difficult scientific problems -- the problem of long-range weather forecasting, to which he remained true in his subsequent research work.

Nikolay Il'ich Zverev is the author of a number of synoptic-statistical and physical-statistical models for the forecasting of anomalies of monthly temperature, the index of zonal circulation of the atmosphere and the monthly quantity of precipitation. After defending his dissertation "Use of Statistics in Weather Forecasting" in 1969 he was awarded the academic degree of Doctor of Physical and Mathematical Sciences.

N. I. Zverev is known as the author of a number of studies devoted to an analysis of regional meteorological conditions and the problems involved in interaction between the atmosphere and troposphere, the influence of the temperature field of the continent and ocean on atmospheric circulation of the Far East.

Another cycle of studies of Nikolay Il'ich Zverev is related to use of the analogue principle in long-range forecasts, objectivization and development of the parameters of similarity of meteorological fields. The parameters which he developed are used extensively in scientific research and operational work. Their use made it possible to automate a series of operations in the work of forecasters. He has published a total of more than 55 scientific studies.

Since 1966 Nikolay Il'ich has headed first the laboratory and then the division of monthly weather forecasts -- one of the responsible and tireless work areas of the USSR Hydrometeorological Center.

The RUKOVODSTVO PO MESYACHNYM PROGNOZAM POGODY (Manual on Monthly Weather Forecasts) was published in 1972 on the initiative of N. I. Zverev and with his most active participation. During recent years under his direction specialists have developed a new synoptic-statistical method for predicting weather for a month in advance and a number of important results have been obtained.

It is impossible to overlook the great organizational and methodological activity of Nikolay Il'ich on directing the specialized and routine work of long-range forecasters at our peripheral institutes and enterprises.

N. I. Zverev devotes much attention to the problems related to the training and enhancing the skills of young specialists in the division and the problems involved in the training of scientific personnel through the graduate student level. Nikolay Il'ich always has advice and he can always be consulted on matters relating to science and operational work.

His name has been entered in the Book of Honor at the USSR Hydrometeorological Center.

We wish Nikolay Il'ich good health, long years and successes in his work research on the problem of long-range weather forecasting.

SIXTIETH BIRTHDAY OF IL'YA ZAYNULOVICH LUTFULIN

Moscow METEOROLOGIYA I GIDROLOGIYA in Russian No 6, Jun 80 p 122

[Article by colleagues and friends]

[Text] The professional meteorologist Il'ya Zaynulovich Lutflin, Doctor of Technical Sciences, Director of the Kazakh Scientific Research Hydrometeorological Institute, marked his 60th birthday on 10 February.

After graduation from the Higher Military Hydrometeorological Institute in May 1944 he was sent to the active army in the post of chief of a meteorological station of an aviation regiment.

The scientific activity of Il'ya Zaynulovich began in 1950 and his civilian service began in 1967. During the period of army service he developed a number of new methods for predicting weather phenomena dangerous for aviation and methods for predicting the altitude of the tropopause and predicting air temperature on tropospheric and stratospheric aviation routes.

In 1951 the Scientific Council of the Central Institute of Forecasts awarded him the academic degree of Candidate of Physical and Mathematical Sciences for his scientific study "Investigation of the Tropospheric Air Flow."

A result of many years of research by Il'ya Zaynulovich was the monograph NOVYYE METODY PREDVYCHISLENIYA METEOROLOGICHESKIKH POLEY (New Methods in Precomputing Meteorological Fields), published in 1966, for which he was awarded the Doctor's degree in 1967.

In 1970 Il'ya Zaynulovich moved to Alma-Ata. At the Kazakh Scientific Research Hydrometeorological Institute he organized investigations on improvement of models for numerical prediction of meteorological fields by taking into account additional physical factors.

Since 1971 he has been engaged in scientific-pedagogic activity in training meteorological engineers at Kazakh State University.

As he reached his 60th birthday he completed investigations for creating a new model for the forecasting of meteorological fields for a time up to five days.

APPROVED FOR RELEASE: 2007/02/08: CIA-RDP82-00850R000300030024-9

In 1976 I. Z. Lutfullin became the director of the Kazakh Scientific Research Hydrometeorological Institute and from that time has combined the work of a scientist with the tasks of director. The Communist I. Z. Lutfulin also does a great amount of Party work.

The many years of productive activity of I. Z. Lutfulin have been highly appreciated by the Motherland: he has been awarded the Order of the Red Star and a number of medals. By a decree of the Supreme Soviet Kazakh SSR he has been awarded the Diploma of Honor of the Supreme Soviet of the Republic in connection with his 60th birthday.

Il'ya Zaynulovich meets his 60th birthday in good health, in good spirit, filled with energy, creative plans and thoughts. In congratulating him on his memorable anniversary the personnel of the institute wish him excellent health, active and productive organizational, scientific and pedagogic activity for long years ahead.

HIGH AWARD TO YEVGENIY KONSTANTINOVICH FEDOROV

Moscow METEOROLOGIYA I GIDROLOGIYA in Russian No 6, Jun 80 p 122

[Unsigned]

[Text] The Presidium of the USSR Supreme Soviet has awarded the Order of Lenin to Academician Yevgeniy Konstantinovich Fedorov for his major services in the development of the earth sciences, active public and political activity and in connection with his seventieth birthday.

AWARDS AT THE USSR EXHIBITION OF ACHIEVEMENTS IN THE NATIONAL ECONOMY

Moscow METEOROLOGIYA I GIDROLOGIYA in Russian No 6, Jun 80 pp 123-126

[Article by M. M. Kuznetsova]

[Text] The main committee of the USSR Exhibition of Achievements in the National Economy has presented awards to participants in the USSR Exhibition of Achievements in the National Economy for 1979 at the main exposition and at the specialized exhibits "Automated Technical Means for the Observation, Collection, Processing and Dissemination of Information on the State of the Environment" and "Instruments for Scientific Investigations in the Field of Hydrometeorology and Environmental Monitoring" held in the "Hydrometeorological Service" Pavilion.

First-Degree Diplomas:

Order of the Red Banner of Labor Main Geophysical Observatory imeni A. I. Voyeykov -- for the development of a hydrodynamic model of the atmosphere making it possible to clarify the physical principles of long-range weather forecasts, natural changes in general circulation of the atmosphere and possible changes in climate as a result of man's economic activity. The hydrodynamic model is at the level of the best existing foreign models.

State Scientific Research Center for the Study of Natural Resources -- for developing a method for computer processing of space TV information, making it possible to increase the information yield of photographs, and also methods for the interpretation and use of SHF information and data in other ranges; for the development and introduction of methods for the processing of space information obtained from the "Meteor" artificial earth satellites at operational subdivisions and on the scientific research ships of the State Committee on Hydrometeorology, which made it possible to improve the hydrometeorological support of organizations concerned with the national economy.

Central Aerological Observatory -- for developing and introducing M-100B rockets and associated apparatus which will ensure measurement of temperature and pressure with a higher accuracy and reliability and which has a high noise immunity of data transmission. The apparatus made possible automated input of the collected information into an electronic computer.

Institute of Experimental Meteorology -- for developing and improving the design of tetroons of different types with a miniature radio responder intended for measurement of the characteristics of transfer and scattering of a contaminating impurity in the atmosphere.

Second-Degree Diplomas:

Kazakh Republic Administration of Hydrometeorology and Environmental Monitoring -- for the high quality of agrometeorological servicing of the virgin lands of Kazakhstan, assurance of regular carrying out of aerial reconnaissance investigations, development of methods and manuals on agrometeorology.

West Siberian Regional Scientific Research Hydrometeorological Institute -- for developing and introducing computation methods for the prediction of fog and visibility in a fog in the presence of industrial haze, low cloud cover, wind velocity and also study of meteorological conditions applicable to the flight of supersonic aircraft and for a recommendation for the diagnosis and prediction of jet streams.

State Order of the Red Banner of Labor Hydrological Institute -- for carrying out expeditionary work for study of the water resources of the virgin and idle lands of northern Kazakhstan and lowland Altay. The economic effect from the use of scientific research in the virgin lands over a period of 25 years was 150 million rubles.

Ural Territorial Administration of Hydrometeorology and Environmental Monitoring -- for the agrometeorological support of programming of high yields of grain crops in Sverdlovskaya Oblast with allowance for agroclimatic factors and the microclimatic characteristics of farm areas.

Ukrainian Weather Bureau of the Ukrainian Republic Administration of Hydrometeorology and Environmental Monitoring -- for high-quality hydrometeorological support of beet production in the Ukrainian SSR with the use of materials from aerial inspections of the state of sugar beet fields and for improvements in the technology for care of fields.

Central Asiatic Regional Scientific Research Institute imeni V. A. Bugayev -- for carrying out a complex of snow-avalanche investigations making it possible to reduce the estimated cost of anti-avalanche structures by a factor of 50 on individual sectors of the Baykal-Amur Railroad and anti-avalanche investigations in the planning and construction of electric power lines in the sector Ust'-Kut - Tynda.

Amderma Territorial Administration of Hydrometeorology and Environmental Monitoring -- for hydrometeorological support of unloading and transport of freight on ice and introduction of a method for constructing a morphological map of shore ice.

Order of Lenin Arctic and Antarctic Scientific Research Institute -- for developing a method for the use of satellite information in evaluating ice conditions.

Central Design Bureau of Hydrometeorological Instrument Making -- for developing the "Potok" instrument for measuring the relative conductivity of water, intended for measuring the change in relative conductivity of water. The economic effect from use of the instrument is about 2,000 rubles annually.

Main Radiometeorological Center -- for developing and coordinating the technical specifications for the "Kurs" coupling apparatus and participation in factory and state tests.

State Oceanographic Institute -- for developing an automatic wave recorder making possible the routine collection of data on the mean values of wave elements and its introduction into expeditionary investigations. The annual economic effect for one coastal wave recorder is 8,400 rubles, for one shipboard wave recorder -- 8,800 rubles.

Third-Degree Diploma

Belogorka Agrometeorological Station of the Northwestern Territorial Administration of Hydrometeorology and Environmental Monitoring -- for hydrometeorological support of programmed yields, formulation of regional scientific research themes and introduction of the results into agricultural production.

Sosnovo Meteorological Station of the Northwestern Territorial Administration of Hydrometeorology and Environmental Monitoring -- for ensuring programmed yields of agricultural production with hydrometeorological information, preparation of a microclimatic map of the "Petrovskiy" Sovkhoz, and carrying out a great volume of reconnaissance investigations in programmed fields.

Leningrad Hydrometeorological Observatory of the Northwestern Territorial Administration of Hydrometeorology and Environmental Monitoring -- for ensuring programmed yields in a vegetable-growing zone with agrometeorological information and preparation of maps for taking into account microclimatic characteristics in the cultivation of agricultural crops.

Vinnitsa Hydrometeorological Bureau of the Ukrainian Republic Administration of Hydrometeorology and Environmental Monitoring -- for high-quality meteorological support of beet production in Vinnitskaya Oblast, study of the regularities in the formation of the yield of sugar beets in dependence on weather conditions during different parts of the growing season.

Gigant Agrometeorological Station of the Northern Caucasus Territorial Administration of Hydrometeorology and Environmental Monitoring -- for highly effective support of the "Gigant" grain sovkhoz. The economic effect from use of the information is more than 500,000 rubles.

Martuni Meteorological Station of the Armenian Republic Administration of Hydrometeorology and Environmental Monitoring -- for meteorological support of the national economy and information which makes it possible to choose the most rational agroengineering procedures directed to the retention of moisture reserves and determination of irrigation norms and times.

Gor'kovskaya Hydrometeorological Observatory of the Verkhne-Volzhskoye Territorial Administration of Hydrometeorology and Environmental Monitoring -- for carrying out agroclimatic regionalization of the territory of the Verkhne-Volzhskoye Administration of the Nonchernozem zone of the RSFSR, used in the long-range planning of agricultural production.

Royka Agrometeorological Station of the Verkhne-Volzhskoye Territorial Administration of Hydrometeorology and Environmental Monitoring -- for carrying out complex microclimatic investigations in meliorated lands over an area of about 5,000 hectares and formulation of recommendations on the use of the studied floodplain of the Kud'ma River by specialized crop rotations.

Morshanskaya Hydrometeorological Station of the Territorial Administration of Hydrometeorology and Environmental Monitoring of the Central Chernozem Oblasts -- for supplying agriculture with hydrometeorological information making it possible to obtain high yields of agricultural crops. The economic effect from its use was about 100,000 rubles.

Leninkan Hydrometeorological Bureau of the Armenian Republic Administration of Hydrometeorology and Environmental Monitoring -- for high-quality hydrometeorological support of the national economy of the Armenian SSR with recommendations and information. The economic effect from the use of hydrometeorological information was about 400,000 rubles.

Penzenskaya Zonal Hydrometeorological Observatory of the Privolzhskoye Territorial Administration of Hydrometeorology and Environmental Monitoring -- for carrying out work on monitoring the state of the environment in Penza city, development of methods and introduction into operational practice of forecasts and warnings concerning the onset of unfavorable meteorological conditions, making it possible for enterprises to proceed to an operating regime with a reduced discharge of contaminating substances and for carrying out hydrochemical work for study of the state of contamination of surface waters in Penza and Kazan' cities.

Alma-Ata Aviation Center of the Kazakh Republic Administration of the Hydrometeorology and Environmental Monitoring -- for high-quality meteorological support of flights of supersonic transport aircraft along the route Moscow - Alma-Ata - Moscow with the use of computation methods for predicting weather phenomena dangerous for aviation, making use of satellite and radar meteorological information.

Omsk Territorial Administration of Hydrometeorology and Environmental Monitoring -- for effective meteorological support of the safety of flights of all types of aircraft, a high probable success of forecasts (97%) and storm war·ing of dangerous weather phenomena, servicing of new air routes in places where petroleum and gas are being exploited.

Nadym Aviation Meteorological Station of the Omsk Territorial Administration of Hydrometeorology and Environmental Monitoring -- for ensuring accident-free highly effective meteorological servicing of civil aviation in regions of the largest gas deposits in the country: Medvezh'ye, and the Nadym-Punga gas pipeline.

A number of workers of the USSR State Committee on Hydrometeorology and Environmental Monitoring have been awarded medals of the All-Union Exhibition of Achievements in the National Economy. [Note: Abbreviations of affiliations are given at end of article.]

Gold Medal:

V. P. Meleshko (GGO), G. N. Isayeva (GosNITs IPR), I. S. Moshnikov, Yu. V. Mel'nichuk (TsAO), Ye. K. Garner, V. V. Smirnov (IEM), V. V. Bogorodskiy, V. B. Smirnov (AANII).

Silver Medal:

G. M. Bondar' (Kazakhskoye UGKS), V. T. Rylova (Zhaltyr Meteorological Station Kazakhskoye UGKS), V. M. Yarkova (ZapSibRNIGMI), A. B. Zavodchikov, A. N. Chizhov (GGI), V. N. Babchenko (Ural'skoye UGKS), L. N. Burtsev (Ukrainskoye UGKS), L. A. Kanayev, Ye. Ya. Ran'kov, V. A. Korobkov (SARNIGMI), B. Ye. Shneyerov, G. B. Brylev (GGO), A. N. Chilingarov (Amderminskoye UGKS), A. V. Bushuyev, V. Ye. Borodachev, V. P. Tripol'nikov, I. N. Kosterin (AANII), A. P. Tishchenko (GosNITs IPR), A. V. Komotskov, A. A. Ivanov, A. G. Voronovskiy, V. I. Kozlov, V. D. Grinchenko, O. V. Shtyrkov, A. F. Chizhov (TsaO), G. S. Rybin, B. P. Seredin (TsKB), V. Ye. Osherov (GRMTs), B. A. Maksimov (GOIN), A. I. Ovsyannikov, V. N. Ivanov, M. I. Allenov, N. D. Tret'yakov (IEM), A. F. Konov (VNIIsel'khoz Meteorologiya), A. Ye. Mikirov (IPG).

Bronze Medal:

R. A. Shishkina, N. I. Sukhanova, Yu. P. Teplov (Kazakhskoye UGKS), A. D. Maslovskaya, D. P. Fedyushina, S. A. Bedarev, V. P. Petrashin, Ye. N. Korobova, R. S. Golubev, Ye. V. Bogolyubova (KazNIGMI), L. Ye. Kaminskaya, M. I. Chernikova, N. V. Vostryakova, V. N. Martynov (ZapSibRNIGMI), V. Ye. Vodogretskiy, I. N. Obraztsov, G. P. Levchenko, S. I. Kharchenko, V. A. Znamenskiy, A. M. Filippov, T. V. Fuksova, V. V. Borodulin, R. V. Donchenko (GGI), V. A. Teplyshov, S. M. Vodovenko (Ural'skoye UGKS), S. M. Malakhova (Belogorka Agricultural Meteorological Station Severo-Zapadnoye UGKS), N. D. Golovina (Sosnovo Meteorological Station Severo-Zapadnoye

UGKS), M. I. Degtyareva (Northwestern UGKS), R. M. Koronatova (Leningrad Hydrometeorological Observatory of the Severo-Zapadnoye UGKS), N. P. Krivenchenko, N. F. Tokar' (Ukrainian UGKS), Zh. P. Kovtun (Vinnitsa Hydrometeorological Bureau of the Ukrainian UGKS), E. R. Sprogis, A. P. Simane (Latvian UGKS), V. V. Kostenko (Gigant Agrometeorological Station of the Severo-Kavkazskoye UGKS), V. N. Karapetyan (posthumously)(Martuni Meteorological Station Armenian UGKS), S. F. Grechkaneva (Gor'kiy Hydrometeorological Observatory of the Verkhne-Volzhskoye UGKS), Yu. V. Syroyegin (Royka Agrometeorological Station of the Verkhne-Volzhskoye UGKS), A. I. Korshunov (Morshanskaya Hydrometeorological Station UGKS Tsentral'no-Chernozemnykh Oblastey), G. Ye. Aslanyan, V. Ye. Pogosyan (Leninakan Hydrometeorological Bureau of the Armyanskoye UGKS), N. P. Bakhtin, V. T. Miklin, T. V. Zaigrayeva (Krasnoyarskoye UGKS), O. I. Orestov, A. A. Chirkova, V. V. Maystrova, V. P. Brekhov, M. I. Getker (SARNIGMI), L. R. Dmitriyeva, P. N. Nikolayev, A. A. Fedorov, A. G. Linev, N. S. Dorozhkin (GGO), V. M. Klimovich, V. Ya. Korzhikov, V. N. Vorob'yev (Amderminskoye UGKS), Yu. D. Bychenkov, S. A. Kolesov, G. B. Savitskiy, G. V. Trepov, G. P. Khokhlov, V. M. Vystavnoy, I. A. Shumilov, R. A. Balakin, P. A. Tsvetkov, V. N. Titov, N. I. Telyayev, V. A. Ul'yev, N. N. Ivanov (AANII), A. F. Kormilkin, O. V. Vereshchagina (Penzenskaya ZMGO of the Privolzhskoye UGKS), I. I. Bobrikov (Alma-Ata Aviation Meteorological Center Kazakhskoye UGKS), S. S. Kazachkov, N. I. Smirnov, P. G. Kondakov (Omskoye UGKS), G. V. Ocheretnyy, N. V. Yermakova (Nadym Aviation Meteorological Station Omskoye UGKS), V. R. Golovchin, V. P. Bocharov, I. G. Rozanov, V. S. Dobrykh, Ye. P. Domkovskaya, I. S. Skuratova, S. V. Shapovalov (GosNITs IPR), A. S. Butko, Ye. V. Lysenko, V. Ya. Rusina, M. F. Mayorov, V. V. Yermakov, V. V. Babenko, G. P. Trifonov, N. A. Kuz'micheva, Ye. N. Kadygrov, Yu. N. Rybin, G. S. Pavlov, A. P. Zhukov, G. M. Rybchenko, A. V. Fedynskiy, V. A. Yushkov, N. I. Brezgin, Ye. A. Polyakova, V. N. Yanin, S. G. Linnik, V. N. Lyakh (TsAO), V. N. Yefimtsev, B. I. Nikolayev, A. S. Mileshin, A. G. Roshchin, A. S. Gromakov, I. T. Baramykin (TsKB), L. V. Petukhov, A. V. Rostkov, V. V. Galushko, Yu. N. Chernetskiy, V. V. Ipatov, G. P. Zhukov, V. I. Ptakhin, S. I. Aksarina (IEM), B. D. Lipavskiy, N. Ye. Saprykin (DVNIGMI), V. M. Rokogon, A. G. Sukhovey, M. G. Mayboroda (Odo GOIN), G. K. Popandopulo, S. A. Folimonov, I. M. Shenerovich, L. S. Kleban, G. N. Mar, B. L. Binder, Ye. N. Uspenskiy, N. S. Varzhenevskiy, A. I. Afanas'yev, A. L. Zlatin (NIIGMP), V. A. Gubanov, Yu. B. Guseynov, N. A. Volkov (GRMTs), I. P. Trubkin, G. V. Matushevskiy, M. V. Kozlov (GOIN), G. M. Osipenko, A. V. Sergiyevskiy (Kuchinskaya EPM NIIGMP), A. A. Gen, V. V. Vol'vach (VNIIsel'khozmeteorologiya), T. V. Li, L. D. Pilyugina (Zapadno-Sibirskoye UGKS), T. V. Kazachevskaya, V. V. Selant'yev, V. Ya. Isyakayev (IPG), A. B. Kot, E. A. Afonyushkin (TsVGMO), G. V. Myakon'kiy, G. V. Stepanov, V. G. Khorguani (VGI).

The total number of participants in the All-Union Exhibition of Achievements in the National Economy in 1979 from the State Committee on Hydrometeorology is 499 persons. In addition to workers of the USSR State Committee on Hydrometeorology and Environmental Monitoring, the Main Exhibition Committee of the USSR All-Union Exhibition of Achievements in the National Economy for the "Gidrometsluzhba" Pavilion awarded prizes to outside organizations taking a direct part in the development of some themes.

ABBREVIATIONS

GGO = Main Geophysical Observatory
GosNITs IPR = State Scientific Research Center for Study of Natural Resources
TsAO = Central Aerological Observatory
IEM = Institute of Experimental Meteorology
AANII = Arctic and Antarctic Scientific Research Institute
Kazakhskoye UGKS = Kazakh Administration of the Hydrometeorological Service
ZapSibRNIGMI = Western Siberian Regional Scientific Research Hydrometeorological Institute
GGI = State Hydrological Institute
Ural'skoye UGKS = Ural Administration of the Hydrometeorological Service
Ukrainskoye UGKS = Ukrainian Administration of the Hydrometeorological Service
SARNIGMI = Central Asian Regional Scientific Research Hydrometeorological Institute
TsKB = Central Design Bureau
Amderminskoye UGKS = Amderma Administration of the Hydrometeorological Service
GOIN = State Oceanographic Institute
VNII sel'khoz Meteorologiya = All-Union Scientific Research Institute of Agricultural Meteorology
IPG = Institute of Applied Geophysics
KazNIGMI = Kazakh Scientific Research Hydrometeorological Institute
Severo-Zapadnoye UGKS = Northwestern Administration of the Hydrometeorological Service
Verkhne-Volzhskoye UGKS = Upper Volga Administration of the Hydrometeorological Service
UGKS Tsentral'no-Chernozemnykh Oblastey (Administration of the Hydrometeorological Service of the Central Chernozem Oblasts)
Krasnoyarskoye UGKS = Krasnoyarsk Administration of the Hydrometeorological Service
Penzenskaya ZMGO = Penza Zonal Hydrometeorological Observatory
Omskoye UGKS -- Omsk Administration of the Hydrometeorological Service
DVNIGMI = Far Eastern Scientific Research Hydrometeorological Institute
Odo GOIN = Odessa Division of the State Oceanographic Institute
TsVGMO = Central Volga Hydrometeorological Observatory
VGI = High-Mountain Geophysical Institute

AT THE USSR STATE COMMITTEE ON HYDROMETEOROLOGY AND ENVIRONMENTAL MONITORING

Moscow METEOROLOGIYA I GIDROLOGIYA in Russian No 6, Jun 80 p 126

[Article by V. N. Zakharov]

[Text] An expanded session of the Board of the USSR State Committee on Hydrometeorology and Environmental Monitoring was held during the period 11-12 March. Those in attendence considered a report by the Chairman of the State Committee on Hydrometeorology Corresponding Member USSR Academy of Sciences Yu. A. Izrael' entitled "Principal Results of Activity During 1979 and Tasks for 1980 in Light of the Resolutions of the November (1979) Plenary Session of the Central Committee CPSU, the Principles and Conclusions Set Forth in an Address by the General Secretary of the Central Committee CPSU Comrade L. I. Brezhnev at the Plenary Session."

The report dealt with the problems involved in the hydrometeorological servicing of the national economy, monitoring of environmental contamination, technical development, scientific research activity, financial-economic activity, work with personnel, major construction, etc.

On 13 March there was a session of the Presidium of the Scientific and Technical Council of the State Committee on Hydrometeorology which dealt with problems relating to improvement of planning, monitoring, reporting on and record keeping on the scientific research work in the system of the USSR State Committee on Hydrometeorology and Environmental Monitoring. A report on this problem was presented by the First Deputy Chairman of the State Committee on Hydrometeorology Yu. S. Sedunov.

The session also examined some problems involved in the work of the scientific councils on different problems.

Participating in the work of the Presidium of the Scientific and Technical Council were the directors of institutes, workers in the central offices of the State Committee on Hydrometeorology and chiefs of the administrations of the Hydrometeorological Service.

CONFERENCES, MEETINGS AND SEMINARS

Moscow METEOROLOGIYA I GIDROLOGIYA in Russian No 6, Jun 80 pp 126-128

[Article by K. M. Lugina and Yu. G. Slatinskiy]

[Text] A conference of experts of the hydrological and meteorological services of Bulgaria, Hungary, East Germany, Poland, Rumania, USSR and Czechoslovakia on the subject "Climatic Change" was held at the State Hydrological Institute during the period 12-16 November 1979. The conference heard 14 reports and informative communications on different aspects of the problem.

An introductory report by Corresponding Member USSR Academy of Sciences M. I. Budyko gave a review of studies of the problem carried out in different countries. It was noted that interest in this problem has increased in virtually all countries.

An informative communication by V. V. Kupriyanov gave a generalization of the principal directions of scientific research at the State Hydrological Institute.

A report by I. A. Shiklomanov was devoted to problems involved in the change in runoff of a number of major rivers in the Soviet Union as a result of the influence of different types of economic activity and the problem of interzonal redistribution of river runoff.

In a report by M. I. Budyko entitled "Future of the Biosphere" it was demonstrated that the anthropogenic increase in carbon dioxide in the atmosphere can lead in the near future to a change in the earth's climate. The author emphasized that by using instrumental and paleoclimatic data, as well as computations by means of climatic models, already in the immediate future it is possible to prepare a prediction of climatic changes at the end of the current and at the beginning of the next century.

A report by K. Ya. Vinnikov, G. V. Gruza, V. F. Zakharov, N. P. Kovyneva and E. Ya. Ran'kova gave a generalization of empirical data on recent changes in the thermal and ice regimes of the northern hemisphere.

The correlation between the quantity of precipitation and the change in air temperature was discussed in a report by O. A. Drozdov. By analyzing paleoclimatic information, historical data and data from instrumental observations, the author demonstrated that an increase in global temperature approximately up to 2° in comparison with the present-day level will lead to a decrease in the meridional thermal gradients and the precipitation associated with them in the continental regions of the temperate latitudes. A further temperature increase will be accompanied by an increase in the quantity of precipitation due to convective factors.

A report by O. Sebek (CzSSR) was devoted to an analysis of a 200-year series of observations of air temperature and a 100-year series of observations of precipitation at the meteorological station Prague-Klementina. The warmest and coldest periods were determined for individual seasons and for the year as a whole. Their correlation with the temperature of other long-series European stations was analyzed.

A communication by A. Leman (East Germany) dealt with the problems involved in the quality of the information used in investigations of climate and its changes. He emphasized the need for formulating unified criteria for evaluating the homogeneity of series of meteorological observations.

M. Sadovski (Poland) informed the conferees about investigations of climatic changes carried out in Poland. These studies are being made for the most part in three directions: 1) determination of climatic norms; 2) evaluation of climatic trends; 3) study of periodic fluctuations of different climatic elements (temperature, precipitation, radiation). The communication also included some results of analysis of data on the snow cover in the Warsaw region.

A communication by E. Koleva (Bulgaria) was devoted to long-term fluctuations of precipitation sums and the mean monthly air temperature in the territory of Bulgaria. The cyclicity of precipitation was investigated using a method proposed by O. A. Drozdov with the use of correlation and spectral functions.

A report by K. M. Lugina was devoted to the problems involved in a spatial averaging method and the accuracy of the characteristics of meteorological fields obtained using this method.

L. G. Polozova discussed the problems involved in investigating climatic changes of the past on the basis of an analysis of archeological and dendroclimatic information and the assimilation of this information with instrumental observation data.

A report by G. V. Gruza dealt in detail with problems involved in an analysis of variability of the mean monthly air temperature and atmospheric pressure fields in the northern hemisphere during the period 1891-1978.

A report by M. V. Muratova and I. A. Suyetova presented the results of use of data from a pollen analysis at 30 points in the Soviet Union for constructing maps of mean temperature and precipitation during the period of the Holocene thermal optimum (5,000-6,000 years ago).

The conference noted that the conclusion that there is a possible anthropogenic change in climate as a result of an increase in the content of carbon dioxide in the atmosphere, contained in the resolutions of a whole series of international conferences and symposia and finding reflection in the Declaration of the World Conference on Climate, obligates professional climatologists to intensify attention to investigations in this field.

The conferees formulated a draft of a program for joint work on the problem of investigation of anthropogenic changes in climate during 1981-1985. The program includes the development of investigations in the following principal directions: development of a method for the use of data from instrumental meteorological measurements for evaluating changes in climate; study of the regularities in recent climatic changes; development of the principles for use of paleoclimatic information for evaluating the climate of the future; evaluation of the changes in climatic conditions possible in the territories of the socialist countries caused by anthropogenic changes in global climate.

The representatives of the countries participating in the conference signed a protocol in which it is emphasized that evaluations of the possible changes in the climatic regime can bring practical advantage in long-range economic planning. At the same time it was noted that the solution of such a complex problem is possible only on the basis of broad international cooperation and interaction.

K. M. Lugina

A republic conference of chiefs of sea and river-mouth subdivisions of the Ukrainian Administration of the Hydrometeorological Service was held during the period 20-22 November 1979 at Sevastopol'.

A report on the operation of sea and river-mouth subdivisions of the Ukrainian Administration of the Hydrometeorological Service in the Tenth Five-Year Plan and the tasks for the coming years was presented by a division chief at this administration, V. I. Kostin, and the chief of the marine division of the Crimean Hydrometeorological Observatory, G. V. Yatsevich. It was noted in the reports that during recent years specialists at the Ukrainian Administration of the Hydrometeorological Service have carried out much work on rationalization of the sea network and the types of observations and increasing the quality of the information received for servicing of national economic organizations and the prognostic divisions of the State Committee on Hydrometeorology.

In accordance with the plan for long-range development of the sea network the Ukrainian Administration of the Hydrometeorological Service in the future is planning the continuation of work on broadening existing and creating new observation points. In particular, on the proposal of the Sevastopol' Division of the State Oceanographic Institute a study is being made of the problem of the possibility of creating a major rivermouth station in the lower reaches of the Dnestr River and a specialized hydrometeorological post on the Belosarayskaya spit. Jointly with representatives of planning organizations there is discussion of a plan for the development of the observational network along the planned route of the Danube-Dnepr Canal.

Each year the sea network of the Ukrainian Administration of the Hydrometeorological Service receives a great volume of information for evaluating the state of the hydrometeorological regime in the coastal zone and in the open sea.

The carrying out of expeditionary investigations occupies an important place in the activity of the sea network. With each passing year more and more work is being done under complex specialized programs formulated by the Sevastopol' Division of the State Oceanographic Institute.

In the reports a major place was devoted to an analysis of operation of the sea network by the card punching of coastal and deep-water hydrological observations and the status of work by the shipboard network was analyzed in detail.

The Sevastopol' Division of the State Oceanographic Institute presented several reports at the conference. A report by A. P. Zhilyayev examined the principal results of carrying out of expeditionary work and the tasks facing subdivisions of the sea network with respect to improving operation of the entire low-tonnage fleet and increasing the effectiveness of its use. V. G. Simov told about a program for the further development of investigations in the mouth regions of the largest rivers in the Ukrainian SSR, and on participation of specialists in the sea network in implementing a number of major national economic projects for the redistribution of fresh runoff in the southern regions of the country. A. D. Bruk gave a detailed analysis of the activity of network hydrochemical laboratories. In particular, the report told of the extensive work carried out by the Sevastopol' Division of the State Oceanographic Institute in optimizing the network of stations, carried out during regular hydrochemical surveys by subdivisions of the sea network.

The directors of a number of network subdivisions of the Ukrainian Administration of the Hydrometeorological Service presented reports at the conference.

NOTES FROM ABROAD

Moscow METEOROLOGIYA I GIDROLOGIYA in Russian No 6, Jun 80 p 128

[Article by B. I. Silkin]

[Text] The oxygen present in the atmosphere at an altitude of about 35 km above the earth's surface absorbs a considerable part of the sun's UV radiation, as a result of which ozone molecules are formed. It is reported in SCIENCE, 22 June 1979, and SCIENCE NEWS, Vol 115, No 25, that by studying this process, highly important for the safeguarding of everything alive from lethal doses of UV, specialists at the Langley Research Center, Hampton, Virginia, of NASA, L. B. Callis, M. Nataradzhan and D. E. Neeley developed a model making it possible to compute the quantity of ozone in the stratosphere and temperature variations in their relationship to known data revealing variations of solar UV radiation during the period between the early 1960's and 1976.

As a result they drew the conclusion that the observed changes in O_3 content and temperature can to a considerable degree be caused by the degree of variability of the flux of solar ultraviolet radiation associated with the 11-year cycle of solar activity. The agreement between the computed and observed ozone contents in the earth's temperate latitudes is deemed to be good: as the flux of UV radiation increased with the solar cycle and decreased in a sine curve, the quantity of ozone followed it closely. The temperature trend was the same.

The changes in the O_3 content were associated with both photochemical and thermal processes. When the intensity of UV radiation increases there is also an increase in the quantity of ozone forming as a result of photochemical processes. However, an increase in the ozone concentration is partially restrained by an increase in temperature, which reduces the number of O_3 molecules. All these interactions were taken into account in a model containing elements associated with the intensity of radiation, convection and photochemical processes. However, in the opinion of the researchers themselves, final conclusions concerning the relationship between solar phenomena and stratospheric phenomena can be drawn when more exhaustive data are obtained concerning variations of ozone, temperature and solar UV radiation for the range of wavelengths less than 300 nm.

ME

18 SEPTEMBER 1980 NO. 6, JUNE 1980 3 OF 3

APPROVED FOR RELEASE: 2007/02/08: CIA-RDP82-00850R000300030024-9

It is also impossible to deny the influence of other natural phenomena such as atmospheric absorption of galactic cosmic rays, the sun's ejection of protons and sudden stratospheric warmings, which can also exert an influence on the formation of ozone molecules in the stratosphere.

[10-5303]

5303
CSO: 1864

-END-